University of Alberta

Satellite Cell Involvement in Activity-Induced Skeletal Muscle Adaptations

by

Karen Janet Bernice Martins (*Nee:* Martinuk)

A thesis submitted to the Faculty of Graduate Studies and Research
in partial fulfillment of the requirements for the degree of

Doctor of Philosophy

Faculty of Physical Education and Recreation

Fall 2009
Edmonton, Alberta

Examining Committee

Charles Putman, Physical Education and Recreation

Walter Dixon, Agricultural, Food and Nutritional Science

George Foxcroft, Agricultural, Food and Nutritional Science

Daniel Syrotuik, Physical Education and Recreation

Karyn Esser, Physiology, University of Kentucky

ABSTRACT

Skeletal muscle is a heterogeneous, multinucleated, post-mitotic tissue that contains many functionally diverse fibre types that are capable of adjusting their phenotypic properties in response to altered contractile demands. This plasticity, or adaptability of skeletal muscle is largely dictated by variations in motoneuron firing patterns. For example, in response to increased tonic firing of slow motoneurons, which occurs during bouts of endurance training or chronic low-frequency stimulation (CLFS), skeletal muscle adapts by transforming from a faster to a slower phenotypic profile. CLFS is an animal model of endurance training that induces fast-to-slow fibre type transformations in the absence of fibre injury in the rat. The underlying signaling mechanisms regulating this fast-to-slow fibre type transformation, however, remain to be fully elucidated. It has been suggested that myogenic stem cells, termed satellite cells, may regulate and/or facilitate this transformational process. Therefore, the signaling mechanisms involved in CLFS-induced satellite cell activation as well as the role satellite cells may play in CLFS-induced skeletal muscle adaptation were investigated in rat. A pharmacological inhibitor of nitric oxide (NO) synthase, N^{ω}-nitro-L-arginine methyl ester, was used to investigate CLFS-induced satellite cell activation in the absence of endogenous NO production. Results suggest that NO is required for early CLFS-induced satellite cell activation, but a yet-to-be defined pathway exists that is able to fully compensate in the absence of prolonged NO production. A novel method of satellite cell ablation (i.e. weekly focal γ-irradiation application) was used to investigate CLFS-induced skeletal

muscle adaptation in the absence of a viable satellite cell population. Myosin heavy chain (MHC), an important structural and regulatory protein component of the contractile apparatus, was used as a cellular marker of the adaptive response to CLFS. It was demonstrated that satellite cell activity may be involved in early fast-to-slow MHC-based transformations to occur at the protein level without delay in the fast fibre population, and may also play an obligatory role in the final transformation from fast type IIA to slow type I fibres. Interestingly, additional results show that NO appears to be a key mediator of MHC isoform gene expression during CLFS-induced fast-to-slow fibre type transformations.

ACKNOWLEDGEMENTS

I would like to express sincere gratitude to my supervisor, Dr. Charles T. Putman for his exceptional academic mentorship and guidance. I am also truly grateful to my current and former committee members, Dr. Walter Dixon, Dr. George Foxcroft and Dr. Tessa Gordon, for their support and advice. Additionally, I would like to thank Dr. John Dunn for catalyzing the expansion of my academic knowledge.

Thank you to Zoltan Kenwall, Dr. Gordon Murdoch, Joan Turchinsky, Neil Tyreman, and particularly Ian MacLean and Jean Pearcy for their gracious assistance, guidance and invaluable technical expertise and support in the laboratory. Of course, I cannot forget the assistance of Mark Burquest, Vanessa Carlson, Carolyn Crowell, Max Levine and Pam McDonald, all of whom spent countless hours in the laboratory and staring into microscopes on my behalf.

Many thanks to my fellow colleagues both past and present, Victoria Cook, Dr. Maria Gallo, Dr. Luke Harris and Yang Shu for their practical help, advice and above all else, camaraderie. I would also like to thank the Gang for morning coffee, lab lunches and high-five Fridays, which provided unforgettable memories and much appreciated levity. Numerous friends outside of academia have helped to keep life in perspective for me. Particular thanks to Bobbi Barbarich, Daryl Lehocky and Shane Mortemore.

Finally, thank you to my Husband for everything, but especially for teaching me balance, to my loving Mom and Dad for supporting their daughter, the proverbial student, to my Brother who is travelling a similar path, and to my entire family for their unconditional love and encouragement - always.

Research support was provided by the Alberta Agricultural Research Institute, the Alberta Heritage Foundation of Medical Research (AHFMR), the Canadian Institutes of Health Research and the Natural Sciences and Engineering Research Council (NSERC). My scholarship funding support was provided by AHFMR, NSERC and the University of Alberta.

Cheers to science!

TABLE OF CONTENTS

LIST OF TABLES

LIST OF FIGURES

CHAPTER ONE

CHAPTER TWO

CHAPTER FOUR

CHAPTER FIVE

CHAPTER SIX

APPENDIX A

APPENDIX B

LIST OF SYMBOLS, NOMENCLATURE AND ABBREVIATIONS

©	copyright
®	registered trademark
™	not yet registered trademark
γ	gamma
μg	microgram
μl	microliter
μm	micrometer
μs	microsecond
^{3}H	tritium-labeled hydrogen
4E-BP1	eukaryotic initiation factor 4E-binding protein-1
AB	Alberta
Ach	acetylcholine
ANOVA	analysis of variance
ATP	adenosine triphosphate
BrdU	5-bromo-2'-deoxyuridine
BS	blocking solution
CA	California
Ca^{2+}	calcium
Ca++	calcium
CAMK	calmodulin-dependent protein kinase
CCAC	Canadian Council for Animal Care
cDNA	complimentary deoxyribonucleic acid
cGMP	cyclic guanosine monophosphate
CLFS	chronic low-frequency stimulation
cm	centimeter
COX	cytochrome c oxidase
CS	citrate synthase
CSA	cross-sectional area
Ct	threshold cycle
DTT	dithiothreitol
DML	dorsal medial lip
DNA	deoxyribonucleic acid
EBI	European Bioinformatics Institute
EDL	extensor digitorum longus
EDTA	ethylenediaminetetraacetic acid
eIF2B	eukaryotic initiation factor 2B
EMBL	European Molecular Biology Laboratory
eNOS	endothelial nitric oxide synthase
ERK1/2	extracellular signal-regulated kinase
FoxO	forkhead box O
g	gram
GAPDH	glyceraldehyde phosphate dehydrogenase
GSK-3β	glycogen synthase kinase-3β
Gy	gray

h	hour
HDAC	histone deacetylase
HGF	hepatocyte growth factor
hr	hour
HRP	horse radish peroxidase
Hz	hertz
IgG	immunoglobulin G
IgM	immunoglobulin M
IN	Indianapolis
Inc.	Incorporation
IRR	weekly doses of γ-irradiation focused on the left leg only
IN	Indiana
iNOS	inducible nitric oxide synthase
JNK	c-jun N-terminal kinase
kDa	kilodalton
kg	kilogram
L-	treated with N^{ω}-nitro-L-arginine methyl ester
L-Arg	L-arginine
L-NAME	N^{ω}-nitro-L-arginine methyl ester
MA	Massachusetts
mA	milliamps
MAPK	mitogen-activated protein kinase
M-Cadherin	muscle-cadherin
MD	Maryland
MEF2	myocyte enhancing factor-2
MGB	minor groove binder
mg	milligram
MHC	myosin heavy chain
min	minute
ml	milliliter
mM	millimolar
mm	millimeter
M-MLV	moloney murine leukemia virus
MMP	matrix metalloproteinase
MRF	myogenic regulatory factor
mRNA	messenger ribonucleic acid
mTOR	mammalian target of rapamycin
MTP	membrane type I
NFAT	nuclear factors of activated T-cells
NJ	New Jersey
nm	nanometer
NMJ	neuromuscular junction
nNOS	neuronal nitric oxide synthase
NO	nitric oxide
NOS	nitric oxide synthase
OCT	optimum cutting temperature

ON	Ontario
Pax	paired box transcription factor
PBS	phosphate-buffered saline
PBS-T	phosphate-buffered saline-Tween-20
PDK1	3'-phosphoinositide-dependent protein kinase-1
PFK	phosphofructokinase
PG	proteoglycans
PQ	Quebec
RNA	ribonucleic acid
RT-PCR	reverse transcriptase-polymerase chain reaction
S6K	ribosomal protein S6 kinase
SA-Ca	stretch-activated calcium ion
SDS-PAGE	sodium dodecyl sulfate-polyacrylamide gel electrophoresis
SEM	standard error of the mean
sGC	soluble guanylate cyclase
Stim	chronic low-frequency stimulation of the left leg only
TA	tibialis anterior
TSC2	tuberous sclerosis complex-2
UK	United Kingdom
USA	United States of America
UV	ultraviolet
V	volts
v	volume
VA	Virginia
VLL	ventral lateral lip
w	weight
wgt	weight
wt	weight
wk	week

CHAPTER ONE

INTRODUCTION

1.1 INTRODUCTION

Adult skeletal muscle is a heterogeneous, multinucleated, post-mitotic tissue containing many functionally diverse fibre types that are capable of adjusting their structural, functional, metabolic and molecular properties in response to altered contractile demands (reviewed by Pette & Staron, 1997; Pette, 1998; Pette & Staron, 2000; Pette, 2001). The underlying signaling mechanisms that lead to phenotypic transformation, however, remain unclear. One possible mechanism that has been suggested to regulate and/or facilitate this transformational process are myogenic stem cells, termed satellite cells that are associated with all skeletal muscle fibres (Schultz *et al.*, 1990).

Named for their location between the basal lamina and the sarcolemma of adult skeletal muscle fibres (Fig. 1.1), satellite cells are undifferentiated, mononucleated, muscle progenitor stem cells that constitute approximately 1-4% of total myonuclei (Schultz & McCormick, 1994). Normally quiescent in adult skeletal muscle, satellite cells become active in response to a number of stimuli including muscle growth, damage, innervation/denervation, stretch, overload and exercise (Putman *et al.*, 1999; Seale & Rudnicki, 2000). It is well established that in response to skeletal muscle hypertrophic stimuli or damage, quiescent satellite cells begin to actively cycle and fuse with existing myofibres or with each other, creating new myonuclei or forming new myofibres, respectively (reviewed by Schultz & McCormick, 1994; Hawke & Garry, 2001; Charge & Rudnicki, 2004; Adams, 2006; O'Connor & Pavlath, 2007). As Schultz & Darr (1990) and Bamman (2007) point out, however, the role of satellite cells in endurance exercise-induced skeletal muscle adaptation is less clear.

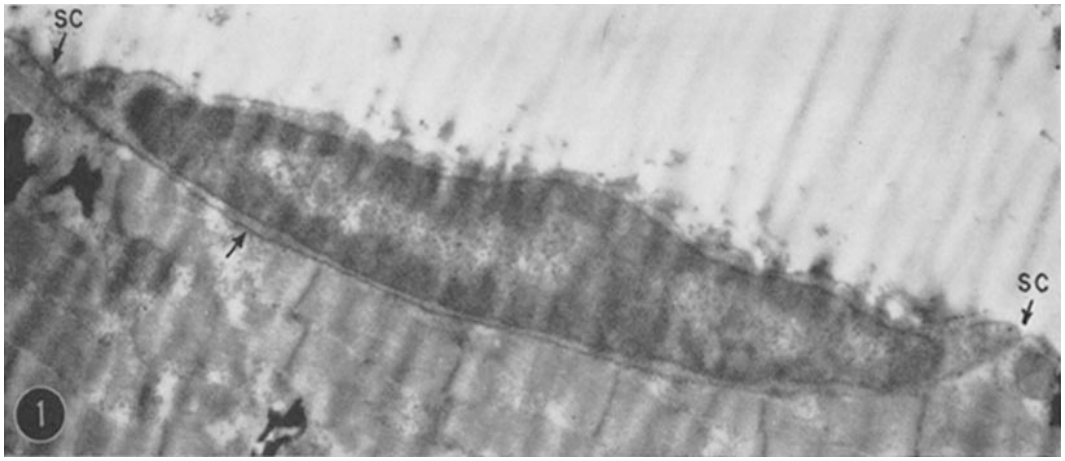

Figure 1.1 First documented satellite cell. Arrows indicate satellite cell. SC=extreme poles of the satellite cell. © Mauro, 1961. Originally published in *J. Biophys. Biochem. Cytol.* 9: 493-494.

The work presented in this thesis examines the activity-induced activating signaling mechanisms and subsequent contributions of satellite cells to skeletal muscle transformations in rat fast-twitch skeletal muscle. The second chapter is a review of the literature, examining the pertinent components of skeletal muscle and the satellite cell population associated with it, specifically focused on rodents. The first section of the literature review provides a general overview of the heterogeneity of adult skeletal muscle and its ability to adapt in response to varying contractile demands such as chronic low-frequency stimulation (CLFS), an animal model of endurance exercise training. The second section reviews the different roles that satellite cells play in skeletal muscle including development, regeneration, hypertrophy and fast-to-slow fibre type transformations. The recent classification of satellite cells as stem cells is also addressed in this section along with the proposed underlying signaling mechanisms controlling the ability of satellite cells to generate both differentiated skeletal muscle progeny and to self-renew. Additionally, the model of gamma (γ)-irradiation as a method of satellite cell ablation is reviewed. The final section addresses the signaling mechanisms involved in satellite cell activation. The nitric oxide (NO)-dependent satellite cell activation pathway that involves NO, hepatocyte growth factor (HGF) and the

satellite cell c-met receptor, is reviewed along with this pathways potential involvement in CLFS-induced satellite cell activation. NO-independent satellite cell activation is also discussed.

The three studies in this thesis are presented as sequential chapters (3-5). The study detailed in Chapter 3 implemented a novel γ-irradiation protocol that successfully ablated satellite cell activity in the rat mixed fast-twitch tibialis anterior muscle throughout 21 days of CLFS. This allowed investigation of the effects of long-term CLFS-induced fast-to-slow skeletal muscle fibre type transformations, in the absence of a viable satellite cell population. Moderate attenuation of CLFS-induced fast-to-slow fibre type transformations was observed in long-term stimulated muscles that were exposed to γ-irradiation. Specifically, the final type IIA to I transformation did not occur in these muscles. Thus, satellite cells appear to play a direct role in fast-to-slow fibre type transformations that is quantitative in nature. Considerable adaptive potential does, however, seem to reside in myonuclei, which indicates that the primary role of satellite cells may be to maintain the long-term stability of the transformed state.

The second study (Chapter 4) examined the involvement of satellite cells in response to short-term (1 to 10 days) CLFS-induced fast-to-slow fibre type transformations in rat tibialis anterior muscle. It was reported that significant satellite cell activation occurred at 1 day of stimulation and confirmed previous results that maximal proliferation occurs between 5 and 10 days of stimulation (Putman *et al.*, 1999). Additionally, in those muscles exposed to γ-irradiation, fast-to-slow fibre type transformations during short-term CLFS were attenuated in the fast fibre population and the final fast-twitch to slow-twitch transformation was prevented, as similarly observed during long-term CLFS. These findings indicate that satellite cell activity may also be important during short-term CLFS. Collectively, it appears that existing myonuclei can support fast-to-slow fibre type transformations up to a certain threshold or myonuclear domain ceiling beyond

which satellite cells may be required, particularly for the final transformation from type IIA to type I fibres.

The final time-course study (Chapter 5) was the first to investigate the signaling mechanisms involved in CLFS-induced satellite cell activation and specifically, the NO-dependent satellite cell activation pathway in rat tibialis anterior. Endogenous NO production was blocked by orally administering a pharmacological inhibitor of NO synthase (NOS) activity, N^{ω}-nitro-L-arginine methyl ester (L-NAME). In those animals that received L-NAME, early CLFS-induced satellite cell activity was blocked, but by 5 days of stimulation, satellite cell activity was able to fully recover. Therefore, it appears that only immediate CLFS-induced satellite cell activation occurs via a NO-dependent pathway, while a yet-to-be identified NO-independent pathway exists that is able to fully compensate during NO suppression. Additionally, in the L-NAME treated animals, the up-regulation of myosin heavy chain (MHC) mRNAs involved in CLFS-induced fast-to-slow transformations was prevented. Therefore, NO also appears to be directly involved in regulating CLFS-induced MHC gene expression.

Collectively, these studies indicate that NO is required for immediate satellite cell activity, which in turn, is involved in both short-term and long-term CLFS-induced fast-to-slow fibre type transformations. Additionally, NO also appears to be a key mediator of MHC gene expression in response to CLFS. The overall results and interpretations of findings are discussed in the final chapter of this thesis (Chapter 6). Rationales for future studies are also presented that would further our understanding of the underlying cellular and molecular mechanisms responsible for activity-induced satellite cell activation and the regulation of fast-to-slow skeletal muscle transformation.

1.2 REFERENCES

Adams GR. (2006). Satellite cell proliferation and skeletal muscle hypertrophy. *Appl Physiol Nutr Metab* **31,** 782-790.

Bamman MM. (2007). Take two NSAIDs and call on your satellite cells in the morning. *J Appl Physiol* **103,** 415-416.

Charge SB & Rudnicki MA. (2004). Cellular and molecular regulation of muscle regeneration. *Physiol Rev* **84,** 209-238.

Hawke TJ & Garry DJ. (2001). Myogenic satellite cells: physiology to molecular biology. *J Appl Physiol* **91,** 534-551.

Katz B. (1961). The termination of the afferent nerve fiber in the muscle spindle of the frog. *Philos Trans R Soc Lond B Biol Sci* **243,** 221-238.

Mauro A. (1961). Satellite cell of skeletal muscle fibers. *J Biophys Biochem Cytol* **9,** 493-494.

O'Connor RS & Pavlath GK. (2007). Point:Counterpoint: Satellite cell addition is/is not obligatory for skeletal muscle hypertrophy. *J Appl Physiol* **103,** 1099-1100.

Pette D. (1998). Training effects on the contractile apparatus. *Acta Physiol Scand* **162,** 367-376.

Pette D. (2001). Historical Perspectives: plasticity of mammalian skeletal muscle. *J Appl Physiol* **90,** 1119-1124.

Pette D & Staron RS. (1997). Mammalian skeletal muscle fiber type transitions. *Int Rev Cytol* **170,** 143-223.

Pette D & Staron RS. (2000). Myosin isoforms, muscle fiber types, and transitions. *Microsc Res Tech* **50,** 500-509.

Putman CT, Düsterhöft S & Pette D. (1999). Changes in satellite cell content and myosin isoforms in low-frequency- stimulated fast muscle of hypothyroid rat. *J Appl Physiol* **86,** 40-51.

Schultz E, Darr KC & Pette D. (1990). The role of satellite cells in adaptive or induced fiber transformations. In *The dynamic state of muscle fibers*, pp. 667-679. Walter de Gruyter, Berlin and New York.

Schultz E & McCormick KM. (1994). Skeletal muscle satellite cells. *Rev Physiol Biochem Pharmacol* **123,** 213-257.

CHAPTER TWO

LITERATURE REVIEW

2.1 ADULT SKELETAL MUSCLE

2.1.1 Diversity

Skeletal muscle is a heterogeneous tissue containing structurally, functionally and metabolically distinct fibre types (reviewed by Pette & Staron, 1997, 2000; Pette, 2002; Spangenburg & Booth, 2003). A summary of some of the characteristics of the current fibre type nomenclature is given in Table 2.1. Differences in MHC isoform content, metabolic enzyme activity levels and myonuclear domain sizes between the various skeletal muscle fibre types are highlighted in this section.

Table 2.1 Characteristics of skeletal muscle fibre types.

Classification scheme				
Myosin heavy chain	MHCI	MHCIIa	MHCIId(x)	MHCIIb
Fibre type	Type I	Type IIA	Type IID(X)	Type IIB
Contractile speed	Slow-twitch	Fast-twitch	Fast-twitch	Fast-twitch
Metabolic Profile	Oxidative	Oxidative-Glycolytic	Glycolytic	Glycolytic

Currently, the most accepted and widely used method of fibre type classification is performed according to MHC isoform content, which is an important myofibrillar protein because it dictates the rate of force development and the maximum shortening velocity of cross-bridge formation (Pette & Staron, 1997). MHC-based fibre types are classified as type I, IIA, IID(X) and IIB that contain the corresponding MHC isoforms listed in increasing order of shortening

velocity: MHCI, MHCIIa, MHCIId(x) and MHCIIb (Table 2.1) (Pette & Staron, 1997).

Metabolic profiles also differ between the different skeletal muscle fibre types (Table 2.1). Type I fibres primarily generate ATP, an intracellular energy transfer molecule, through mitochondrial pathways of aerobic substrate oxidation. Carbohydrate, fatty acid, keytone body and amino acid oxidation that involve the production of acetyl coenzyme A fuel this process. In the mitochondria, the citric acid cycle begins with the reaction between acetyl coenzyme A and oxalocateate to from citrate, which is catalysed by the "aerobic-oxidative" enzyme, citrate synthase (CS). Subsequently, the high-energy electrons produced by the citric acid cycle are passed down the electron-transport chain to electron acceptors such as oxygen. Part of the energy released during this process is used for ATP resynthesis via oxidative phosphorylation. Conversely, the type II fast-twitch skeletal muscle fibres generate most of their energy through the glycolytic pathway, which represents the initial reactions of glycogen and glucose catabolism. This process involves a series of enzymatic steps, in which, glyceraldehyde phosphate dehydrogenase (GAPDH) is involved.

In addition to distinct MHC isoforms and metabolic properties, skeletal muscle fibre types also contain varying myonuclear domain sizes. A myonuclear domain is the finite volume of cytoplasm surrounding and controlled by the gene products of a single myonucleus (Cheek, 1985; Hall & Ralston, 1989; Pavlath *et al.*, 1989; Allen *et al.*, 1999). Slow-twitch skeletal muscle fibres (i.e. type I) contain a larger number of myonuclei, smaller cross-sectional areas and cytoplasmic volume (Gibson & Schultz, 1982, 1983) and therefore, smaller myonuclear domain sizes compared with fast-twitch skeletal muscle fibres (i.e. type IIB) (Cheek, 1985; Schultz *et al.*, 1990; Tseng *et al.*, 1994; Roy *et al.*, 1999). Because slow-twitch skeletal muscle fibres are recruited first and therefore most often, the smaller myonuclear domain sizes of these fibres are presumably a

requirement of their higher biosynthetic activity levels and greater protein turnover compared with fast-twitch skeletal muscle fibres (Schultz *et al.*, 1990).

2.1.2 Plasticity

Skeletal muscle displays a great deal of plasticity or adaptability that is largely dictated by variations in motoneuron activity. The dominant influence of the motoneuron was demonstrated most clearly by nerve cross-union studies that showed the cross-reinnervation of a fast-twitch muscle with a slow-twitch nerve (or visa versa) resulted in a fast-to-slow transformation (or visa versa) (Buller et al., 1960). The resultant phenotypic changes following cross-reinnervation have been shown to be primarily due to the motoneuron-specific impulse patterns delivered to the muscle (Salmons & Verbová, 1969). During this transformation, it is not uncommon for a fibre to simultaneously express two or more different MHC isoforms (Pette & Staron, 1997; Pette, 2001). These "transitional" or "hybrid" fibres presumably reflect the dynamic remodeling state of a muscle undergoing adaptation to altered physiological demands (Pette & Staron, 1997; Putman et al., 2000; Pette, 2001). For example, skeletal muscle fast-to-slow transformation follows the "next nearest-neighbour" rule; according to this rule, hybrid fibre types bridge the gaps between the pure fibre types undergoing a predictable pattern of transformation as follows (with minor exceptions to certain pathological conditions): IIB→IID(X)/B→IID(X)→IIA/D(X)→IIA→I/IIA→I (Fig. 2.1) (reviewed by Pette & Staron, 1997, 2000; Pette, 2002). It should be noted that in response to certain altered physiological demands, hybrid fibres cans simultaneously express three or more MHC isoforms (Pette, 2002). Additional factors that also play important roles in both the maintenance and transformation of skeletal muscle fibres, but are beyond the scope of this literature review, include mechanical overload/unloading, hormones and ageing.

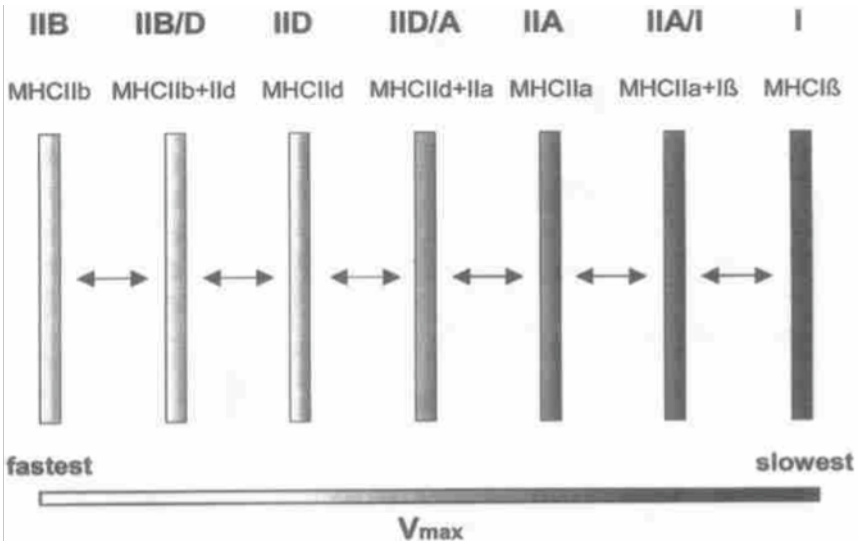

Figure 2.1 Schematic representation of reversible fibre type transformations in response to altered neuromuscular activity. With permission from Pette (2002).

2.1.2.1 Chronic Low-Frequency Stimulation

CLFS is an endurance exercise model that is ideal for studying the effects of enhanced neuromuscular activity on various structural, functional, metabolic and molecular properties of skeletal muscle in the absence of fibre injury in the rat (Simoneau & Pette, 1988; Delp & Pette, 1994; Putman *et al.*, 1999, 2000; Putman *et al.*, 2001). Figure 2.2 illustrates the CLFS model in rat and summarises CLFS-induced transformations. The sustained tonic pattern of motor nerve activity induced by CLFS mimics the electrical discharge pattern of slow motoneurons innervating slow-twitch muscles, but does not mimic voluntary muscle activation for two reasons (Pette & Vrbová, 1999; Ljubicic *et al.*, 2005). First, during voluntary contractions, motor units (a motoneuron and all the muscle fibres it innervates) are recruited in a strict hierarchical order according size, known as Henneman's Size Principle (Henneman *et al.*, 1981). Second, these motor units fire asynchronously and with different frequencies. Normally, the smallest motor units fire first followed by larger motor units when more force is needed. CLFS overrides both of these activation patterns by imposing the electrical discharge pattern of slow motoneurons as well as activating all motor units synchronously.

Despite the differences between normal and electrically induced skeletal muscle activity, CLFS has certain advantages. First, all motor units receive the same pattern of activity, thus providing a standardised regime. Second, since the targeted motor units are all recruited synchronously, the adaptive potential of skeletal muscle is maximally challenged. Specifically, the large motor units that are not normally recruited experience the greatest transformations in response to CLFS (Pette & Vrbová, 1999; Ljubicic *et al.*, 2005). Third, having CLFS restricted to the target muscle allows for comparison to an internal contralateral control muscle and minimal secondary systemic effects. Taken together, the standardised and highly reproducible conditions of CLFS allows for higher levels of activity-induced fast-to-slow transformations to occur in a well-defined shorter period of time compared with voluntary exercise (Pette, 2002; Ljubicic *et al.*, 2005).

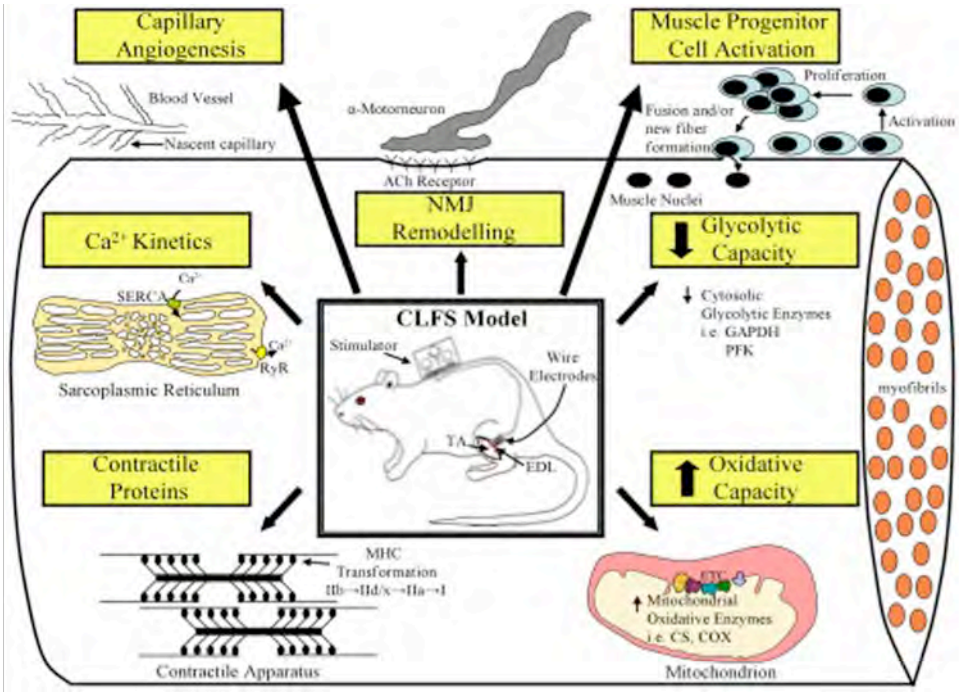

Figure 2.2 The CLFS model and a summary of the CLFS-induced adaptations. Ach=acetylcholine; Ca^{2+}=calcium; CLFS=chronic low-frequency stimulation; CS=citrate synthase; COX=cytochrome c oxidase; EDL=extensor digitorum longus; GAPDH=glyceraldehyde phosphate dehydrogenase; NMJ=neuromuscular junction; PFK= phosphofructokinase; TA=tibialis anterior. With permission from Ljubicic *et al.* (2005).

CLFS-induced fast-to-slow fibre type transformations occur in a specific time-dependent manner. Jaschinski *et al.* (1998) detected fast-to-slow MHC isoform transformations beginning at the mRNA level at 1 day after the onset of stimulation that rapidly continued to change through 10 days in rat fast-twitch skeletal muscle (Fig. 2.3*A*). Corresponding changes at the MHC protein level first occurred at 5 days of stimulation and were found to be most rapidly transforming by 10 days of CLFS (Fig. 2.3*B*). At 21 days of stimulation, 80-90% of fast-to-slow fibre type transformations have occurred (Fig. 2.3*A* and *B*). CLFS-induced metabolic energy adaptations also occur in a time-dependent and sequential manner as demonstrated by Simoneau & Pette (1988). They showed CLFS-induced time-dependent increases in CS (aerobic-oxidative pathway enzyme) and concomitant decreases in GAPDH (glycolytic pathway enzyme) in fast-twitch skeletal muscle across different species, including rat (Fig. 2.4; rat species denoted by the symbol x). This observed increase in mitochondrial enzyme production by CLFS is considered to be reflective of mitochondrial biogenesis. For example, linear correlations have been shown to exist between the increase in CS activity, total mitochondrial volume and aerobic-oxidative capacity (Reichmann *et al.*, 1985). Therefore, CLFS-induced reciprocal changes in enzyme activity patterns ultimately alter the metabolic profile of the muscle fibre type from glycolytic to predominantly aerobic-oxidative. CLFS-induced fast-to-slow fibre type transformations were also associated with increases in satellite cell activity, number and fusion to transforming fibres (Putman *et al.*, 1999). Interestingly, maximum satellite cell activity has been shown to occur between 5 and 10 days of CLFS in rat fast-twitch skeletal muscle, when fast-to-slow fibre type transformations are most readily transforming (Fig. 2.5).

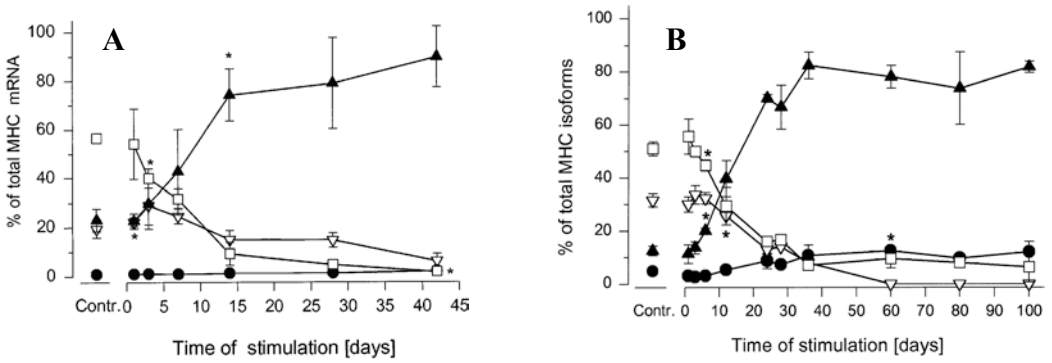

Figure 2.3 Changes in MHC mRNA (*A*) and protein isoforms (*B*) in extensor digitorum longus muscle of rat. MHCIIb (□), MHCIId/x (▽), MHCIIa (▲), and MHCI (●). Statistical symbol indicates: * first time point that was significantly different versus control. With permission from Jaschinski *et al.* (1998).

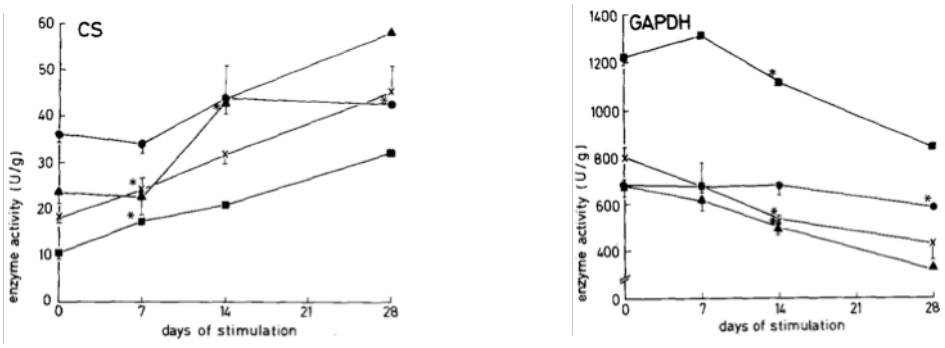

Figure 2.4 Changes in activities of CS and GAPDH in tibialis anterior muscles of mouse (●), rat (x), guinea pig (▲) and rabbit (■). Statistical symbol indicates: * first time point at which changes reach significance compared to zero time. With permission from Simoneau & Pette (1988).

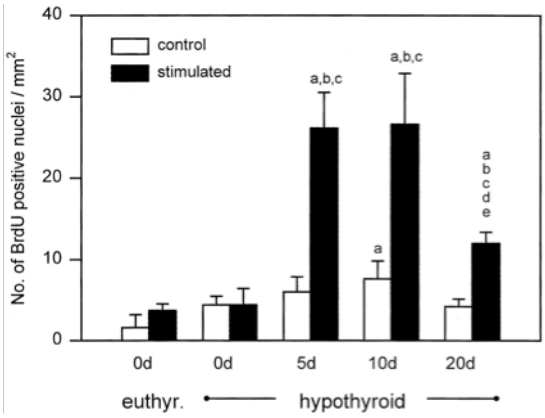

Figure 2.5 Number of previously or currently proliferating satellite cells in rat extensor digitorum longus muscles. Statistical symbols indicate difference from: [a] euthyroid (euthyr.), [b] hypothyroid, [c]contralateral controls, [d] 5d stimulated, and [e] 10d stimulated. With permission from Putman *et al.* (2000).

2.2 SATELLITE CELLS

2.2.1 Satellite Cell Function

As mentioned in Chapter 1, section 1.1, satellite cells are mononucleated muscle progenitor cells associated with all post-mitotic skeletal muscle fibres. The different roles that satellite cells play in skeletal muscle are discussed in this section.

2.2.1.1 Muscle Development

Skeletal muscle and satellite cell development are considered a synonymous process. Additionally, satellite cell regulation in adult skeletal muscle closely parallels the program manifested during myogenesis (Seale & Rudnicki, 2000). It is therefore essential to review the developmental process of skeletal muscle and satellite cells. Pownall *et al.* (2002) presents an excellent review of skeletal muscle development and the key role myogenic regulatory factors (MRFs; Myf5, MyoD, MRF4 and myogenin) play in this process. MRFs are a family of transcription factors that have been identified as key regulators of muscle cell specification and differentiation that possess the capacity to convert non-muscle cell types into muscle (Pownall *et al.*, 2002). Each of the MRFs has been shown to heterodimerize with the ubiquitous basic helix-loop-helix proteins. This protein structural motif binds to DNA at E-boxes (i.e. CANNTG) that are present in the promoter and enhancer regions of many skeletal muscle specific genes. Figure 2.6 illustrates the developmental process of the structures involved in embryonic skeletal muscle and satellite cell development from the presomitic paraxial mesoderm to the dermomyotome.

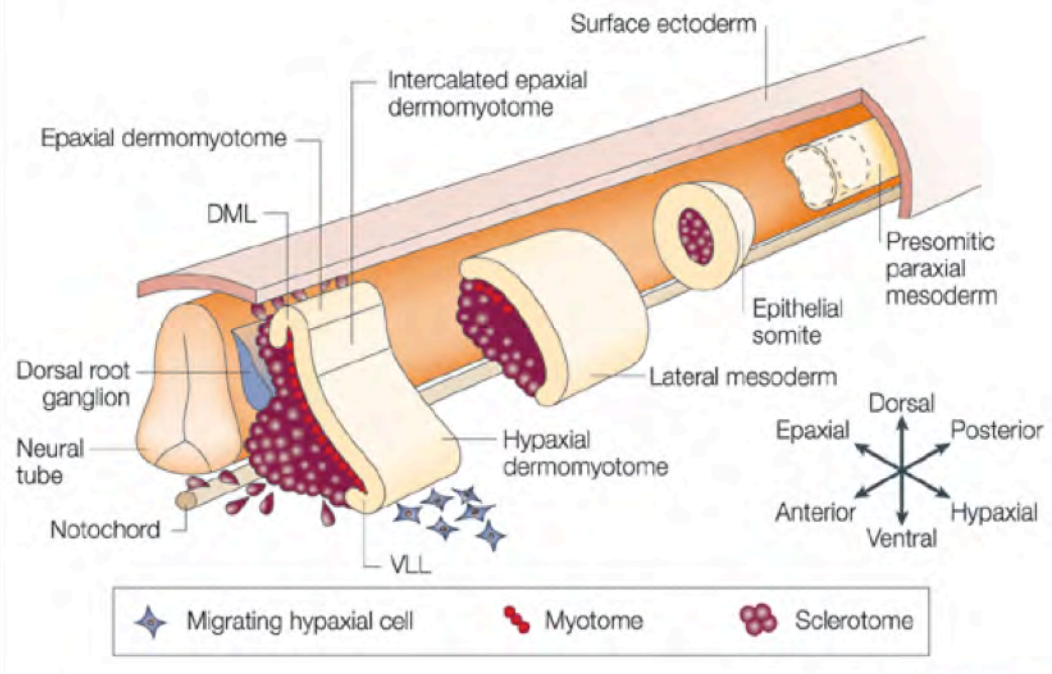

Figure 2.6 Embryonic origins of skeletal muscle and satellite cells. DML=dorsal medial lip; VLL=ventral lateral lip. With permission from Parker *et al.* (2003).

Embryonic myogenesis begins in newly formed, transitory structures, termed somites that rapidly give rise to the sclerotome and dermomyotome, from which muscle and satellite cell precursors originate (Pownall *et al.*, 2002). These precursors are characterized by their expression of the paired-box transcription factors (Pax)3 and Pax7. Pax3 has been shown to be involved in the delamination and subsequent migration of embryonic myogenic progenitor cells (Parker *et al.*, 2003), while Pax7 appears to be essential for satellite cell specification, survival and self-renewal (Kuang *et al.*, 2007). Upon migration to the primary myotome and sites of skeletal muscle limb formation, these transcription factors decline and MRFs are up-regulated, which further enforce commitment to the myogenic lineage (Cossu *et al.*, 1996; Parry, 2001; Pownall *et al.*, 2002; Chargé & Rudnicki, 2004). The dermomyotome, however, is a transient structure that can only produce a limited number of muscle progenitor cells, which are not capable of supporting continued skeletal muscle growth during the late embryonic and fetal stages of development.

Recently, a distinct population of cells has been identified that is vital for the continued development of skeletal muscle (Gros *et al.*, 2005; Kassar-Duchossoy *et al.*, 2005; Relaix *et al.*, 2005). These satellite cell precursor cells originate in the central region of the dermomyotome, express both Pax3 and Pax7 and continue to proliferate during embryonic and fetal myogenesis (Gros *et al.*, 2005; Kassar-Duchossoy *et al.*, 2005; Relaix *et al.*, 2005). Subsequently, they either i) become committed myogenic progenitor cells by up-regulating MRFs, fuse with existing primary or secondary myofibres and contribute myonuclei or ii) take up residence in the satellite cell niche of these myofibres and maintain expression of Pax7 and for the most part, down-regulate Pax3 (Gros *et al.*, 2005; Relaix *et al.*, 2005; Kuang *et al.*, 2007). These results suggest that satellite cell precursor cells maintain muscle growth during late embryonic and fetal development (Gros *et al.*, 2005; Relaix *et al.*, 2005; Kuang *et al.*, 2007).

2.2.1.2 Stem Cells

Stem cells are defined by their ability to generate differentiated progeny and undergo self-renewal. In response to a number of stimuli, satellite cells become active and proliferate, thus generating a pool of muscle progenitor cells. Subsequently, about 80% of these cells terminally differentiate and contribute myonuclei, while the other 20% repopulate the satellite cell niche and become quiescent, thus representing the self-renewing potential of satellite cells (Schultz & McCormick, 1994; Schultz, 1996; Rouger *et al.*, 2004; Zammit *et al.*, 2004; Collins *et al.*, 2005; Mitchell *et al.*, 2005). Additionally, satellite cells can also give rise to non-myogenic cells such as osteoblasts and adipocytes (Shefer *et al.*, 2004). Because of their ability to generate differentiated progeny and undergo self-renewal, satellite cells have recently been accepted as a stem cell population (reviewed by Collins *et al.*, 2005; Holterman & Rudnicki, 2005; Zammit *et al.*, 2006).

A number of models have been proposed to explain the underlying mechanisms controlling the ability of satellite cells to generate both differentiated

skeletal muscle progeny and to self-renew (reviewed by Dhawan & Rando, 2005; Holterman & Rudnicki, 2005; Scime & Rudnicki, 2006). Two of these models include asymmetric cell division (Fig. 2.7*a*) and the differential expression of MRFs (Fig. 2.7*b*), which are not considered to be mutually exclusive.

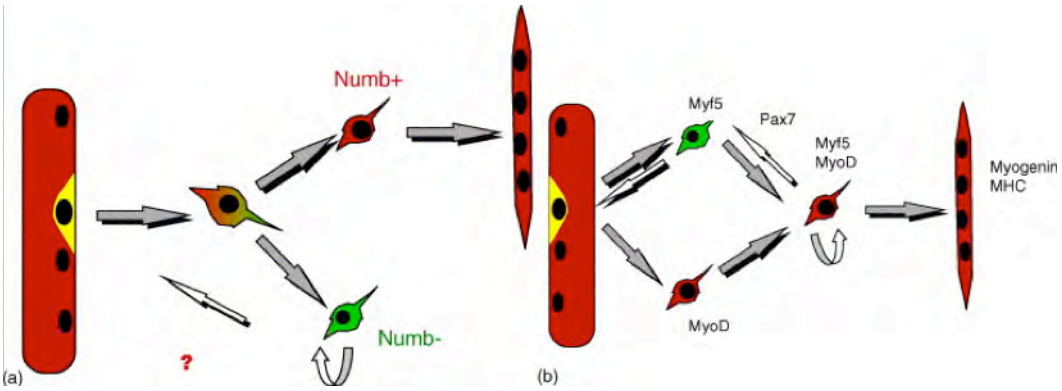

Figure 2.7 Models of satellite cell self-renewal: asymmetric cell division (*a*) and differential expression of the myogenic regulatory factors (*b*). With permission from Holterman & Rudnicki (2005).

The asymmetric cell division model (Fig. 2.7*a*) involves the production of two daughter cells, which differentially express Numb. Upon activation, satellite cells express Notch, which inhibits myogenic differentiation and therefore supports the proliferative state. One of the daughter cells, however, subsequently up-regulates the Notch inhibitor, Numb (i.e. Numb+) and progresses through the myogenic pathway becoming a myonucleus. The daughter cell that expresses low or absent levels of Numb (i.e. Numb-) returns to quiescence and repopulates the satellite cell niche. The differential expression of MRFs model (Fig. 2.7*b*) is considered to parallel events of embryonic myogenesis. In this model, satellite cell progeny first express Myf5 or MyoD followed by their co-expression during the proliferative state. MyoD is considered necessary for the progression to terminal differentiation while Myf5 seems necessary for proliferation. Subsequently, a few daughter cells down-regulate MyoD and return to the quiescent state, whereas most daughter cells maintain MyoD expression and go on

to terminally differentiate by up-regulating MRF4 and myogenin and contribute myonuclei.

2.2.1.3 Muscle Regeneration

In response to muscle injury, numerous lines of evidence have shown that muscle regeneration requires satellite cell activity. Specifically, the obligatory role that satellite cells play in muscle regeneration was clearly established using selective irradiation (model to be discussed in section 2.2.1.4.1) to ablate satellite cells in damaged skeletal muscle (Robertson et al., 1992). An excellent review by Chargé & Rudnicki (2004) details the regulation of skeletal muscle regeneration and the role that satellite cells play in this process. Briefly, in response to damage, satellite cells re-enter the cell cycle and contribute myonuclei in order to repair injured fibres or in the case of extensive muscle damage where fibres have actually been destroyed, satellite cells can also initiate the de novo formation of skeletal muscle fibres by fusing with each other (Fig. 2.8). As well, a portion of activated satellite cells return to quiescence in order to repopulate the satellite cell pool.

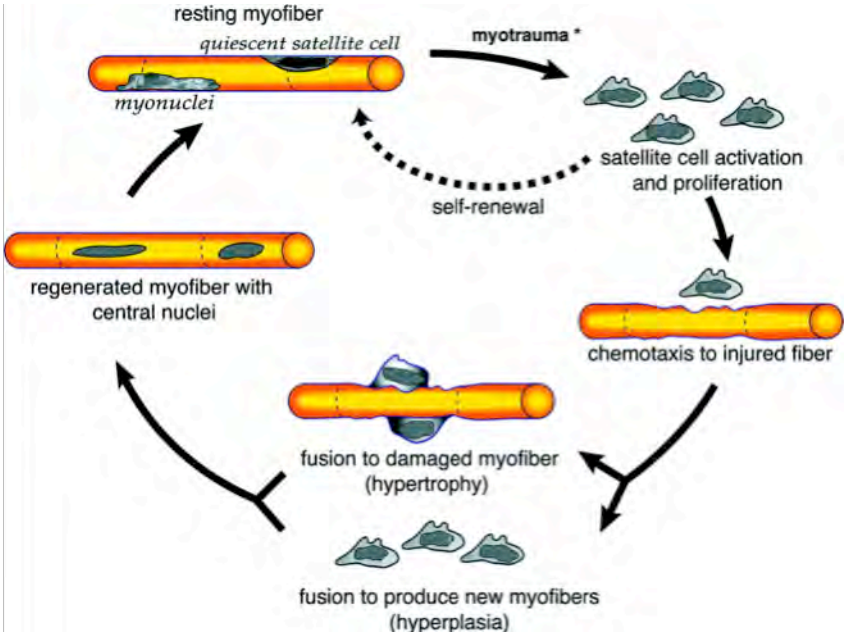

Figure 2.8 Satellite cell response to skeletal muscle damage. With permission from Hawke & Garry (2001).

2.2.1.4 Muscle Hypertrophy

Skeletal muscle hypertrophy is defined by an increase in cell size resulting from increased myofibrillar protein content and mass (O'Connor & Pavlath, 2007) that occurs in response to muscle growth and overload. In both cases, satellite cells are responsible for providing the additional myonuclei to enlarging fibres in order to maintain a relatively constant myonuclear domain size (Fig. 2.9) (reviewed by Schultz, 1989; Adams, 2006; O'Connor & Pavlath, 2007). The involvement of satellite cells in growing post-natal skeletal muscle has been the focus of numerous studies. For example, Moss & Leblond (1970) were the first to document how post-mitotic muscle fibres gained myonuclei during growth by showing that after a single [^{3}H]-thymidine injection only proliferating satellite cell nuclei were labeled and that these cells then fused with muscle fibres, thereby contributing myonuclei. In support of this observation, ablation of satellite cell activity by γ-irradiation or hindlimb suspension in the muscles of young and rapidly growing rodents resulted in negligible hypertrophy (Darr & Schultz, 1989; Barton-Davis *et al.*, 1999).

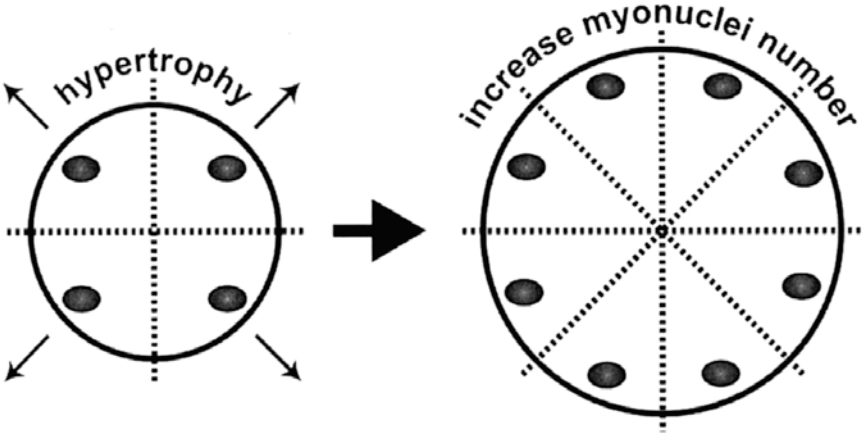

Figure 2.9 Satellite cell contribution of myonuclei to hypertrophying skeletal muscle fibres. Note that the cross-sectional area within each of the triangles (i.e. myonuclear domain) of the myofibres is similar in size. With permission from Hawke (2005).

A number of studies have also investigated the involvement of satellite cells in adult skeletal muscle hypertrophy due to functional overload. The removal of synergist muscles (i.e. synergist ablation) has long been used as a model of functional overload that results in hypertrophy as well as fast-to-slow fibre type transformations (Rosenblatt & Parry, 1992, 1993; Adams *et al.*, 2002). The most conclusive evidence that satellite cells play an obligatory role in overload-induced hypertrophy comes from studies where γ-irradiation was applied to rodent hindlimbs, which were subsequently overloaded by synergist ablation (Rosenblatt & Parry, 1992, 1993; Adams *et al.*, 2002) or voluntary wheel running (Li *et al.*, 2006). Results uniformly indicate that ionising radiation suppresses or prevents all of the hypertrophy normally seen in these overload models. Collectively, these studies show that satellite cell activity is required for skeletal muscle hypertrophy. It is important to note, however, that small increases in myofibre cross-sectional area and cytoplasmic volume can be supported by existing myonuclei up to a certain threshold, or myonuclear domain "ceiling", above which myonuclear accretion from satellite cells is required to support continued hypertrophy (Kadi *et al.*, 2004; Petrella *et al.*, 2006; O'Connor & Pavlath, 2007).

2.2.1.4.1 Gamma Irradiation

The structure of DNA contains two strands, each of which has a "back-bone" of alternating phosphate and sugar groups with attached bases. The two strands are connected by hydrogen bonds between the paired bases, adenine with thymine and guanine with cytosine. DNA exposed to low levels of ionising radiation such as γ-irradiation can produce three major types of damage: single and double strand breaks and base damage (Coggle, 1983). After exposure to γ-irradiation, post-mitotic myonuclei are able to quickly repair their damaged DNA and maintain normal cellular functions (Wheldon *et al.*, 1982; Mozdziak *et al.*, 1996; Phelan & Gonyea, 1997). DNA possesses an amazing ability to repair itself, mostly due to the double-helical structure that allows for the complementary undamaged strand to serve as a template in repairing the other,

which is enzymatically controlled. The detailed mechanisms of repair are, however, beyond the scope of this literature review, but an excellent multi-author review titled, "DNA Repair in Mammalian Cells" (Nouspikel, 2009b) discusses a number of DNA repair processes in depth, including direct damage reversal (Eker *et al.*, 2009), base excision repair (Robertson *et al.*, 2009), nucleotide excision repair (Nouspikel, 2009a; Tornaletti, 2009), mismatch repair (Kunz *et al.*, 2009) and single- and double-strand break repair (Pardo *et al.*, 2009).

On the other hand, when irradiated and thus damaged mitotic cells such as satellite cells attempt to divide, mitotic failure (Wakeford *et al.*, 1991) and apoptosis (Wheldon *et al.*, 1982) ensue. Single doses of ionising radiation ranging from 16 to 30 Gy (Wheldon *et al.*, 1982; Gulati, 1987; Mozdziak *et al.*, 1996; Phelan & Gonyea, 1997; Heslop *et al.*, 2000; Adams *et al.*, 2002) and up to 60 Gy (Lewis, 1954) have been used to ablate satellite cell activity while maintaining normal skeletal muscle fibre morphology and function. The collective results of these studies, however, indicate that the success of these doses to ablate satellite cell activity is dependent on the amount of ionising radiation administered, on the nature and severity of physiological stimuli leading to satellite cell activation, and on the species investigated.

Although most satellite cells seem to be ablated after a single 20 to 30 Gy dose of ionising radiation, it has been noted that a single 25 Gy dose of γ-irradiation disrupts mitotic activity of avian satellite cells in vivo for only 7 days (Mozdziak *et al.*, 1996), with significant recovery occurring between 9 and 12 days post-irradiation (Wakeford *et al.*, 1991; McGeachie *et al.*, 1993; Mozdziak *et al.*, 1996). In support of these observations, studies utilising a rat model reported a significant increase in myotube formation 7 days after a single 20 Gy dose of ionising radiation (Gulati, 1987), and greater skeletal muscle DNA content 15 days after a single 25 Gy dose of ionising radiation (Adams *et al.*, 2002). The reason for the apparent radiation resistance of some satellite cells may include the capacity to undergo at least one mitotic division before cell death (Coggle, 1983;

McGeachie *et al.*, 1993; Mozdziak *et al.*, 1996), the ability to recover and thus remain fusion-competent, and/or differentiated satellite cell progeny, which are past the radiosensitive phase, may fuse directly to existing fibres (Wakeford *et al.*, 1991; Robertson *et al.*, 1992; McGeachie *et al.*, 1993; Mozdziak *et al.*, 1996, 1997; Adams *et al.*, 2002).

2.2.1.5 Fast-to-Slow Fibre Type Transformations

Consistent with the uneven myonuclear distribution between the different fibre types, as mentioned in section 2.1.1, slow-twitch skeletal muscle fibres also contain a larger number of satellite cells compared with fast-twitch fibres (Gibson & Schultz, 1982, 1983). Additionally, satellite cells become active in response to a number of stimuli including exercise-induced fast-to-slow fibre type transformations (Putman *et al.*, 1999). Based on these observations, satellite cell-derived myonuclear addition may be a prerequisite for exercise-induced skeletal muscle fast-to-slow fibre type transformations or be involved in the maintenance of the transformed state (Schultz *et al.*, 1990).

To date, there have been a limited number of studies that have directly investigated the involvement of satellite cells in exercise-induced fast-to-slow fibre type transformations (Rosenblatt & Parry, 1992, 1993; Adams *et al.*, 2002; Li *et al.*, 2006). Collectively, these studies reported no attenuation of fast-to-slow fibre type transformations in response to functional overload (Rosenblatt & Parry, 1992, 1993; Adams *et al.*, 2002) or voluntary wheel running (Li *et al.*, 2006) in muscles that were also exposed to ionising radiation. Unfortunately, these studies were not without their shortcomings. First, only a single 25 Gy dose of ionising radiation was administered before the onset of exercise. Consequently, a significant amount of satellite cell proliferation was observed in response to 14 days of voluntary wheel running in mouse plantaris muscles (Li *et al.*, 2006) and greater skeletal muscle DNA content was reported after 15 days of functional overload in rat plantaris muscles (Adams *et al.*, 2002). Secondly, only Li *et al.* (2006) directly measured proliferating and previously proliferating satellite cells

in vivo by DNA labeling with 5-bromo-2′-deoxyuridine (BrdU), while Adams *et al.* (2002) measured DNA content and Rosenblatt & Parry reported myonuclear-to-myoplasmic volume ratio (1993) or assumed ablation of satellite cell activity (1992). Thirdly, fast-to-slow fibre type transformations were assessed by measuring only MHC protein isoforms (Adams *et al.*, 2002; Li *et al.*, 2006), or just the four adult pure fibre types (Rosenblatt & Parry, 1992, 1993), which does not allow the detection of hybrid fibre types, whose appearance is a hallmark indication of skeletal muscle undergoing transformation (Pette & Staron, 1997; Putman *et al.*, 2000; Pette, 2001). Lastly, synergist ablation overload models are considered to be only modest fast-to-slow fibre type transformational stimuli (Pette & Staron, 1997). Based on the limitations of these studies, the question still remains as to the involvement of satellite cells in fast-to-slow fibre type transformations.

2.2.2 Satellite Cell Activation

The signaling mechanism(s) involved in exercise-induced activation of satellite cells in the absence of fibre damage have yet to be investigated. To date, HGF is the only confirmed growth factor that provides a signal that can activate quiescent satellite cells (Allen *et al.*, 1995; Tatsumi *et al.*, 1998), and it is located downstream of NO (Fig. 2.10, pathway A). The NO-dependent satellite cell activation pathway will be discussed in this section as well as its potential involvement in CLFS-induced satellite cell activation. The possibility of NO-independent satellite cell activation will also be reviewed (Fig. 2.10, pathway B).

2.2.2.1 Nitric Oxide

NO is a gaseous short-lived ubiquitous signaling molecule that is controlled at the synthesis level by NOS, which converts L-arginine and molecular oxygen to L-citrulline and NO. Since NOS synthesises NO, which can only diffuse short distances, the localisation of NOS must be spatially associated with its downstream targets.

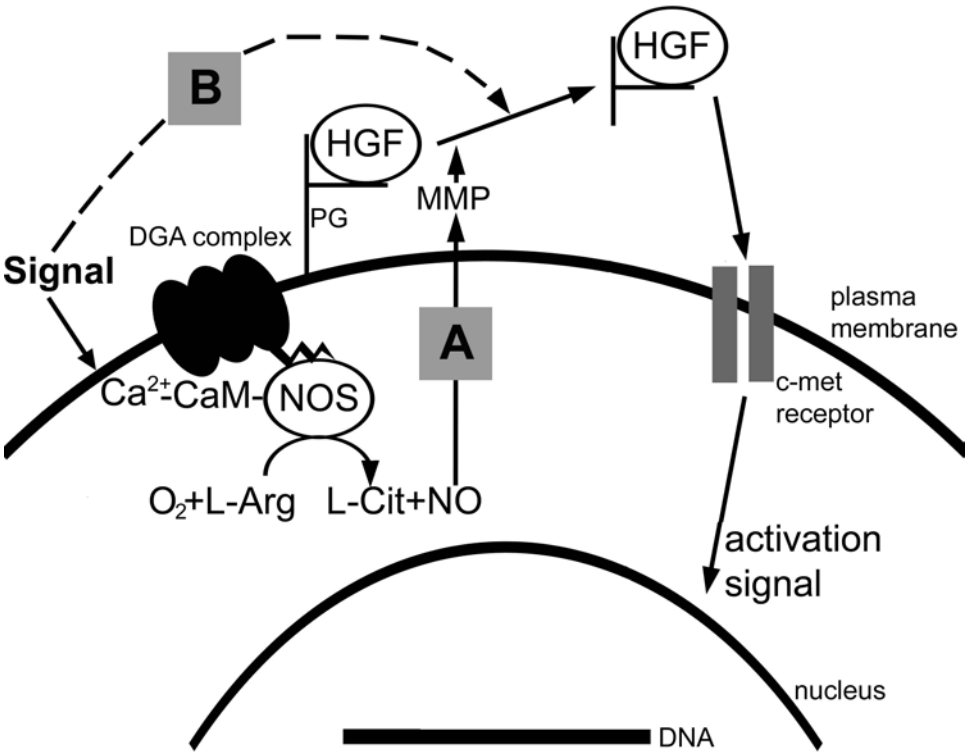

Figure 2.10 Proposed signaling cascade for satellite cell activation. Ca^{2+}-CaM=calcium-calmodulin complex; DGA=dystrophin-glycogen associated; HGF=hepatocyte growth factor protein (active form); L-Arg=L-arginine; L-Cit=L-citruline; MMP=matrix metalloproteinase; NO=nitric oxide; NOS=nitric oxide synthase; PG=proteoglycans; straight arrows=NO-dependent satellite cell activation pathway (A); dashed arrows=potential NO-independent activation pathways (B).

Skeletal muscle expresses three NOS isoforms: endothelial (e)NOS is specifically associated with mitochondria, inducible (i)NOS is pathologically expressed and neuronal (n)NOS is the most abundant NOS isoform in skeletal muscle (Stamler & Meissner, 2001). nNOS is anchored to the sarcolemma via the dystrophin-glycoprotein complex (Kobzik *et al.*, 1995; Stamler & Meissner, 2001) and is primarily regulated by intracellular calcium (Ca^{2+}) through calmodulin binding (Bredt, 2003). In addition to increasing in response to shear damage, stretch and overload, nNOS activity and NO production have been shown to increase in response to a variety of electrical stimulation protocols (i.e. 2 Hz/min, 25 Hz/60 min, 100 Hz/5min and 10 Hz/3 weeks) that include CLFS (Stamler & Meissner, 2001).

2.2.2.2 Hepatocyte Growth Factor

HGF is localised in the extracellular matrix of uninjured skeletal muscle fibres (Tatsumi *et al.*, 1998), where it may associate with glycosaminoglycan chains of proteoglycans. Specifically, the inactive form of HGF (90 kDa single chain) is first synthesized in the cytosol and then exported to the extracellular matrix where specific proteases such as urokinase and tissue-type plasminogen activator, cleave it into heterodimers (60 kDa α-chain and 30 kDa β-chain) held together by a disulfide bond (Tatsumi & Allen, 2004).

2.2.2.3 Nitric Oxide-Dependent Satellite Cell Activation

The role of NO and HGF as positive regulators of satellite cell activation has been demonstrated by a variety of investigative approaches that include in vitro, in vivo and cultured single fibres that retain their resident satellite cells in a quiescent state. Bischoff (1986) first showed that satellite cells on single fibres became activated when exposed to crushed muscle extract. It was later shown that HGF contained within the crushed muscle extract, and specifically its colocalisation with the satellite cell c-met receptor, was the mechanism responsible for activation (Tatsumi *et al.*, 1998). NO was first implicated in HGF-mediated satellite cell activation by Anderson (2000) who showed that treatment with L-NAME just prior to crush injury prevented both the colocalisation of HGF with c-met, as well as immediate satellite cell activation in vivo. Subsequent NO inhibition studies support this observation (Anderson & Pilipowicz, 2002; Tatsumi *et al.*, 2002; Sakata *et al.*, 2006; Tatsumi *et al.*, 2006). Additionally, satellite cell activation can be augmented in response to supplemental NO administration (Anderson & Pilipowicz, 2002; Tatsumi *et al.*, 2002; Betters *et al.*, 2008a; Betters *et al.*, 2008b). Collectively, these studies show that NO is released upstream of HGF and influences HGF-mediated satellite cell activation (Fig. 2.10, pathway A). Recently, Tatsumi & Allen (2008) elaborated on the NO-dependent satellite cell activation pathway, suggesting that NO may activate HGF release from its tethering in the extracellular matrix by stimulating matrix metalloproteinase (MMP)-2. MMPs are a large family of

endopeptidases that collectively degrade one or several extracellular matrix constituents including collagens, elastin, fibronectin, laminin and proteoglycans (reviewed by Haas, 2005). Once active, MMP-2 appears to liberate HGF with its associated extracellular segment of proteoglycan that is subsequently presented to the satellite cell c-met receptor, generating a signal for activation (Yamada *et al.*, 2008). Interestingly, Haas *et al.* (2000) found that both MMP-2 mRNA and the active 62 kDa form of the protein increased significantly in response to CLFS.

2.2.2.4 Nitric Oxide-Independent Satellite Cell Activation

It has been proposed that signaling mechanisms involved in satellite cell activation may also function in a NO-independent pathway (Fig. 2.10, pathway B) (Wozniak *et al.*, 2005). This idea was originally supported by results from $nNOS^{-/-}$ mice that showed only delayed satellite cell activation after muscle injury and were capable of full regeneration (Anderson, 2000). The possibility of alternative NO production sources from eNOS and/or iNOS, however, could not be ruled out. On the other hand, Sellman *et al*. (2006) and Gordon *et al.* (2007) found that satellite cell activity and subsequent myonuclear addition, respectively, in 7-12 day overloaded plantaris muscles of rats that received L-NAME were similar to control overloaded muscles. Additionally, stretch-induced increases in satellite cell activity have been observed as early as 2 days after hindlimb suspension in rats treated with L-NAME (Tatsumi *et al.*, 2006). Collectively, these results indicate that both NO-dependent and NO-independent mechanisms may play a role in satellite cell activation.

2.3 REFERENCES

Adams GR. (2006). Satellite cell proliferation and skeletal muscle hypertrophy. *Appl Physiol Nutr Metab* **31,** 782-790.

Adams GR, Caiozzo VJ, Haddad F & Baldwin KM. (2002). Cellular and molecular responses to increased skeletal muscle loading after irradiation. *Am J Physiol Cell Physiol* **283,** C1182-C1195.

Allen DL, Roy RR & Edgerton VR. (1999). Myonuclear domains in muscle adaptation and disease. *Muscle Nerve* **22,** 1350-1360.

Allen RE, Sheehan SM, Taylor RG, Kendall TL & Rice GM. (1995). Hepatocyte growth factor activates quiescent skeletal muscle satellite cells in vitro. *J Cell Physiol* **165,** 307-312.

Anderson J & Pilipowicz O. (2002). Activation of muscle satellite cells in single-fiber cultures. *Nitric Oxide* **7,** 36-41.

Anderson JE. (2000). A role for nitric oxide in muscle repair: nitric oxide-mediated activation of muscle satellite cells. *Mol Biol Cell* **11,** 1859-1874.

Barton-Davis ER, Shoturma DI & Sweeney HL. (1999). Contribution of satellite cells to IGF-I induced hypertrophy of skeletal muscle. *Acta Physiol Scand* **167,** 301-305.

Betters JL, Lira VA, Soltow QA, Drenning JA & Criswell DS. (2008a). Supplemental nitric oxide augments satellite cell activity on cultured myofibers from aged mice. *Exp Gerontol* **43,** 1094-1101.

Betters JL, Long JH, Howe KS, Braith RW, Soltow QA, Lira VA & Criswell DS. (2008b). Nitric oxide reverses prednisolone-induced inactivation of muscle satellite cells. *Muscle Nerve* **37,** 203-209.

Bischoff R. (1986). A satellite mitogen from crushed adult muscle. *Dev Biol* **115,** 140-147.

Bredt DS. (2003). Nitric oxide signaling specificity--the heart of the problem. *J Cell Sci* **116,** 9-15.

Buller AJ, Eccles JC & Eccles RM. (1960). Interactions between motoneurones and muscles in respect of the characteristic speeds of their responses. *J Physiol* **150,** 417-439.

Chargé SB & Rudnicki MA. (2004). Cellular and molecular regulation of muscle regeneration. *Physiol Rev* **84,** 209-238.

Cheek DB. (1985). The control of cell mass and replication. The DNA unit--a personal 20-year study. *Early Hum Dev* **12,** 211-239.
Coggle JE. (1983). *Biological effects of radiation*. Taylor and Francis, London.

Collins CA, Olsen I, Zammit PS, Heslop L, Petrie A, Partridge TA & Morgan JE. (2005). Stem cell function, self-renewal, and behavioral heterogeneity of cells from the adult muscle satellite cell niche. *Cell* **122,** 289-301.

Cossu G, Tajbakhsh S & Buckingham JA. (1996). How is myogenesis initiated in the embryo? *Trends Genet* **12** 218-223.

Darr KC & Schultz E. (1989). Hindlimb suspension suppresses muscle growth and satellite cell proliferation. *J Appl Physiol* **67,** 1827-1834.

Delp MD & Pette D. (1994). Morphological changes during fiber type transitions in low-frequency- stimulated rat fast-twitch muscle. *Cell Tissue Res* **277,** 363-371.

Dhawan J & Rando TA. (2005). Stem cells in postnatal myogenesis: molecular mechanisms of satellite cell quiescence, activation and replenishment. *Trends Cell Biol* **15,** 666-673.

Eker AP, Quayle C, Chaves I & van der Horst GT. (2009). DNA repair in mammalian cells: Direct DNA damage reversal: elegant solutions for nasty problems. *Cell Mol Life Sci* **66,** 968-980.

Gibson MC & Schultz E. (1982). The distribution of satellite cells and their relationship to specific fiber types in soleus and extensor digitorum longus muscles. *Anat Rec* **202,** 329-337.

Gibson MC & Schultz E. (1983). Age-related differences in absolute numbers of skeletal muscle satellite cells. *Muscle Nerve* **6,** 574-580.

Gordon SE, Westerkamp CM, Savage KJ, Hickner RC, George SC, Fick CA & McCormick KM. (2007). Basal, but not overload-induced, myonuclear addition is attenuated by NG-nitro-L-arginine methyl ester (L-NAME) administration. *Can J Physiol Pharmacol* **85,** 646-651.

Gros J, Manceau M, Thome V & Marcelle C. (2005). A common somitic origin for embryonic musle progenitors and satellite cells. *Nature* **435,** 954-958.

Gulati AK. (1987). The effect of X-irradiation on skeletal muscle regeneration in the adult rat. *J Neurol Sci* **78,** 111-120.

Haas TL. (2005). Endothelial cell regulation of matrix metalloproteinases. *Can J Physiol Pharmacol* **83,** 1-7.

Haas TL, Milkiewicz M, Davis SJ, Zhou AL, Egginton S, Brown MD, Madri JA & Hudlicka O. (2000). Matrix metalloproteinase activity is required for activity-induced angiogenesis in rat skeletal muscle. *Am J Physiol Heart Circ Physiol* **279,** H1540-1547.

Hall ZW & Ralston E. (1989). Nuclear domains in muscle cells. *Cell* **59,** 771-772.

Hawke TJ. (2005). Muscle stem cells and exercise training. *Exerc Sport Sci Rev* **33,** 63-68.

Hawke TJ & Garry DJ. (2001). Myogenic satellite cells: physiology to molecular biology. *J Appl Physiol* **91,** 534-551.

Henneman E & Mendell LM. (1981). Functional organization of the motoneurone pool and its inputs. In *Handbook of physiology Sect. I Vol. II. The nervous system: motor control Part I*, ed. Brooks VB, pp. 345-442. American Physiology Society, Washington, D.C., USA.

Heslop L, Morgan JE & Partridge TA. (2000). Evidence for a myogenic stem cell that is exhausted in dystrophic muscle. *J Cell Sci* **113** (Pt 12), 2299-2308.

Holterman CE & Rudnicki MA. (2005). Molecular regulation of satellite cell function. *Semin Cell Dev Biol* **16,** 575-584.

Jaschinski F, Schuler MJ, Peuker H & Pette D. (1998). Changes in myosin heavy chain mRNA and protein isoforms of rat muscle during forced contractile activity. *Am J Physiol Cell Physiol* **274,** C365-C370.

Kadi F, Schjerling P, Andersen LL, Charifi N, Madsen JL, Christensen LR & Andersen JL. (2004). The effects of heavy resistance training and detraining on satellite cells in human skeletal muscles. *J Physiol* **558,** 1005-1012.

Kassar-Duchossoy L, Giacone E, Gayraud-Morel B, Jory A, Gomes D & Tajbakhsh S. (2005). Pax3/Pax7 mark a novel population of primitive myogenic cells during development. *Genes Dev* **19,** 1426-1431.

Kobzik L, Stringer B, Balligand JL, Reid MB & Stamler JS. (1995). Endothelial type nitric oxide synthase in skeletal muscle fibers: mitochondrial relationships. *Biochem Biophys Res Commun* **211,** 375-381.

Kuang S, Kuroda K, Le Grand F & Rudnicki MA. (2007). Asymmetric self-renewal and commitment of satellite stem cells in muscle. *Cell* **129,** 999-1010.

Kunz C, Saito Y & Schar P. (2009). DNA repair in mammalian cells: Mismatched repair: variations on a theme. *Cell Mol Life Sci* **66,** 1021-1038.

Lewis RB. (1954). Changes in striated muscle following single intense doses of X-rays. *Lab Invest* **3,** 48-55.

Li P, Akimoto T, Zhang M, Williams RS & Yan Z. (2006). Resident stem cells are not required for exercise-induced fiber-type switching and angiogenesis but are necessary for activity-dependent muscle growth. *Am J Physiol Cell Physiol* **290,** C1461-C1468.

Ljubicic V, Adhihetty PJ & Hood DA. (2005). Application of animal models: chronic electrical stimulation-induced contractile activity. *Can J Appl Physiol* **30,** 625-643.

McGeachie JK, Grounds MD, Partridge TA & Morgan JE. (1993). Age-related changes in replication of myogenic cells in mdx mice: quantitative autoradiographic studies. *J Neurol Sci* **119,** 169-179.

Mitchell PO, Mills T, O'Connor RS, Graubert T, Dzierzak E & Pavlath GK. (2005). Sca-1 negatively regulates proliferation and differentiation of muscle cells. *Dev Biol* **283,** 240-252.

Moss FP & Leblond CP. (1970). Nature of dividing nuclei in skeletal muscle of growing rats. *J Cell Biol* **44,** 459-462.

Mozdziak PE, Schultz E & Cassens RG. (1996). The effect of in vivo and in vitro irradiation (25 Gy) on the subsequent in vitro growth of satellite cells. *Cell Tissue Res* **283,** 203-208.

Mozdziak PE, Schultz E & Cassens RG. (1997). Myonuclear accretion is a major determinant of avian skeletal muscle growth. *Am J Physiol* **272,** C565-C571.

Nouspikel T. (2009a). DNA repair in mammalian cells : Nucleotide excision repair: variations on versatility. *Cell Mol Life Sci* **66,** 994-1009.

Nouspikel T. (2009b). DNA repair in mammalian cells: So DNA repair really is that important? *Cell Mol Life Sci* **66,** 965-967.

O'Connor RS & Pavlath GK. (2007). Point:Counterpoint: Satellite cell addition is/is not obligatory for skeletal muscle hypertrophy. *J Appl Physiol* **103,** 1099-1100.

Pardo B, Gomez-Gonzalez B & Aguilera A. (2009). DNA repair in mammalian cells: DNA double-strand break repair: how to fix a broken relationship. *Cell Mol Life Sci* **66,** 1039-1056.

Parker MH, Seale P & Rudnicki MA. (2003). Looking back to the embryo: defining transcriptional networks in adult myogenesis. *Nat Rev Genet* **4,** 497-507.

Parry DJ. (2001). Myosin heavy chain expression and plasticity: role of myoblast diversity. *Exerc Sport Sci Rev* **29,** 175-179.

Pavlath GK, Rich K, Webster SG & Blau HM. (1989). Localization of muscle gene products in nuclear domains. *Nature* **337,** 570-573.

Petrella JK, Kim JS, Cross JM, Kosek DJ & Bamman MM. (2006). Efficacy of myonuclear addition may explain differential myofiber growth among resistance-trained young and older men and women. *Am J Physiol Endocrinol Metab* **291,** E937-E946.

Pette D. (2001). Historical Perspectives: plasticity of mammalian skeletal muscle. *J Appl Physiol* **90,** 1119-1124.

Pette D. (2002). The adaptive potential of skeletal muscle fibers. *Can J Appl Physiol* **27,** 423-448.

Pette D & Staron RS. (1997). Mammalian skeletal muscle fiber type transitions. *Int Rev Cytol* **170,** 143-223.

Pette D & Staron RS. (2000). Myosin isoforms, muscle fiber types, and transitions. *Microsc Res Tech* **50,** 500-509.

Pette D & Vrbová G. (1999). What does chronic electrical stimulation teach us about muscle plasticity? *Muscle Nerve* **22,** 666-677.

Phelan JN & Gonyea WJ. (1997). Effect of radiation on satellite cell activity and protein expression in overloaded mammalian skeletal muscle. *Anat Rec* **247,** 179-188.

Pownall ME, Gustafsson MK & Emerson CP, Jr. (2002). Myogenic regulatory factors and the specification of muscle progenitors in vertebrate embryos. *Annu Rev Cell Dev Biol* **18,** 747-783.

Putman CT, Düsterhöft S & Pette D. (1999). Changes in satellite cell content and myosin isoforms in low-frequency- stimulated fast muscle of hypothyroid rat. *J Appl Physiol* **86,** 40-51.

Putman CT, Düsterhöft S & Pette D. (2000). Satellite cell proliferation in low-frequency stimulated fast muscle of hypothyroid rat. *Am J PhysiolCell Physiol* **279,** C682-C690.

Putman CT, Sultan KR, Wassmer T, Bamford JA, Skorjanc D & Pette D. (2001). Fiber-type transitions and satellite cell activation in low-frequency-stimulated muscles of young and aging rats. *J Gerontol A Biol Sci Med Sci* **56,** B510-B519.

Reichmann H, Hoppeler H, Mathieu-Costello O, von Bergen F & Pette D. (1985). Biochemical and ultrastructural changes of skeletal muscle mitochondria after chronic electrical stimulation in rabbits. *Pflügers Arch* **404,** 1-9.

Relaix F, Rocancourt D, Mansouri A & Buckingham M. (2005). A Pax3/Pax7-dependent population of skeletal muscle progenitor cells. *Nature* **435,** 948-953.

Robertson AB, Klungland A, Rognes T & Leiros I. (2009). DNA repair in mammalian cells: Base excision repair: the long and short of it. *Cell Mol Life Sci* **66,** 981-993.

Robertson TA, Grounds MD & Papadimitriou JM. (1992). Elucidation of aspects of murine skeletal muscle regeneration using local and whole body irradiation. *J Anat* **181 (Pt 2),** 265-276.

Rosenblatt DJ & Parry DJ. (1992). Gamma irradiation prevents compensatory hypertrophy of overloaded mouse extensor digitorum longous muscle. *J Appl Physiol* **73,** 2538-2543.

Rosenblatt DJ & Parry DJ. (1993). Adaptation of rat extensor digitorium longous muscle to gamma irradiation and overload. *Pflügers Arch* **423,** 255-264.

Rouger K, Brault M, Daval N, Leroux I, Guigand L, Lesoeur J, Fernandez B & Cherel Y. (2004). Muscle satellite cell heterogeneity: in vitro and in vivo evidences for populations that fuse differently. *Cell Tissue Res* **317,** 319-326.

Roy RR, Monke SR, Allen DL & Edgerton VR. (1999). Modulation of myonuclear number in functionally overloaded and exercised rat plantaris fibers. *J Appl Physiol* **87,** 634-642.

Sakata T, Tatsumi R, Yamada M, Shiratsuchi S, Okamoto S, Mizunoya W, Hattori A & Ikeuchi Y. (2006). Preliminary experiments on mechanical stretch-induced activation of skeletal muscle satellite cells *in vivo*. *Animal Science Journal* **77,** 518-525.

Schultz E. (1989). Satellite cell behaviour during skeletal muscle growth and regeneration. *Med Sci Sports Exerc* **21,** S181-S186.

Schultz E. (1996). Satellite cell proliferative compartments in growing skeletal muscles. *Dev Biol* **175,** 84-94.

Schultz E, Darr KC & Pette D. (1990). The role of satellite cells in adaptive or induced fiber transformations. In *The dynamic state of muscle fibers*, pp. 667-679. Walter de Gruyter, Berlin and New York.

Schultz E & McCormick KM. (1994). Skeletal muscle satellite cells. *Rev Physiol Biochem Pharmacol* **123,** 213-257.

Scime A & Rudnicki MA. (2006). Anabolic potential and regulation of the skeletal muscle satellite cell populations. *Curr Opin Clin Nutr Metab Care* **9,** 214-219.

Seale P & Rudnicki MA. (2000). A new look at the origin, function, and "stem-cell" status of muscle satellite cells. *Dev Biol* **218,** 115-124.

Sellman JE, Deruisseau KC, Betters JL, Lira VA, Soltow QA, Selsby JT & Criswell DS. (2006). In vivo inhibition of nitric oxide synthase impairs up-regulation of contractile protein mRNA in overloaded plantaris muscle. *J Appl Physiol* **100**, 258-265.

Shefer G, Wleklinski-Lee M & Yablonka-Reuveni Z. (2004). Skeletal muscle satellite cells can spontaneously enter an alternative mesenchymal pathway. *J Cell Sci* **117,** 5393-5404.

Salmons S & Vrbová G. (1969). The influence of activity on some contractile characteristics of mammalian fast and slow muscles. *JPhysiol* **201,** 535-549.

Simoneau JA & Pette D. (1988). Species-specific effects of chronic nerve stimulation upon tibialis anterior muscle in mouse, rat, guinea pig and rabbit. *Pflügers Arch* **412,** 86-92.

Spangenburg EE & Booth FW. (2003). Molecular regulation of individual skeletal muscle fibre types. *Acta Physiol Scand* **178,** 413-424.

Stamler JS & Meissner G. (2001). Physiology of nitric oxide in skeletal muscle. *Physiol Rev* **81,** 209-237.

Tatsumi R & Allen RE. (2004). Active hepatocyte growth factor is present in skeletal muscle extracellular matrix. *Muscle Nerve* **30,** 654-658.

Tatsumi R & Allen RE. (2008). Mechano-biology of resident myogenic stem cells: molecular mechanism of stretch-induced activation of satellite cells. *Animal Science Journal* **79,** 279-290.

Tatsumi R, Anderson JE, Nevoret CJ, Halevy O & Allen RE. (1998). HGF/SF is present in normal adult skeletal muscle and is capable of activating satellite cells. *Dev Biol* **194,** 114-128.

Tatsumi R, Hattori A, Ikeuchi Y, Anderson JE & Allen RE. (2002). Release of hepatocyte growth factor from mechanically stretched skeletal muscle satellite cells and role of pH and nitric oxide. *Mol Biol Cell* **13,** 2909-2918.

Tatsumi R, Liu X, Pulido A, Morales M, Sakata T, Dial S, Hattori A, Ikeuchi Y & Allen RE. (2006). Satellite cell activation in stretched skeletal muscle and the role of nitric oxide and hepatocyte growth factor. *Am J Physiol Cell Physiol* **290,** C1487-1494.

Tornaletti S. (2009). DNA repair in mammalian cells: Transcription-coupled DNA repair: directing your effort where it's most needed. *Cell Mol Life Sci* **66,** 1010-1020.

Tseng BS, Kasper CE & Edgerton VR. (1994). Cytoplasm-to-myonucleus ratios and succinate dehydrogenase activities in adult rat slow and fast muscle fibers. *Cell Tissue Res* **275,** 39-49.

Wakeford S, Watt DJ & Partridge TA. (1991). X-irradiation improves mdx mouse muscle as a model of myofiber loss in DMD. *Muscle Nerve* **14,** 42-50.

Wheldon TE, Michalowski AS & Kirk J. (1982). The effect of irradiation on function in self-renewing normal tissues with differing proliferative organisation. *Br J Radiol* **55,** 759-766.

Wozniak AC, Kong J, Bock E, Pilipowicz O & Anderson JE. (2005). Signaling satellite-cell activation in skeletal muscle: markers, models, stretch, and potential alternate pathways. *Muscle Nerve* **31,** 283-300.

Yamada M, Sankoda Y, Tatsumi R, Mizunoya W, Ikeuchi Y, Sunagawa K & Allen RE. (2008). Matrix metalloproteinase-2 mediates stretch-induced activation of skeletal muscle satellite cells in a nitric oxide-dependent manner. *Int J Biochem Cell Biol* **40,** 2183-2191.

Zammit PS, Golding JP, Nagata Y, Hudon V, Partridge TA & Beauchamp JR. (2004). Muscle satellite cells adopt divergent fates: a mechanism for self-renewal? *J Cell Biol* **166,** 347-357.

Zammit PS, Partridge TA & Yablonka-Reuveni Z. (2006). The Skeletal Muscle Satellite Cell: The Stem Cell That Came In From the Cold. *J Histochem Cytochem*.

Zhang M, Koishi K & McLennan IS. (1998). Skeletal muscle fibre types: detection methods and embryonic determinants. *Histol Hisopathol* **13,** 201-207.

[1]CHAPTER THREE

EFFECTS OF SATELLITE CELL ABLATION ON LOW-FREQUENCY-STIMULATED FAST-TO-SLOW FIBRE TYPE TRANSFORMATIONS IN RAT SKELETAL MUSCLE

3.1 INTRODUCTION

Satellite cells are quiescent myoblasts associated with post-mitotic skeletal muscle fibres that underlie the regenerative, and possibly adaptive, potential of muscle fibres. In this regard, satellite cells seem to function primarily as a source of new myonuclei by leaving their quiescent state, actively cycling, and fusing to existing skeletal muscle fibres or to each other, forming new myofibres (Bischoff *et al.*, 1994; Putman *et al.*, 1999b). The role of these muscle precursor cells during postnatal growth, overload-induced hypertrophy and regeneration is well documented (reviewed by Schultz & McCormick, 1994; Charge & Rudnicki, 2004). The role of satellite cells in activity-induced fibre type transformations is, however, less clear.

Slow-twitch (oxidative) skeletal muscle fibres are known to contain a larger number of myonuclei and satellite cells compared with fast-twitch (glycolytic) fibres (Gibson & Schultz, 1982, 1983). CLFS is a model of muscle training that induces maximal fast-to-slow fibre type transformations in the absence of fibre injury in rat (Simoneau & Pette, 1988; Delp & Pette, 1994; Putman *et al.*, 1999a; Putman *et al.*, 1999b; Putman *et al.*, 2001). These properties make the application of CLFS to rat fast-twitch muscle an ideal experimental model in which to study the contributions of satellite cells to fibre type transformations. Previous studies have shown that fast-to-slow fibre type transformations are associated with increases in satellite cell activation, number

[1] A version of this chapter has been published. Martins, KJB, Gordon T, Pette D, Dixon WT, Foxcroft GR, MacLean IM and Putman CT. (2006). Effects of satellite cell ablation on low-frequency-stimulated fast-to-slow fibre type transitions in rat skeletal muscle. *Journal of Physiology (London)*, **572**: 281-94.

and fusion to transforming fibres, especially within the IIB fibre population (Putman *et al.*, 1999b). Collectively, these findings suggest that higher myonuclear content is a prerequisite for fast-to-slow fibre type transformations in rat skeletal muscle, and that satellite cells play an important role in this adaptive response.

Rosenblatt *et al.* (1992, 1993) reported that satellite cell ablation by exposure to a single 25 Gy dose of γ-irradiation prevented fibre hypertrophy but did not prevent fast-to-slow fibre type transformations after 4 weeks of compensatory overload in rodent extensor digitorum longus muscle following removal of the synergist tibialis anterior. They concluded that satellite cell involvement was not a requirement for fibre type transformations. Furthermore, it has been noted that a single 25 Gy dose of γ-irradiation disrupts mitotic activity of avian satellite cells in culture for only 7 days (Mozdziak *et al.*, 1996) with significant recovery occurring between 9 and 12 days post-irradiation (Wakeford *et al.*, 1991; McGeachie *et al.*, 1993; Mozdziak *et al.*, 1996). In support of these observations, studies utilising a rat model reported a significant increase in myotube formation 7 days after a single 20 Gy dose of ionising irradiation (Gulati, 1987), and greater skeletal muscle DNA content 15 days after a single 25 Gy dose of ionising irradiation (Adams *et al.*, 2002). Thus the question remains as to the involvement of satellite cells in fast-to-slow fibre type transformations.

The purpose of this study was to test the hypothesis that fast-to-slow fibre type transformations would be attenuated in rat tibialis anterior muscles exposed to γ-irradiation after 21 days of CLFS. In order to sustain complete satellite cell ablation throughout 21 days of CLFS, tibialis anterior muscles were exposed to a 25 Gy dose of γ-irradiation every 7 days. A single 60 Gy dose of ionising irradiation has been shown to not cause muscle fibre damage or abnormalities in rabbit skeletal muscle (Lewis, 1954). Likewise, the three weekly 25 Gy doses of γ-irradiation used in the present study did not cause any muscle fibre damage or abnormalities in rat skeletal muscle. Thus, this model allowed us to successfully

investigate fibre type transformations during 21 days of CLFS, in the absence of a viable satellite cell population.

Immunohistochemical detection and quantification of satellite cell content was assessed with a number of different antibodies. The Ca^{2+}-dependent transmembrane satellite cell anchor protein, muscle (M)-cadherin, was used to assess quiescent satellite cells (Kuschel *et al.*, 1999; Putman *et al.*, 2001). Continuous DNA labeling with BrdU, followed by immunolocalisation was used to detect satellite cell proliferation (Schultz, 1996), while the muscle-specific transcription factor myogenin was used to determine the number of satellite cell progeny committed to terminal differentiation (Putman *et al.*, 1999b). Total myonuclear content was evaluated on serial sections stained with hematoxylin and anti-laminin (Putman *et al.*, 2001). The activities of the reference enzymes CS and GAPDH were also measured to investigate coordinate changes in metabolic properties. MHC-based fibre type transformations were evaluated at the protein level by gel electrophoresis, by immunohistochemical staining of frozen serial sections with monoclonal antibodies (Putman *et al.*, 1999b), and at the mRNA level by reverse transcriptase-polymerase chain reaction (RT-PCR) (Jaschinski *et al.*, 1998; Bamford *et al.*, 2003). Complete ablation of the satellite cell pool significantly attenuated, but did not abolish, MHC-based fast-to-slow fibre type transformations during 21 days of CLFS.

3.2 METHODS

3.2.1 Animals

Twenty-nine adult male Wistar rats (Charles River Laboratories, Montreal PQ, Canada) weighing 296 ± 13.7 g (mean ± SEM) were used in this study. All animal procedures were carried out in accordance with the guidelines of the Canadian Council for Animal Care (CCAC) and received ethical approved from the University of Alberta. Animals were individually housed under controlled environmental conditions (i.e. 22ºC with alternating 12 h light and dark cycles)

and received standard rat chow and water *ad libitum*. Animals were randomly assigned to one of the following three groups receiving either: sham operation + weekly doses of γ-irradiation focused on the left leg only (IRR, n=8), IRR + 21-days of CLFS of the left leg (IRR-Stim, n=11), or 21-days of CLFS (Stim, n=10). The application of CLFS tended to elicit a compensatory effect in the contralateral control muscles due to increased weight bearing (data shown in Appendix A), as previously observed (Putman *et al.*, 2000). Therefore, comparisons were evaluated against the right contralateral control leg of IRR (Control, n=8).

3.2.2 Chronic Low-Frequency Stimulation and BrdU Labeling

CLFS was applied across the left common peroneal nerve as previously described (Simoneau & Pette, 1988; Putman *et al.*, 2004). Bipolar electrodes were implanted under general anaesthesia [75 mg (kg body wgt)$^{-1}$ ketamine and 10 mg (kg body wgt)$^{-1}$ xylezine] lateral to the common peroneal nerve of the left hindlimb, externalised at the dorsal intrascapular region, and connected to a small, portable stimulator. CLFS (10 Hz, impulse width 380 μs, 12 h day^{-1}) was applied for 21 consecutive days; strong persistent dorsiflexion was observed in the left legs of IRR-Stim and Stim twice daily throughout the study. This time point was selected because fibre type transformations are essentially 80-90% complete after 21-days of CLFS, at both the protein and mRNA levels (Jaschinski *et al.*, 1998). Animals received a continuous infusion of the thymidine analogue BrdU (5 mg/200 μl) via subcutaneously implanted Alzet® mini-osmotic pumps (model 2004, 0.25 μl/hr release rate and 200 μl volume) (Schultz, 1996).

3.2.3 Gamma Irradiation

On days 1, 7 and 14, animals were anaesthetised by an intraperitoneal injection of Somnotol [45 mg (kg body mass)$^{-1}$] and placed in a Gammacell 40 Cesium-137 Irradiation Unit (Health Services Laboratory Animal Services, University of Alberta). Satellite cells of the left tibialis anterior muscle were ablated by exposing the left anterior crural compartment to a total of 25 Gy of γ-

irradiation (0.56 Gy per min^{-1}) (Rosenblatt *et al.*, 1994), while the remainder of the animal was shielded by two 2.5 cm thick lead plates. Irradiation was interrupted at regular intervals to monitor the heart rate and respiratory rate of the animals.

3.2.4 Muscle Sampling

Upon completion of the stimulation period, animals were euthanised with an overdose of Somnotol [100 mg $(kg\ body\ mass)^{-1}$], followed by exsanguination, and the tibialis anterior muscles were excised from both hindlimbs, weighed, fixed in a slightly longitudinally stretched position, and frozen in melting isopentane (-159ºC). Muscles were stored in liquid nitrogen (-196ºC) until analysed.

3.2.5 Antibodies

The following monoclonal antibodies directed against adult and embryonic MHC isoforms (Schiaffino *et al.*, 1988; Schiaffino *et al.*, 1989) were harvested from the supernatant of hybridoma cell lines obtained from the American Type Culture Collection (Manassas, VA, U.S.A.): BA-D5 (IgG, anti-MHCI), SC-71 (IgG, anti-MHCIIa), BF-F3 (IgM, anti-MHCIIb), BF-35 [IgG, not MHCIId(x)], and BF-45 (IgG, anti-MHC-embryonic). Anti-dystrophin monoclonal antibody (clone DYS2, Dy8/6C5), directed against the carboxyl terminus, was obtained from Novocastra Laboratories (Newcastle, U.K.). Monoclonal anti-desmin (clone DE-U-10) and monoclonal anti-vimentin (clone V9) were obtained from Sigma (Deisenhofen, Germany). Goat polyclonal anti-M-cadherin (N-19) and mouse monoclonal anti-myogenin (clone F5D) antibodies were obtained from Santa Cruz Biochemicals (Santa Cruz, CA, U.S.A.). Mouse monoclonal anti-5-bromo-2'-deoxyuridine (clone BMC 9318) was obtained from Roche Diagnostics Corporation (Indianapolis, IN, U.S.A.). Rabbit polyclonal anti-laminin (IgG) was obtained from ICN Biochemicals (Costa Mesa, CA, U.S.A.). Biotinylated horse-anti-mouse-IgG (rat-absorbed, affinity-purified), biotinylated horse-anti-goat-IgG, biotinylated goat anti-rabbit IgG, and

biotinylated goat anti-mouse IgM were obtained from Vector Laboratories, Inc. (Burlingame, CA, U.S.A.). Non-specific control mouse-IgG was obtained from Santa Cruz Biochemicals.

3.2.6 Immunohistochemistry for Myosin, Dystrophin, Vimentin, Desmin and Laminin

Tibialis anterior muscles were mounted in embedding medium (Tissue-Tek O.C.T. Compound, Miles Scientific, U.S.A.) at -20ºC and 16 μm-thick frozen sections were collected from the mid point of each muscle, also at -20ºC. Immunostaining was completed according to established protocols (Putman *et al.*, 2001). Briefly, sections were air-dried, washed in phosphate-buffered saline (PBS) with 0.1% (v/v) Tween-20 (PBS-T), with PBS, and then incubated for 15 minutes in 3% (v/v) H_2O_2 in methanol. Sections stained for MHC isoforms (i.e., BA-D5, SC-71, BF-35, BF-45), dystrophin, vimentin, or desmin were then incubated at room temperature for 1 h in a blocking solution [BS-1: 1% (w/v) bovine serum albumin, 10% (v/v) horse serum in PBS-T, pH 7.4] containing Avidin-D Blocking Reagent (Vector Laboratories Inc.). Sections stained with anti-laminin or anti-MHCIIb (BF-F3) were incubated at room temperature for 1 hour in a similar blocking solution, with the exception that goat serum was substituted for horse serum (BS-2). Sections were incubated overnight at 4°C with a primary antibody that was diluted in its corresponding blocking solution, also containing Biotin Blocking Reagent (Vector Laboratories Inc.), as follows: BA-D5, 1:400 in BS-1; SC-71, 1:100 in BS-1; BF-35, 1:10,000 in BS-1; BF-F3, 1:400 in BS-2; BF-45, 1:50 in BS-1; DYS2, 1:10 in BS-1; V9, 1:20 in BS-1; DE-U-10, 1:100 in BS-1; anti-laminin, 1:100 in BS-2. These dilutions were determined by applying different concentrations of the primary antibody (i.e. neat, 1:10, 1:20, 1:40, 1:100, 1:200, 1:400, 1:500, 1:1,000 and 1:10,000) to skeletal muscle tissue and choosing the dilution with the best signal-to-noise ratio. Sections were washed as before and one of biotinylated horse-anti-mouse-IgG (BA-D5; SC-71; BF-35; BF-45; DYS2; V9; DE-U-10), biotinylated goat-anti-mouse-IgM (BF-F3), or biotinylated goat-anti-rabbit-IgG (anti-laminin) was

applied for 1 hour at a dilution of 1:200. After several washings, sections were incubated with Vectastain ABC Reagent [i.e. avidin-biotin Horse Radish Peroxidase (HRP) complex], according to the manufacturer's instructions (Vector Laboratories Inc.). Sections were then washed and reacted with 0.07% (w/v) diaminobenzidine, 0.05% (v/v) H_2O_2, and 0.03% (w/v) $NiCl_2$ in 50 mM Tris-HCl (pH 7.5); sections stained for desmin and laminin were reacted with the same substrate solution, but without $NiCl_2$. Control samples were run in parallel in which the primary IgM antibody was omitted, or a non-specific mouse IgG antibody was substituted (Santa Cruz). Those sections stained for laminin were counterstained with Harris' Haematoxylin (Fisher Diagnostics, Fair Lawn, NJ, U.S.A.) and used to evaluate the total number of intrafibre myonuclei. All sections were subsequently dehydrated, cleared, and mounted with Entellan (Merck, Darmstadt, Germany).

3.2.7 Immunohistochemistry for BrdU, Myogenin and M-cadherin

Immunostaining for BrdU was completed according to Schultz *et al.* (1996), while myogenin and M-cadherin staining were completed according to established procedures (Putman *et al.*, 2000). Briefly, 16 μm-thick sections of tibialis anterior muscles were air-dried. Sections stained for BrdU were fixed for 15 minutes in 70% (v/v) ethanol at room temperature, whereas sections that were stained for myogenin or M-cadherin were prefixed for 10 min in cold acetone (-20°C). Sections were then washed in PBS-T and PBS, incubated for 15 minutes in 3% (v/v) H_2O_2 in methanol, and washed again. Sections stained for BrdU were further incubated in 2N HCl for 1 hour at room temperature and washed. All sections were incubated for 1 hour in a blocking solution (BS-1) containing Avidin-D Blocking Reagent (Vector Laboratories Inc.) and washed. Sections were then incubated overnight at 4°C with primary anti-BrdU (1:10), anti-myogenin (1:10), or anti-M-cadherin (1:50) that were diluted in BS-1, also containing Biotin Blocking Reagent (Vector Laboratories Inc.). Sections were washed as before and biotinylated horse-anti-mouse-IgG (anti-BrdU; anti-myogenin) or biotinylated horse-anti-goat-IgG (anti-M-cadherin) was applied for

1 hour at a dilution of 1:200. After several washings, sections were incubated with Vectastain ABC Reagent. The sections were washed and reacted with DAB, H_2O_2, and $NiCl_2$ in 50 mM Tris-HCl, pH 7.5. All sections were subsequently dehydrated, cleared, and mounted with Entellan (Merck, Darmstadt, Germany).

3.2.8 Immunohistochemical Analyses

All semi-quantitative analyses were completed with a Leitz Diaplan microscope (Enrst Leitz Wetzlar GmbH, Germany) fitted with a Pro Series High Performance CCD camera (Media Cybernetics, U.S.A.) and a custom designed analytical imaging program (Putman *et al.*, 2000). A similar number of fibres stained for the various MHC isoforms were examined from three distinct cross sectional areas (CSA) of tibialis anterior (deep, middle, and superficial) for each of the Control (total fibres: 426 ± 14 fibres/muscle), IRR (total fibres: 417 ± 16 fibres/muscle), IRR-Stim (total fibres: 451 ± 12 fibres/muscle), Stim (total fibres: 452 ± 35 fibres/muscle), IRR-Stim contralateral control (total fibres: 404 ± 15 fibres/muscle), and Stim contralateral control (total fibres: 453 ± 35 fibres/muscle) legs. A total of 19,121 fibres were examined for fibre type distribution analyses. Fibre cross-sectional area analyses were performed on the same fibres. Types I, IIA and IIB fibres were identified by positive staining of fibres and type IID(X) fibres were identified by the absence of staining. Fibre damage was evaluated using anti-desmin, anti-vimentin, and anti-dystrophin (Putman *et al.*, 1999b; Putman *et al.*, 2001; Peters *et al.*, 2003). Damaged fibres were considered to be vimentin positive, dystrophin negative, and/or to display an altered pattern of desmin staining (i.e. absence of staining or foci of positivity). The entire cross section of each muscle was examined. The mean CSA examined for quiescent satellite cells (M-cadherin), proliferating satellite cell progeny (BrdU), terminally differentiating satellite cell progeny (myogenin), and total intrafibre myonuclei (Harris' Hematoxylin with laminin) were 4.6 ± 0.04, 19.5 ± 2.1, 1.2 ± 0.1, and 1.1 ± 0.005 mm^2, respectively.

3.2.9 Electrophoretic Analysis of Myosin Heavy Chain Protein Isoforms

Quantitative MHC isoform analyses were completed according to the methods described by Hämäläinen & Pette (1996) and Putman *et al.* (2004). Muscle samples were homogenised on ice in 6-volumes of buffer containing 100 mM NaP_2O_7 (pH 8.5), 5 mM EGTA, 5 mM $MgCl_2$, 0.3 mM KCl, 10 mM DTT, and 5 mg ml^{-1} of a protease inhibitor cocktail (Complete™, Roche Diagnostics Corporation, Indianapolis, IN, U.S.A.). This protease inhibitor cocktail is a proprietary blend of protease inhibitors used for the inhibition of serine, cysteine and metalloproteases. Samples were stirred for 30 minutes on ice and centrifuged at 12,000x*g* for 5 minutes at 4°C, and the supernatants were diluted 1:1 with glycerol. Samples were then stored at -20°C until analysed. Prior to gel loading, muscle extracts were diluted to 0.2 μg μl^{-1} in a modified Laemmli-lysis buffer (Laemmli, 1970) and boiled for 6 minutes. MHC isoforms were separated electrophoretically on 7% (w/v) polyacrylamide gels containing glycerol, under denaturing conditions. Samples (1 μg total protein per lane) were electrophoresed in duplicate at 275 V for 24 hours at 8°C. Gels were then immediately fixed and MHC isoforms were detected by silver staining and evaluated by densitometry (Syngene ChemiGenius, GeneSnap™ and GeneTools™, Syngene, U.K.).

3.2.10 Myosin Heavy Chain mRNA Analyses by Reverse Transcriptase-Polymerase Chain Reaction

MHC isoform expression was further examined at the mRNA level using RT-PCR according to established procedures (Jaschinski *et al.*, 1998; Bamford *et al.*, 2003). Briefly, frozen powdered tibialis anterior muscles were homogenised in TRIzol® and subsequently centrifuged. Chloroform was then added to the supernatant and centrifuged to obtain phase separation. Isopropanol was added to the aqueous phase and RNA was allowed to precipitate overnight at -20°C. After centrifugation, the pellet was washed in 75% (v/v) ethanol and air-dried. The pellet was resuspended with DEPC water and treated with a DNAse kit according to manufacturers' instructions (Ambion/Applied Biosystems, Austin, TX, USA). The concentrations and purity of the RNA extracts were evaluated by measuring

the absorbance at 260 and 260/280 nm, respectively, using a microplate reader (Spectra Max 190, Molecular Devices, Sunnyvale, CA, U.S.A.) and 96-well flat bottom UV-transparent plates (Costar®, Corning Incorporated Life Sciences, Acton, MA, U.S.A.). Oligo (dT15) primers (Invitrogen, Life technologies, Burlington, ON, Canada) and Moloney murine leukemia virus (M-MLV) DNA polymerase (Invitrogen, Life Technologies) were added to diluted samples (1 μg μl^{-1}) and reverse transcription was performed for 1 h at 37°C. α-actin was used as an internal standard and its primers did not cross-react with primers for any of the MHC isoforms (Bamford *et al.*, 2003). Therefore, the α-actin assay was multiplexed with each of the assays for the various MHC isoforms. The number of cDNA amplification cycles was optimised for each MHC isoform [i.e., MHCI: 25 cycles; MHCIIa: 22 cycles; MHCIId(x): 22 cycles; MHCIIb: 22 cycles] to ensure cycles were within the geometric phase of amplification. Primer sequences, annealing temperatures, and Mg^{2+} concentrations for the various primer sets have been described previously (Bamford *et al.*, 2003). MHCI, MHCIIa, and MHCIId(x) amplicons were resolved on 2% (w/v) agarose gels for 4 hours at 100 mA. MHCIIb amplicons were resolved on 4% (w/v) agarose gels, also for 4 hours at 100 mA. Gels were subsequently stained for 30 minutes with an ethidium bromide solution, visualised under UV light, and analysed by densitometry (Syngene ChemiGenius, GeneSnap™ and GeneTools™, Syngene, U.K.) (Bamford *et al.*, 2003). The quantity of cDNA within each lane of the agarose gels was well within the established linear range for detection and quantification (i.e. 50 pg μl^{-1} - 10 μg μl^{-1}). All samples were normalised to the internal standard α-actin, and each MHC mRNA isoform was expressed as the percent of total MHC mRNA. The within-sample coefficient of variation was consistently low (11 ± 1%).

3.2.11 Enzyme Measurements

The reference enzymes CS (EC 4.1.3.7) and GAPDH (EC 1.2.1.12) were extracted in a high-salt medium containing 5 mM EDTA, 100 mM sodium potassium phosphate buffer (pH 7.2) (Reichmann *et al.*, 1983), with the addition

of 0.1% (v/v) Triton X-100, in order to ensure complete extraction of soluble and structure-bound activities. To stabilise GAPDH, DTT was added to an aliquot of the supernatant fraction yielding a 2 mM final concentration. The use of DTT has been imperically derived from Reichmann *et al.*, (1983) who found that the activities of glycolytic enzymes (i.e. GAPDH and phosphofructokinase) were better preserved in a reduced environment. GAPDH activities were immediately measured at 30°C (Bass *et al.*, 1969; Putman *et al.*, 2004). CS activities were subsequently measured at 30°C (Srere & Lowenstein, 1969; Putman *et al.*, 2004).

3.2.12 Statistical Analyses

Data are presented as mean ± SEM. Differences between group means were assessed using a two-way [i.e. treatment (irradiation, stimulation or irradiation plus stimulation) X leg (manipulated or control)] Analysis of Variance (ANOVA). When a significant *F*-ratio was found for the interaction, differences were located using the [2]Least Significant Difference post-hoc analysis. Differences were considered significant at $P < 0.05$.

3.3 RESULTS

3.3.1 Animal and Muscle Weights

The animals initially weighed 296 ± 14 g and at the end of the experiment weighed 340 ± 12 g. The absolute weight gain was similar for all groups. There was no difference in weight of the tibialis anterior of IRR (691 ± 34 g) compared with Control (691 ± 24 g). The weights of the tibialis anterior muscles of IRR-Stim (499 ± 30 g) and Stim (460 ± 8 g) were significantly less than Control. The reduction in muscle mass in Stim and IRR-Stim was attributed to the transformation from a fast to a slower phenotype (Fig. 3.11), as opposed to fibre

[2] In all statistical analyses perfomed throughout this thesis, both the Least Significant Difference and Newman-Keuls post-hoc analyses were run and found to yield the same results.

degeneration (section 3.3.3) or pathological atrophy. This finding is consistent with previous studies of CLFS in rat muscle (Putman *et al.*, 1999c).

3.3.2 Satellite Cells

Quiescent satellite cells were identified by strong positive staining for M-cadherin (Fig. 3.1*A*), while activated and previously activated satellite cells were determined by quantifying BrdU staining (Fig. 3.1*B*). Terminally differentiating satellite cell progeny were identified by strong nuclear staining for myogenin (Fig. 3.1*C*). Serial sections were also stained with anti-laminin and counterstained with hematoxylin to identify satellite cells and their progeny, as well as myonuclei (Fig. 3.1*D*). The number of myonuclei was calculated by subtracting the number of M-cadherin-, BrdU-, and myogenin-positive cells (Fig. 3.2).

Similar results were observed in all states of satellite cell activity (Fig. 3.2). In all cases, IRR and IRR-Stim did not differ from Control (Fig. 3.2*A*, *B*, *C* and *D*). In contrast, a 7.7-fold increase in M-cadherin positive nuclei (Fig. 3.2*A*), 8-fold increase in BrdU positive nuclei (Fig. 3.2*B*), 3.8-fold increase in myogenin positive nuclei (Fig. 3.2*C*) and 3.3-fold increase in the number of myonuclei were observed in Stim compared to Control.

3.3.3 Structural Morphology

Serial sections stained with vimentin, dystrophin, and desmin were used to identify damaged fibres (Fig. 3.3), as previously described (Putman *et al.*, 1999b). The entire CSA of 58 tibialis anterior muscles were examined and only 7 fibres were vimentin-positive, dystrophin-negative, and displayed foci of positivity and/or the absence of desmin staining. These 7 fibres were evenly distributed between all groups. Further inspection of hematoxylin and eosin stained cross sections did not reveal fibre necrosis or fibres with centrally located nuclei (Fig. 3.4).

3.3.4 Myosin Heavy Chain mRNA Expression

Examples of the semi-quantitative analytical methods used to determine mRNA expression levels of adult MHC isoforms are illustrated in Fig. 3.5. IRR was not different compared with Control in all MHC mRNA expression levels (Fig. 3.6). Twenty-one days of CLFS induced transformations in the fast-to-slow direction that were detected at the mRNA level. Specifically, IRR-Stim and Stim MHCI mRNA (Fig. 3.6*A*) and MHCIIa mRNA (Fig. 3.6*B*) similarly increased, while MHCIIb mRNA (Fig. 3.6*D*) decreased compared with Control. Changes in MHCIId(x) mRNA levels were unremarkable (Fig. 3.6*C*).

3.3.5 Myosin Heavy Chain Isoform Transformations

A representative gel showing the quantitative analytical method used to measure MHC isoform content in muscle extracts is illustrated in Fig. 3.7. A similar MHC isoform distribution was observed between IRR and Control (Fig. 3.8). As similarly observed at the mRNA level, CLFS induced fast-to-slow MHC-based transformations at the protein level. Specifically, IRR-Stim and Stim resulted in similar 3.0-fold increases in MHCIIa (Fig. 3.8*B*) and 2.0-fold decreases in MHCIIb (Fig. 3.8*D*) compared with Control. In contrast, MHCI content was 1.75-fold greater in Stim compared with IRR, which remained unchanged in IRR-Stim (Fig. 3.8*A*). MHCIId(x) content remained largely unchanged by CLFS and/or weekly exposure to γ-irradiation (Fig. 3.8*C*).

3.3.6 Fibre Type Transformations

Fibre type transformations were assessed by semi-quantitative immunohistochemical analyses on serial sections (Fig. 3.9) in the deep, middle, and superficial regions of each tibialis anterior muscle, in order to ensure representative sampling. When data were summarised as the proportion of fibres expressing a particular MHC isoform (Fig. 3.10), no differences were observed between IRR and Control. As similarly observed in MHC isoform proportions, CLFS induced fast-to-slow fibre type transformations. Specifically, Stim

displayed increases in the percentage of fibres expressing slower MHCI and MHCIIa, and decreases in the percentage of fibres expressing faster MHCIId(x) and MHCIIb compared with Control. When, however, muscles were also exposed to weekly doses of γ-irradiation, fibre type transformations only occurred amongst fibres expressing fast MHC isoforms. Specifically, IRR-Stim only displayed increases in the percentage of fibres expressing MHCIIa and decreases in MHCIId(x) compared with Control.

Detailed fibre type analysis, which included the detection of all pure and hybrid fibre types revealed similar results (Fig. 3.11). For the most part, IRR was similar to Control, the lone exception being a 1.3% increase in type IID(X)/B hybrid fibres compared with Control. CLFS induced fast-to-slow fibre type transformations. Specifically, Stim displayed increases in the proportions of the slower type I (Fig. 3.7*A*), I/IIA (Fig. 3.7*B*), IIA (Fig. 3.7*C*), IIA/D(X) (Fig. 3.7*D*) and IIA/D(X)/B (Fig. 3.7*E*) fibres with concomitant decreases in the proportion of the faster type IID(X) (Fig. 3.7*F*) and IIB (Fig. 3.7*H*) fibres compared with Control. In IRR-Stim, however, these fast-to-slow fibre type transformations were again limited to the fast fibre population. Specifically, IRR-Stim only displayed increases in the proportions of the slower type IIA (Fig. 3.7*C*) and IIA/D(X)/B (Fig. 3.7*E*) fibres with concomitant decreases in the faster type IID(X) (Fig. 3.7*F*) and IIB (Fig. 3.7*H*) types compared with Control. Moreover, the proportion of the slowest type I (Fig. 3.7*A*) and I/IIA (Fig. 3.7*B*) fibres of Stim were significantly greater compared with IRR-Stim. A small population of type I/IIA/D(X)/B hybrid fibres differed between IRR-Stim and Stim (Fig. 3.7*I*). MHC-embryonic was not detected in extrafusal fibres (data not shown).

3.3.7 Fibre Cross-Sectional Areas

For the most part, weekly doses of γ-irradiation (i.e. IRR) had no effect on fibre CSA (Table 3.1). When data were summarised according to the CSA of a particular MHC isoform expressed, those fibres expressing MHCI and MHCIIa in IRR-Stim were significantly larger compared with Stim and Control. Both IRR-

Stim and Stim displayed similar decreases in the CSA of fibres expressing MHCIIb compared with Control. The CSA of individual fibre types varied in IRR-Stim in a manner that was consistent with attenuation of fast-to-slow fibre type transformations. The CSA of individual fibres revealed that type I fibres of IRR-Stim were larger than Control, whereas, Stim did not differ from Control. Additionally, the CSA of type IID(X) fibres in IRR-Stim were 2.5-fold larger compared with Stim.

3.3.8 Enzyme Activities

Mitochondrial CS and glycolytic GAPDH activities of IRR and Control were the same (Fig. 3.12). IRR-Stim and Stim similarly displayed greater than 2-fold increases in CS activity and greater than 1.5-fold decreases in GAPDH activity.

3.4 DISCUSSION

The findings of the present study extend those of Rosenblatt *et al.* (1992, 1993) and Putman *et al.*, (1999b). The current study shows that exposure to three weekly doses of 25 Gy of γ-irradiation completely ablated the satellite cell population and did not cause muscle fibre damage or any structural abnormalities within the target muscle after 21 days of CLFS. This novel approach allowed for direct investigation of the role that satellite cell recruitment plays in activity-induced fibre type transformations, in the absence of fibre regeneration. The main finding of this study was that fast-to-slow fibre type transformations were attenuated, but not abolished, in rat tibialis anterior muscles that were devoid of satellite cell mitotic activity.

3.4.1 Satellite Cell Ablation by Irradiation

Exposure to low levels of γ-irradiation causes multiple single and double strand breaks as well as base damage in target DNA (Coggle, 1983). Once

irradiated satellite cells attempt to divide, mitotic failure (Wakeford *et al.*, 1991) and apoptosis (Wheldon *et al.*, 1982) ensue. Post-mitotic myonuclei, on the other hand, reportedly maintain normal cellular functions after exposure to comparable levels of γ-irradiation (Wheldon *et al.*, 1982; Mozdziak *et al.*, 1996; Phelan & Gonyea, 1997). Previous irradiation models used to ablate skeletal muscle satellite cells have used single doses ranging from 16 to 30 Gy (Wheldon *et al.*, 1982; Gulati, 1987; Mozdziak *et al.*, 1996; Phelan & Gonyea, 1997; Heslop *et al.*, 2000; Adams *et al.*, 2002). The collective results of those studies indicate that the success of satellite cell ablation is dependent on the dose of ionising irradiation administered, on the nature and severity of physiological stimuli leading to satellite cell activation, and on the species investigated. Although most satellite cells seem to be ablated after a single 20 to 30 Gy dose of ionising irradiation, the basis for muscle fibre regeneration after 7 days (Gulati, 1987) appears to be the survival of a small population of radiation-resistant satellite cells (Heslop *et al.*, 2000). The reason for the apparent radiation resistance of some satellite cells may include the capacity to undergo at least one mitotic division before cell death (Coggle, 1983; McGeachie *et al.*, 1993; Mozdziak *et al.*, 1996), the ability to recover and thus remain fusion-competent, and/or differentiated satellite cell progeny, which are past the radiosensitive phase, may fuse directly to existing fibres (Wakeford *et al.*, 1991; Robertson *et al.*, 1992; McGeachie *et al.*, 1993; Mozdziak *et al.*, 1996, 1997; Adams *et al.*, 2002).

In the present study, a total dose of 75 Gy was administered over a 3-week period that may have exceeded the minimum dose required to sustain complete satellite cell ablation, including any potentially radiation-resistant satellite cells. Exposure to a 25 Gy dose of γ-irradiation each week, however, was high enough to continuously disrupt satellite cell mitotic activity, yet was low enough that it did not cause skeletal muscle damage, skeletal morphology abnormalities, or interfere with CLFS-induced changes in muscle gene expression as shown by changes in the expression of MHC isoforms, which are known to be transcriptionally regulated (Jaschinski *et al.*, 1998). The absence of increases in

M-cadherin- and BrdU-positive cells in IRR-Stim clearly shows that satellite cell mitosis was inhibited. Further, the absence of increases in terminally differentiating satellite cells and myonuclear content indicates that direct fusion of satellite cells to transforming muscle fibres did not occur.

3.4.2 Fibre Type Transformations in Normal and Irradiated Muscles

In order to elicit a pronounced stimulus for fast-to-slow fibre type transformations in the absence of muscle fibre regeneration, CLFS was employed, which is a highly standardised and reproducible model of muscle training that mimics the electrical discharge pattern of slow motoneurons innervating slow-twitch muscles. CLFS is an ideal model for studying the effects of enhanced contractile activity on various structural, functional, metabolic, and molecular properties (Pette & Vrbová, 1992, 1999; Ljubicic *et al.*, 2005) because it activates all motor units of the stimulated muscle and, therefore fully challenges the adaptive potential of the target muscle (Pette & Staron, 2000). In the presence of a viable satellite cell population, CLFS is known to induce increases in satellite cell number and activity, and large fast-to-slow phenotypic changes, specifically within the fast fibre population, which are further advanced at the mRNA level compared with protein expression levels (Putman *et al.*, 1999b). This delayed adaptation at the protein level likely reflects the more advanced state of change at the mRNA level compared with the much slower rate of MHC protein turnover. In the current study, these findings were confirmed at the MHC protein and mRNA levels.

Weekly doses of 25 Gy of γ-irradiation alone did not affect cellular metabolism or MHC isoform expression, which is consistent with previous findings (Wheldon *et al.*, 1982; Weller *et al.*, 1991; Rosenblatt & Parry, 1992, 1993). Since γ-irradiation only affected mitotically active satellite cells, any changes that occurred within γ-irradiated muscles that underwent 21 days of CLFS were due solely to the fast-to-slow fibre type transformational stimulus mediated through existing intrafibre myonuclei.

In contrast to the works of Rosenblatt & Parry (1992, 1993), which showed no attenuation of fast-to-slow fibre type transformations in the extensor digitorum longus in response to 4 weeks of compensatory overload after exposure to a single dose of γ-irradiation, the results of the present study showed a modest, yet significant attenuation of CLFS-induced fast-to-slow transformations at the protein level during weekly exposure to ionising irradiation. Specifically the final fast type IIA to I transformation did not occur. Interestingly, MHC mRNA expression was not different between IRR-Stim and Stim. Therefore, in those muscles that were exposed to γ-irradiation, the limiting factor in CLFS-induced fast-to-slow fibre type transformation does not appear to be the ability to produce MHC mRNA, but the signalling pathways associated with post-transcriptional and/or translational regulation. Results of the current study also show that the CLFS-induced metabolic transformations, as reflected by the similar changes in the activity levels of marker enzymes of glycolytic (GAPDH) and aerobic-oxidative (CS) energy metabolism (Pette & Vrbová, 1992; Pette & Staron, 1997), are unaffected by exposure to satellite cell ablation. Collectively, the findings of the present study indicate that although considerable plasticity occurs within existing myonuclei to support fibre type transformations, satellite cell contributions may further facilitate this process.

3.4.3 Conclusions

Results of the present study show that CLFS-induced fast-to-slow fibre type transformations are moderately attenuated at the protein level in rat tibialis anterior muscles exposed to γ-irradiation. Specifically, the final fast type IIA to type I transformation did not occur. Thus, it appears that the roles of satellite cells during CLFS-induced fast-to-slow fibre type transformations may be to maintain stability of the transformed state within the fast fibre types and allow the final fast-twitch to slow-twitch transformation to occur.

Table 3.1 Fibre cross sectional areas of rat tibialis anterior muscles.

	Fibre cross sectional area (μm^2)									Fibre cross sectional area expressing a particular MHC isoform (μm^2)			
Condition	I	I/IIA	IIA	IIA/D(X)	IIA/D(X)/ IIB	IID(X)	IID(X)/ IIB	IIB	I/IIA/ IID(X)/IIB	I	IIA	IID(X)	IIB
Control	818 ± 45	635±191	975±55	479±228		1335±71	255±255	2593±130		854±57	976±56	1334±71	2591±129
IRR	1037±123 c	604±244	1154±151	550±265	231±231	1507±152	717±340	2971±221		1019±122	1152±148	1498±150	2938±220
IRR-Stim	1018±40 c	952±227	988±78	592±222	1563±129 γ	930±276 γ	204±204	966±345 c, γ	1113±416	1104±73 c	1310±73 c	1217±277	1277±347 c, γ
Stim	893±47	558±125	919±79 γ	584±176	1262±121	369±183 c, γ, *		652±166 c, γ	578±287	889±47 *	1064±92 *	974±171 γ	922±202 c, γ

Data are means ± SEM expressed as muscle fibre areas. Statistical symbols indicate difference from: [c] Control, [γ] IRR, [*] IRR-Stim

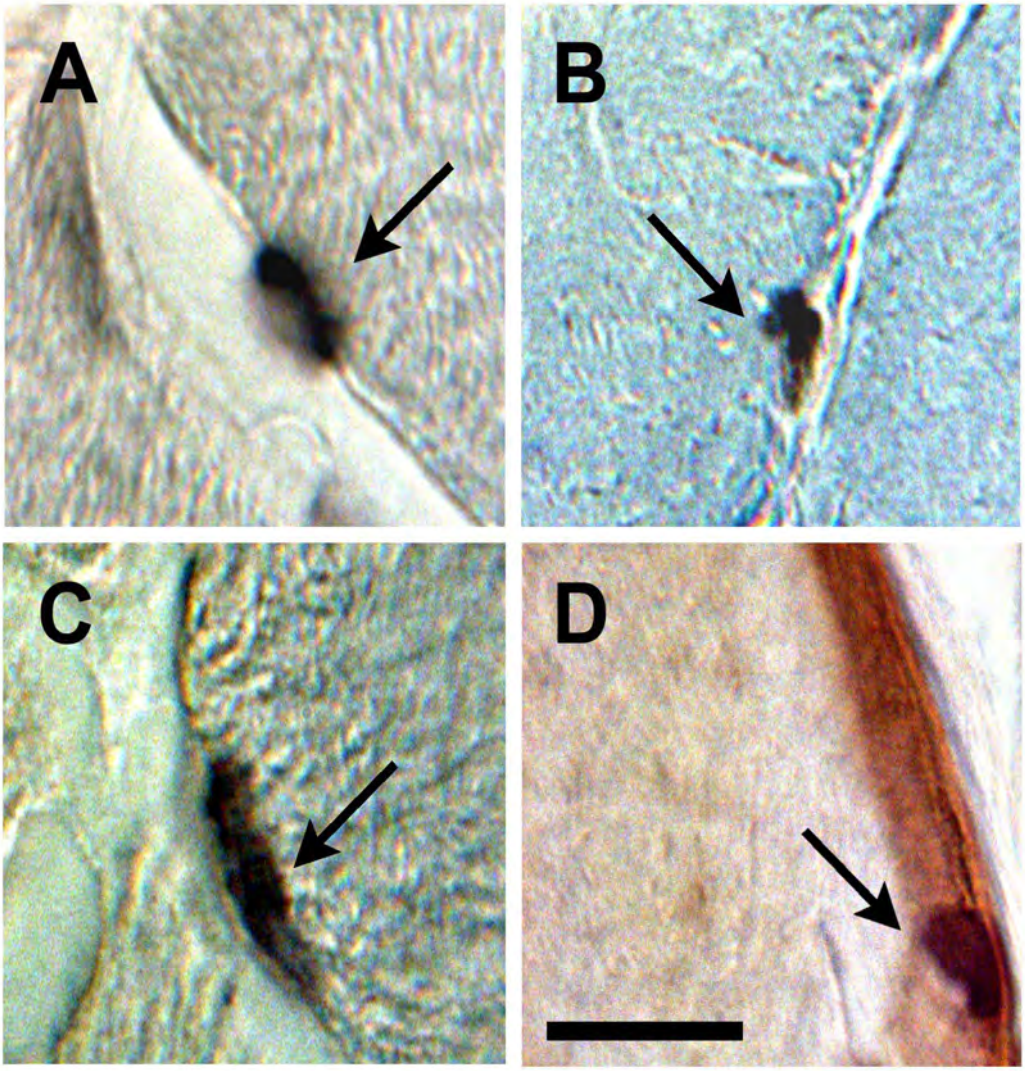

Figure 3.1 Photomicrographs of representative immunohistochemical stains of M-cadherin (*A*), BrdU (*B*), myogenin (*C*), and laminin and haematoxylin (*D*). These stains were used to identify quiescent satellite cells (*A*; arrow), proliferating satellite cells (*B*; arrow), terminally differentiating satellite cell progeny (*C*; arrow) and intrafibre muscle nuclei (*D*; arrow) in rat tibialis anterior muscles. Scale bar represents 40 μm.

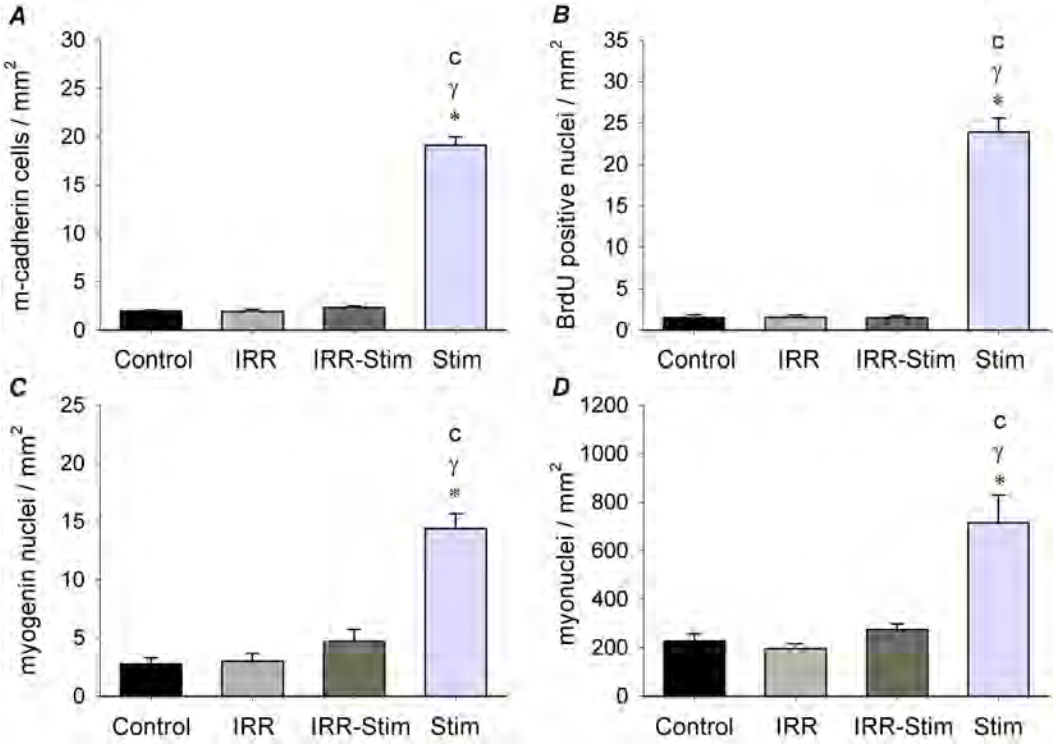

Figure 3.2 Number of quiescent satellite cells (*A*), proliferating satellite cells (*B*), satellite cell progeny committed to or in the later stages of terminal differentiation (*C*), and intrafibre muscle nuclei (*D*) per unit area in rat tibialis anterior muscles. Statistical symbols indicate difference from: ^{c} Control, $^{\gamma}$ IRR, * IRR-Stim ($P < 0.05$).

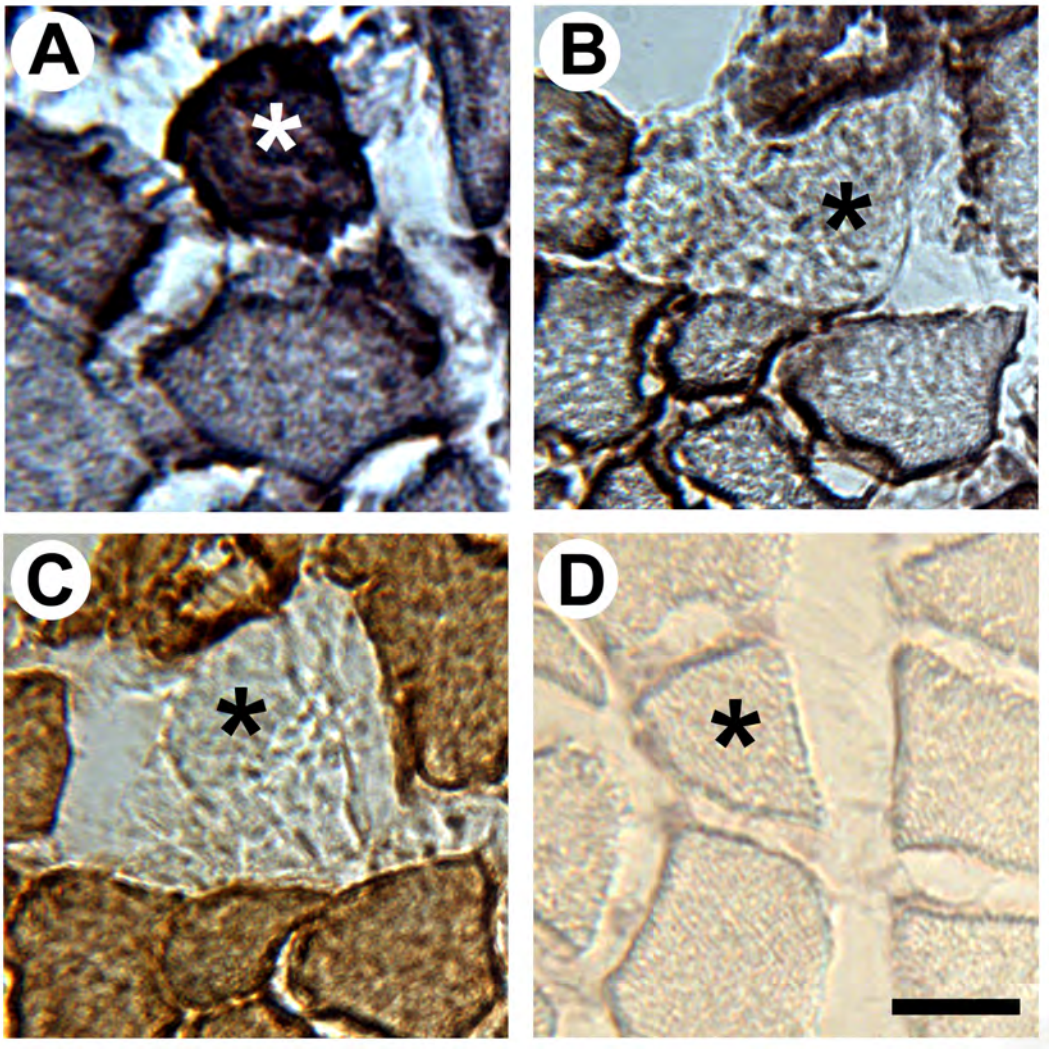

Figure 3.3 Example of the criteria used to determine a damaged fibre in rat tibialis anterior muscle (asterisk), which required positive staining for vimentin (*A*), the absence of dystrophin (*B*) and the absence of desmin positivity (*C*). IgG control (*D*). Scale bar represents 30 μm.

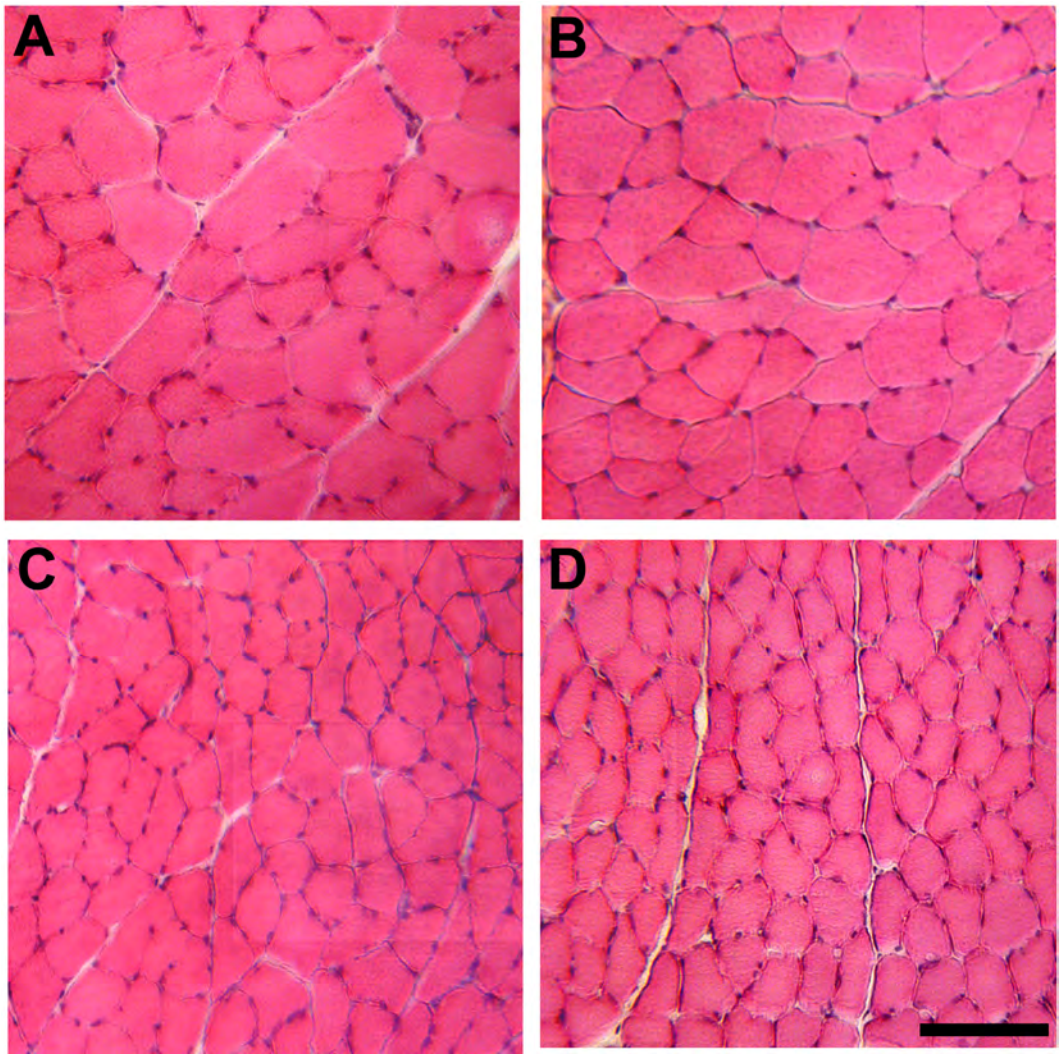

Figure 3.4 Representative photomicrographs of haematoxylin and eosin stains of Control (*A*), IRR (*B*), IRR-Stim (*C*) and Stim (*D*) in rat tibialis anterior muscles. Scale bar represents 100 μm.

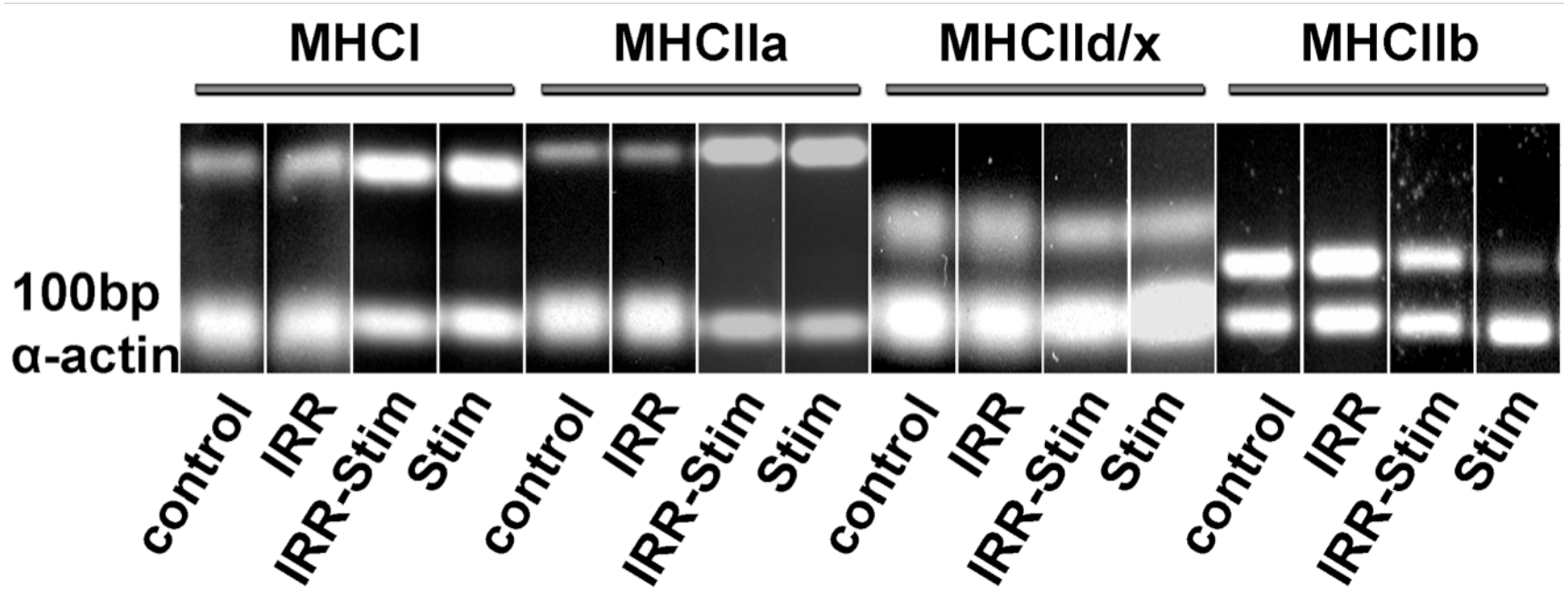

Figure 3.5 RT-PCR method used to evaluate relative mRNA expression in adult MHC isoforms and α-actin mRNA in rat tibialis anterior muscles.

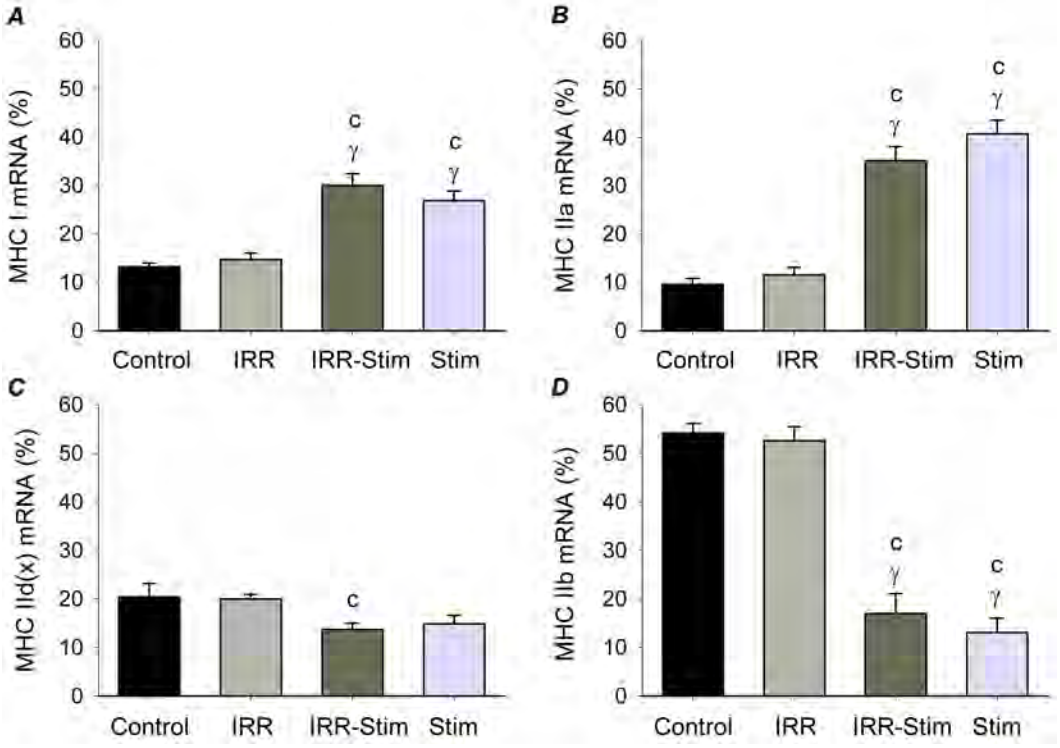

Figure 3.6 MHCI mRNA (*A*), MHCIIa mRNA (*B*), MHCIId(x) mRNA (*C*), and MHCIIb mRNA (*D*) expression displayed as the percent of total MHC mRNA content in rat tibialis anterior muscles. Statistical symbols indicate difference from: ^{c} Control, $^{\gamma}$ IRR, * IRR-Stim ($P < 0.05$).

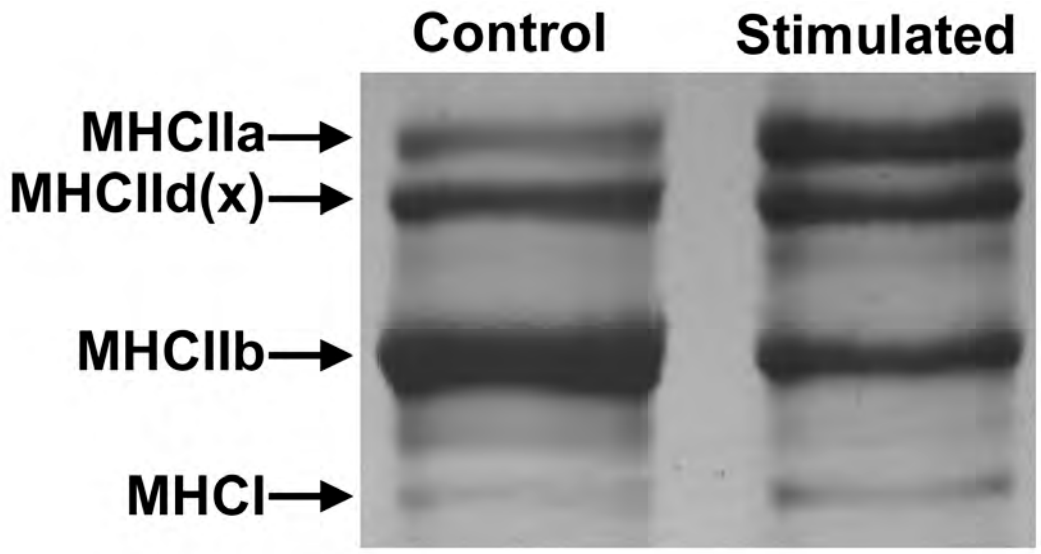

Figure 3.7 Example of the electrophoretic method used to quantify MHC isoform composition of rat tibialis anterior muscle. Control and Stimulated (Stim) are shown.

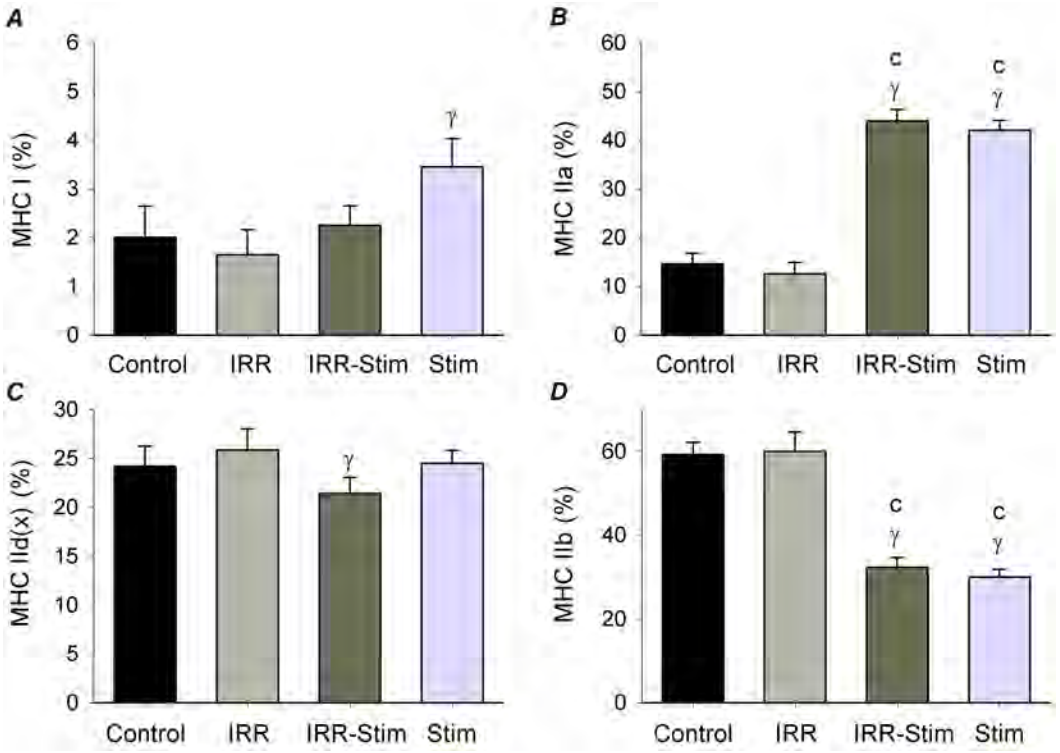

Figure 3.8 Percentage of MHCI (*A*), MHCIIa (*B*), MHCIId(x) (*C*) and MHCIIb (*D*) distribution in rat tibialis anterior muscles as determined by densitometric evaluation of triplicate gels. Statistical symbols indicate difference from: ^{c} Control, $^{\gamma}$ IRR, * IRR-Stim ($P < 0.05$).

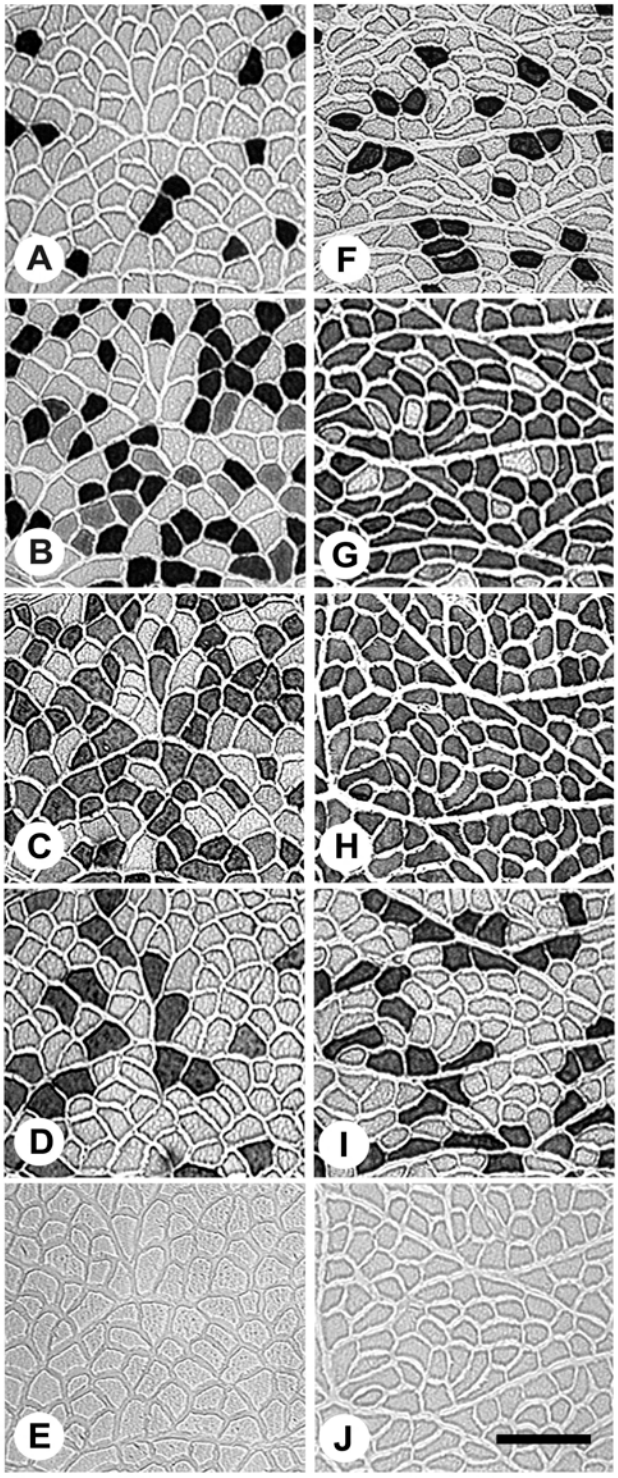

Figure 3.9 Representative photomicrographs of MHC immunohistochemistry of Control (*A, B, C, D, E*) and IRR-Stim (*F, G, H, I, J*) in rat tibialis anterior muscles. *A* and *F*, immunostains for MHCI (clone BA-D5); *B* and *G*, immunostains for MHCIIa (clone SC-71); *C* and *H*, immunostains for all MHC's except MHCIId(x) (clone BF-35); *D* and *I*, immunostains for MHCIIb (clone BF-F3); *E* and *J*, IgG control. Scale bar represents150 μm.

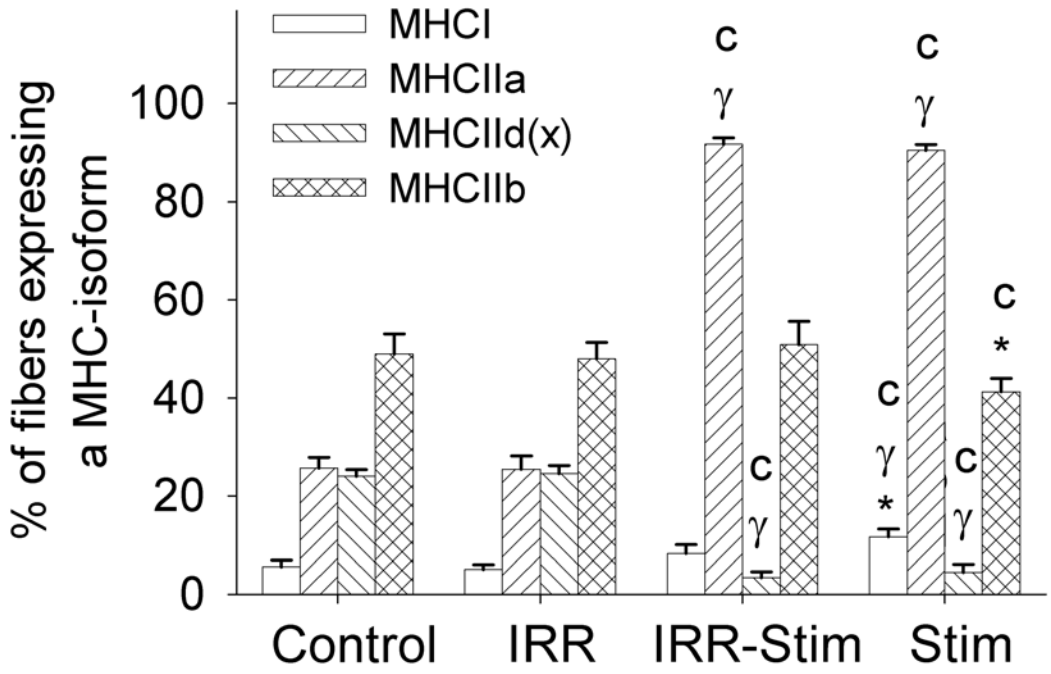

Figure 3.10 The percentage of fibres expressing a particular MHC isoform in rat tibialis anterior muscles. Statistical symbols indicate difference from: ^{c} Control, $^{\gamma}$ IRR, * IRR-Stim ($P < 0.05$).

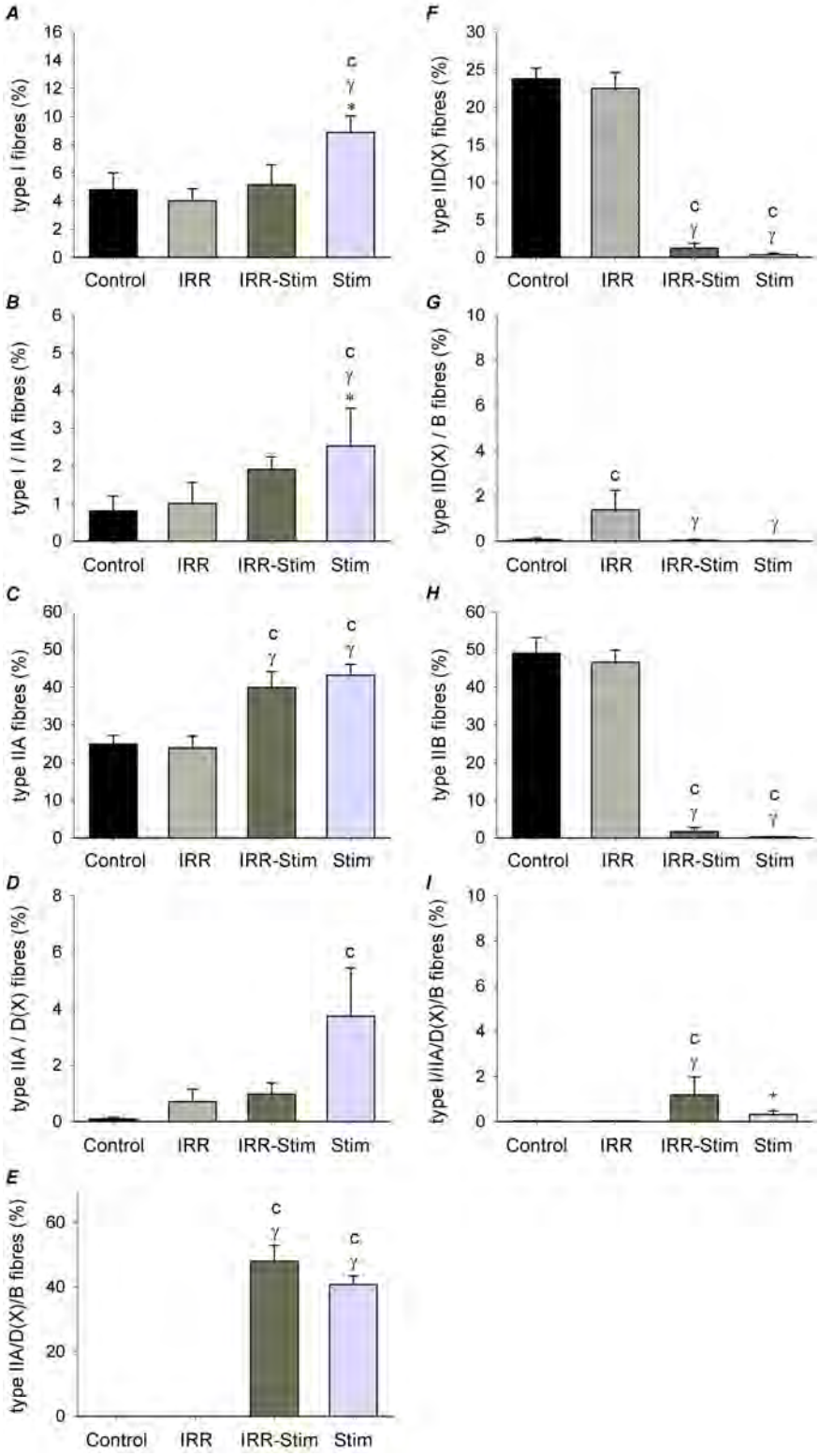

Figure 3.11 The proportion of pure and hybrid fibre types I (*A*), I/IIA (*B*), IIA (*C*), IIA/D(X) (*D*), IIA/D(X)/B (*E*), IID(X) (*F*), IID(X)/B (*G*), IIB (*H*), and I/IIA/D(X)/B (*I*) in rat tibialis anterior muscles. Statistical symbols indicate difference from: ^{c} Control, $^{\gamma}$ IRR, * IRR-Stim ($P < 0.05$).

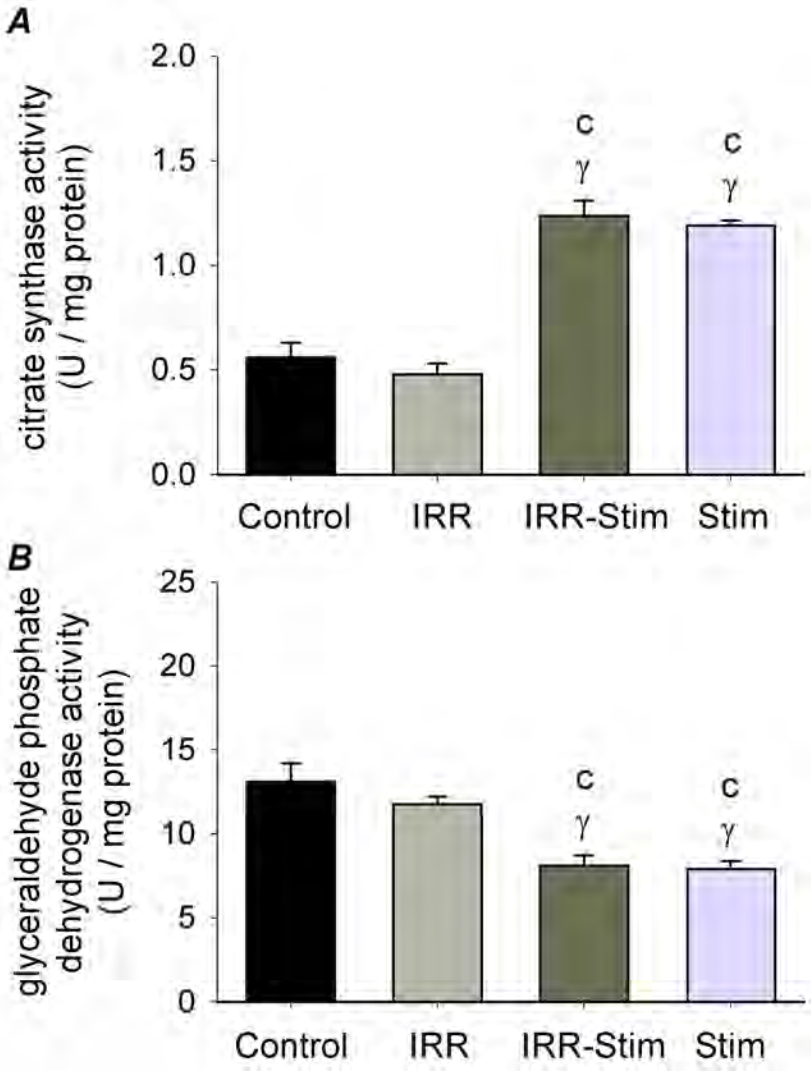

Figure 3.12 Citrate synthase (*A*) and glyceraldehyde phosphate dehydrogenase (*B*) activities in rat tibialis anterior muscles. Statistical symbols indicate difference from: ^{c} Control, $^{\gamma}$ IRR, * IRR-Stim ($P < 0.05$).

3.5 REFERENCES

Adams GR, Caiozzo VJ, Haddad F & Baldwin KM. (2002). Cellular and molecular responses to increased skeletal muscle loading after irradiation. *Am J Physiol Cell Physiol* **283,** C1182-C1195.

Bamford JA, Lopaschuk GD, MacLean IM, Reinhart ML, Dixon WT & Putman CT. (2003). Effects of chronic AICAR administration on the metabolic and contractile phenotypes of rat slow- and fast-twitch skeletal muscles. *Can J Physiol Pharmacol* **81,** 1072-1082.

Bass A, Brdiczka D, Eyer P, Hofer S & Pette D. (1969). Metabolic differentiation of distinct muscle types at the level of enzymatic organization. *Eur J Biochem* **10,** 198-206.

Bischoff R, Engel AG & Franzini-Armstrong C. (1994). The satellite cell and muscle regeneration. In *Myology*, pp. 97-112. McGraw-Hill, N.Y.

Charge SB & Rudnicki MA. (2004). Cellular and molecular regulation of muscle regeneration. *Physiol Rev* **84,** 209-238.

Coggle JE. (1983). *Biological effects of radiation*. Taylor and Francis, London.

Delp MD & Pette D. (1994). Morphological changes during fiber type transitions in low-frequency- stimulated rat fast-twitch muscle. *Cell Tissue Res* **277,** 363-371.

Gibson MC & Schultz E. (1982). The distribution of satellite cells and their relationship to specific fiber types in soleus and extensor digitorum longus muscles. *Anat Rec* **202,** 329-337.

Gibson MC & Schultz E. (1983). Age-related differences in absolute numbers of skeletal muscle satellite cells. *Muscle Nerve* **6,** 574-580.

Gulati AK. (1987). The effect of X-irradiation on skeletal muscle regeneration in the adult rat. *J Neurol Sci* **78,** 111-120.

Hämäläinen N & Pette D. (1996). Slow-to-fast transitions in myosin expression of rat soleus muscle by phasic high-frequency stimulation. *FEBS Lett* **399,** 220-222.

Heslop L, Morgan JE & Partridge TA. (2000). Evidence for a myogenic stem cell that is exhausted in dystrophic muscle. *J Cell Sci* **113 (Pt 12),** 2299-2308.

Jaschinski F, Schuler MJ, Peuker H & Pette D. (1998). Changes in myosin heavy chain mRNA and protein isoforms of rat muscle during forced contractile activity. *Am J Physiol Cell Physiol* **274,** C365-C370.

Kuschel R, Yablonka-Reuveni Z & Bornemann A. (1999). Satellite cells on isolated myofibers from normal and denervated adult rat muscle. *J Histochem Cytochem* **47,** 1375-1383.

Laemmli UK. (1970). Cleavage of structural proteins during the assembly of the head of bacteriophage T4. *Nature* **227,** 680-685.

Lewis RB. (1954). Changes in striated muscle following single intense doses of X-rays. *Lab Invest* **3,** 48-55.

Ljubicic V, Adhihetty PJ & Hood DA. (2005). Application of animal models: chronic electrical stimulation-induced contractile activity. *Can J Appl Physiol* **30,** 625-643.

McGeachie JK, Grounds MD, Partridge TA & Morgan JE. (1993). Age-related changes in replication of myogenic cells in mdx mice: quantitative autoradiographic studies. *J Neurol Sci* **119,** 169-179.

Mozdziak PE, Schultz E & Cassens RG. (1996). The effect of in vivo and in vitro irradiation (25 Gy) on the subsequent in vitro growth of satellite cells. *Cell Tissue Res* **283,** 203-208.

Mozdziak PE, Schultz E & Cassens RG. (1997). Myonuclear accretion is a major determinant of avian skeletal muscle growth. *Am J Physiol* **272,** C565-C571.

Peters D, Barash IA, Burdi M, Yuan PS, Mathew L, Friden J & Lieber RL. (2003). Asynchronous functional, cellular and transcriptional changes after a bout of eccentric exercise in the rat. *J Physiol* **553,** 947-957.

Pette D, Sketelj J, Skorjanc D, Leisner E, Traub I & Bajrovic F. (2002). Partial fast-to-slow conversion of regenerating rat fast-twitch muscle by chronic low-frequency stimulation. *J Muscle Res Cell Motil* **23,** 215-221.

Pette D & Staron RS. (1997). Mammalian skeletal muscle fiber type transitions. *Int Rev Cytol* **170,** 143-223.

Pette D & Staron RS. (2000). Myosin isoforms, muscle fiber types, and transitions. *Microsc Res Tech* **50,** 500-509.

Pette D & Vrbová G. (1992). Adaptation of mammalian skeletal muscle fibers to chronic electrical stimulation. *Rev Physiol Biochem Pharmacol* **120,** 115-202.

Pette D & Vrbová G. (1999). What does chronic electrical stimulation teach us about muscle plasticity? *Muscle Nerve* **22,** 666-677.

Phelan JN & Gonyea WJ. (1997). Effect of radiation on satellite cell activity and protein expression in overloaded mammalian skeletal muscle. *Anat Rec* **247,** 179-188.

Putman CT, Conjard A, Peuker H & Pette D. (1999a). Alpha-cardiac like myosin heavy chain MHCI-alpha is not upregulated in transforming rat muscle. *J Muscle Res Cell Motil* **20,** 155-162.

Putman CT, Dixon WT, Pearcey J, MacLean IM, Jendral MJ, Kiricsi M, Murdoch GK & Pette D. (2004). Chronic low-frequency stimulation up-regulates uncoupling protein-3 in transforming rat fast-twitch skeletal muscle *Am J Physiol Regul Integr Comp Physiol* **287,** R1419-R1426.

Putman CT, Düsterhöft S & Pette D. (1999b). Changes in satellite cell content and myosin isoforms in low-frequency- stimulated fast muscle of hypothyroid rat. *J Appl Physiol* **86,** 40-51.

Putman CT, Düsterhöft S & Pette D. (1999c). Satellite cell proliferation and myogenin expression during fast-to-slow muscle fibre type transformation. *FASEB J* **13,** A409.

Putman CT, Düsterhöft S & Pette D. (2000). Satellite cell proliferation in low-frequency stimulated fast muscle of hypothyroid rat. *Am J Physiol Cell Physiol* **279,** C682-C690.

Putman CT, Sultan KR, Wassmer T, Bamford JA, Skorjanc D & Pette D. (2001). Fiber-type transitions and satellite cell activation in low-frequency-stimulated muscles of young and aging rats. *J Gerontol A Biol Sci Med Sci* **56,** B510-B519.

Reichmann H, Srihari T & Pette D. (1983). Ipsi- and contralateral fibre transformations by cross-reinnervation. A principle of symmetry. *Pflügers Arch* **397,** 202-208.

Robertson TA, Grounds MD & Papadimitriou JM. (1992). Elucidation of aspects of murine skeletal muscle regeneration using local and whole body irradiation. *J Anat* **181 (Pt 2),** 265-276.

Rosenblatt DJ & Parry DJ. (1992). Gamma irradiation prevents compensatory hypertrophy of overloaded mouse extensor digitorum longous muscle. *J Appl Physiol* **73,** 2538-2543.

Rosenblatt DJ & Parry DJ. (1993). Adaptation of rat extensor digitorium longous muscle to gamma irradiation and overload. *Pflügers Arch* **423,** 255-264.

Rosenblatt DJ, Yong D & Parry DJ. (1994). Satellite cell activity is required for hypertrophy of overloaded adult rat muscle. *Muscle Nerve* **17,** 608-613.

Schiaffino S, Gorza L, Pitton G, Saggin L, Ausoni S, Sartore S & Lomo T. (1988). Embryonic and neonatal myosin heavy chain in denervated and paralyzed rat skeletal muscle. *Dev Biol* **127,** 1-11.

Schiaffino S, Gorza L, Sartore S, Saggin L, Ausoni S, Vianello M, Gundersen K & Lomo T. (1989). Three myosin heavy chain isoforms in type 2 skeletal muscle fibres. *J Muscle Res Cell Motil* **10,** 197-205.

Schultz E. (1996). Satellite cell proliferative compartments in growing skeletal muscles. *Dev Biol* **175,** 84-94.

Schultz E & McCormick KM. (1994). Skeletal muscle satellite cells. *Rev Physiol Biochem Pharmacol* **123,** 213-257.

Simoneau JA & Pette D. (1988). Species-specific effects of chronic nerve stimulation upon tibialis anterior muscle in mouse, rat, guinea pig and rabbit. *Pflügers Arch* **412,** 86-92.

Srere PA & Lowenstein JM. (1969). Citrate synthase. In *Citric Acid Cycle*, ed. Colowick SP & Kaplan NO, pp. 3-11. Academic Press, New York, London.

Wakeford S, Watt DJ & Partridge TA. (1991). X-irradiation improves mdx mouse muscle as a model of myofiber loss in DMD. *Muscle Nerve* **14,** 42-50.

Weller B, Karpati G, Lehnert S, Carpenter S, Ajdukovic B & Holland P. (1991). Inhibition of myosatellite cell proliferation by gamma irradiation does not prevent the age-related increase of the number of dystrophin-positive fibers in soleus muscles of mdx female heterozygote mice. *Am J Pathol* **138,** 1497-1502.

Wheldon TE, Michalowski AS & Kirk J. (1982). The effect of irradiation on function in self-renewing normal tissues with differing proliferative organisation. *Br J Radiol* **55,** 759-766.

[3]CHAPTER FOUR

SATELLITE CELL ABLATION ATTENUATES SHORT-TERM FAST-TO-SLOW FIBRE TYPE TRANSFORMATIONS IN RAT FAST-TWITCH SKELETAL MUSCLE

4.1 INTRODUCTION

Adult skeletal muscle contains heterogeneous, post-mitotic fibres that are capable of adjusting their structural, functional, metabolic and molecular properties in response to altered contractile demands such as endurance exercise. MHC is an important myofibrillar protein that largely dictates the rate of force development and maximum shortening velocity of cross-bridge formation, thus forming the basis for the most accepted and widely used method of fibre type classification (Pette & Staron, 1997). MHC-based fibre types are classified as type I, IIA, IID(X) and IIB that contain the corresponding MHC isoforms listed in increasing order of shortening velocity: MHCI, MHCIIa, MHCIId(x) and MHCIIb (Pette & Staron, 1997). CLFS is a model of endurance exercise training that induces fast-to-slow fibre type transformations that follow the "next nearest-neighbour" rule (reviewed by Pette & Staron, 2000; Pette, 2002). According to this rule, hybrid fibre types, which co-express MHC isoforms within a single fibre, bridge the gaps between the pure fibre types undergoing a predictable pattern of fast-to-slow transformation as follows: IIB→IID(X)/B→IID(X)→ IIA/D(X)→IIA→I/IIA→I. Additionally, CLFS-induced fast-to-slow fibre type transformations occur in the absence of fibre injury in the rat and are associated with increases in satellite cell number, activity and fusion to transforming fibres (Delp & Pette, 1994; Putman *et al.*, 1999, 2000; Putman *et al.*, 2001; [4]Martins *et al.*, 2006).

---

[3] A version of this chapter has been published and all tables and figures have been reproduced with permission from Martins KJ, Murdoch GK, Shu Y, Harris RL, Gallo M, Dixon WT, Foxcroft GR, Gordon T and Putman CT. (2009). *Pflügers Arch* **458**, 325-335.

[4] Martins *et al*. 2006, which is a published version of Chapter 3, will hereafter be referred to as Chapter 3.

Satellite cells are myogenic stem cells associated with adult skeletal muscle fibres that underlie the regenerative, and possibly adaptive, potential of muscle. It is well established that in response to skeletal muscle hypertrophic stimuli or damage, quiescent satellite cells begin to actively cycle and fuse with existing myofibres or with each other, creating new myonuclei or forming new myofibres, respectively (reviewed by Schultz & McCormick, 1994; Hawke & Garry, 2001; Charge & Rudnicki, 2004; Adams, 2006; O'Connor & Pavlath, 2007). As Schultz & Darr (1990) and Bamman (2007) point out, however, the role of satellite cells in endurance exercise-induced skeletal muscle fast-to-slow fibre type adaptation in the absence of injury is less clear. Results from Chapter 3 show that in rat tibialis anterior muscles exposed to weekly doses of γ-irradiation, long-term (21 days) CLFS-induced fast-to-slow fibre type transformations within the fast fibre population occurred normally, while the final fast type IIA to slow type I fibres was prevented. This model of γ-irradiation was shown to completely ablate the satellite cell population (Chapter 3). At this time point, 80-90% of fast-to-slow fibre type transformations have already occurred (Jaschinski *et al.*, 1998), suggesting the primary roles of satellite cells during long-term CLFS-induced fast-to-slow fibre type transformations may be to i) maintain stability of the transformed state (Schultz *et al.*, 1990) within the fast fibre types and ii) allow the final fast-twitch to slow-twitch transformation to occur (Chapter 3).

On the other hand, CLFS-induced fast-to-slow fibre type transformations are known to go through a unique period of rapid transformation within the first 10 days. Jaschinski *et al.* (1998) detected fast-to-slow MHC isoform transformations beginning at the mRNA level after 3 days of CLFS that rapidly continued to change through 10 days. Corresponding changes at the MHC protein level first occurred at 5 days of stimulation and were found to be most rapidly transforming by 10 days of CLFS (Jaschinski *et al.*, 1998; Putman *et al.*, 1999). Interestingly, maximum satellite cell activity and fusion to transforming fibres, mostly within the fast fibre population, have also been shown to occur between 5 and 10 days of CLFS (Putman *et al.*, 1999). Collectively, these observations

suggest satellite cells may play an active role in the early phase of transformation to CLFS, especially within the fast fibre population.

The purpose of the present study was therefore to test the hypothesis that in those muscles exposed to γ-irradiation, short-term (1 to 10 days) CLFS-induced fast-to-slow fibre type transformations would be i) attenuated in the fast fibre population and ii) prevented from the final fast-twitch to slow-twitch transformation. Additionally, CLFS-induced satellite cell activation has not been investigated at time points earlier than 5 days in vivo. In light of the rapid CLFS-induced fast-to-slow transformations seen at the MHC mRNA and protein levels, it seems plausible that substantial satellite cell activation may occur within the first 4 days. CLFS was therefore applied for 1 to 10 days. In order to sustain a nonviable satellite cell population throughout this time, tibialis anterior muscles were exposed to a 25 Gy dose of γ-irradiation before the onset of CLFS and at regular intervals throughout the stimulation period (Chapter 3). Satellite cell proliferation was assessed by continuous DNA labeling with BrdU in vivo, followed by immunolocalisation (Schultz, 1996). MHC-based fibre type transformations were evaluated at the mRNA level by real-time RT-PCR (Vinsky *et al.*, 2007), and at the protein level by SDS-PAGE (Hämäläinen & Pette, 1996; Putman *et al.*, 2004) and immunohistochemistry (Putman *et al.*, 2001; Putman *et al.*, 2003).

4.2 METHODS

4.2.1 Animal Treatment and Care

Fifty-four adult male Wistar rats (Charles River Laboratories, Montreal, PQ, Canada) weighing 320 ± 3 g (mean ± SEM) were used in this study. Animals were individually housed under controlled environmental conditions (22°C with alternating 12 h light and dark cycles) and received standard rat chow and water *ad libitum*. All animal procedures were carried out in accordance with the guidelines of the CCAC and received ethical approval from the University of

Alberta. Animals were randomly assigned to one of the following nine groups receiving: sham operation of the left leg only (Control); γ-irradiation plus 1 day (1d IRR-Stim), 2 days (2d IRR-Stim), 5 days (5d IRR-Stim) or 10 days (10d IRR-Stim) of CLFS of the left leg only; 1 day (1d Stim), 2 days (2d Stim), 5 days (5d Stim) or 10 days (10d Stim) of CLFS only (n = 6, animals each group).

It has been previously shown that low doses of γ-irradiation alone (i.e. a single 60 Gy dose or three weekly 25 Gy doses) do not cause skeletal muscle fibre damage (Lewis, 1954) or MHC protein, mRNA expression and metabolic abnormalities (Chapter 3). In accordance with the guidelines of the CCAC, a Control plus γ-irradiation group could not be justified as ethically appropriate and was therefore not included in this study. Unstimulated contralateral right legs served as internal controls. The application of CLFS, however, elicited a compensatory effect in the contralateral control muscles due to increased weight bearing (data not shown), as previously observed (Putman *et al.*, 2000; Chapter 3), therefore comparisons were made to Control.

4.2.2 Chronic Low-Frequency Stimulation and BrdU Labeling

CLFS (10 Hz, impulse width 380 μs, 12 h day^{-1}) was applied across the left common peroneal nerve, directed to the tibialis anterior muscle for 1, 2, 5 or 10 consecutive days (Simoneau & Pette, 1988; Putman *et al.*, 2004). Animals received a continuous infusion of BrdU (10 mg ml^{-1}) via subcutaneously implanted Alzet® mini-osmotic pumps (model 2ML1, 10 μl hr^{-1} release rate and 2 ml volume) (Schultz, 1996), which were replaced 1 wk later in those animals receiving 10 days of stimulation.

4.2.3 Gamma Irradiation

One day before the onset of stimulation, satellite cells of the left tibialis anterior muscle were sterilised as before (Chapter 3). Briefly, anesthetised animals [75 mg (kg body wt)$^{-1}$ ketamine, 10 mg (kg body wt)$^{-1}$ xylezine and 0.5

mg (kg body wt)$^{-1}$ acepromazine maleate] were placed in a Gammacell 40 cesium-137 irradiation unit (Health Services Laboratory Animal Services, University of Alberta) and the left anterior crural compartment was exposed to a 25 Gy dose of γ-irradiation (0.56 Gy min^{-1}) while the remainder of the animal was shielded by two 2.5 cm thick lead plates. 10d IRR-Stim received a second 25 Gy dose of γ-irradiation 1 wk later.

4.2.4 Muscle Sampling

Upon completion of the stimulation period, animals were anesthetised and the tibialis anterior muscles were excised from both hindlimbs, quickly fixed in a slightly longitudinally stretched position and frozen in melting isopentane (-159°C). Muscles were stored in liquid nitrogen (-196°C). Animals were then euthanised with an overdose of Euthanyl [100 mg (kg body wt)$^{-1}$] (Bimedia-MTC Animal Health Inc., Cambridge, ON, Canada), followed by exsanguination.

4.2.5 Antibodies

The following monoclonal antibodies directed against adult and embryonic MHC isoforms (Schiaffino *et al.*, 1988; Schiaffino *et al.*, 1989) were harvested from the supernatant of hybridoma cell lines obtained from the American Type Culture Collection (Manassas, VA, USA): BA-D5 (IgG, anti-MHCI), SC-71 (IgG, anti-MHCIIa), BF-F3 (IgM, anti-MHCIIb) and BF-45 (IgG, anti-MHC-embryonic). Clone BF-35 (purified IgG, not MHCIIx) (also known as MHCIId) was a generous gift from Prof. S. Schiaffino (Padova, Italy). Mouse monoclonal anti-BrdU (clone BMC 9318) was obtained from Roche Diagnostics Corporation (Indianapolis, IN, USA). Biotinylated horse anti-mouse IgG (rat-absorbed, affinity-purified) and biotinylated goat anti-mouse IgM were obtained from Vector Laboratories, Inc. (Burlingame, CA, USA).

4.2.6 Immunohistochemistry for Myosin and BrdU

10 μm-thick transverse frozen sections were collected from the mid belly of each tibialis anterior muscle. Immunostaining was completed according to established protocols for MHC isoforms (Putman *et al.*, 2001; Putman *et al.*, 2003) and BrdU (Schultz, 1996). Briefly, sections were fixed for 15 min in 70% (v/v) ethanol, washed once in PBS-T, twice with PBS and then incubated for 15 min in 3% (v/v) H_2O_2 in methanol. Sections stained for BrdU were then incubated for 1 h in 2N HCl and washed as before. Sections stained for BA-D5, SC-71, BF-35, BF-45 and BrdU were incubated for 1 h in BS-1 containing avidin-D blocking reagent (Vector Laboratories Inc.). Sections stained for BF-F3 were incubated in BS-2. Sections were incubated overnight at 4°C with a primary antibody that was diluted in its corresponding blocking solution containing biotin blocking reagent (Vector Laboratories Inc.) Biotinylated horse anti-mouse IgG (BA-D5; SC-71; BF-35; BF-45; anti-BrdU) or biotinylated goat anti-mouse IgM (BF-F3) was then applied for 1 h (Vector Laboratories Inc.). After several washings, sections were incubated with Vectastain ABC Reagent according to the manufacturer's instructions (Vector Laboratories Inc.) and reacted with 0.07% (w/v) diaminobenzidine, 0.05% (v/v) H_2O_2 and 0.03% (w/v) $NiCl_2$ in 50 mM Tris-HCl (pH 7.5). All sections were subsequently dehydrated, cleared, and mounted in Entellan (Merck, Darmstadt, Germany).

4.2.7 Immunohistochemical Analyses

MHC isoform semi-quantitative analyses were completed with a Leitz Diaplan microscope (Ernst Leitz Wetzlar GmbH, Germany) fitted with a Pro-Series High Performance Charge-Coupled Digital camera (Cohu Inc., San Diego, CA, USA), Image-Pro Plus imaging software (Media Cybernetics Inc., Bethesda, MD, USA) and a custom-designed analytical program (Putman *et al.*, 2000). A similar number of fibres, totaling 60,996, were examined from each group for the various MHC isoforms from three representative cross-sectional areas of tibialis anterior muscles (i.e. deep, middle and superficial regions). Type I, IIA, IIB and

embryonic fibres were identified by positive staining and type IID(X) fibres were identified by the absence of staining with all antibodies directed against the various MHC isoforms. BrdU semi-quantitative analysis was completed with a Leka DMRBE microscope (Leica Microsystems GmbH Wetzal, Germany) at 640x magnification. BrdU positive nuclei were enumerated on cross-sections of all tibialis anterior muscles. A total area of 4.4 ± 0.06 mm^2 was examined for each muscle.

4.2.8 Electrophoretic Analysis of Myosin Heavy Chain Protein Isoforms

Quantitative MHC isoform analyses were completed as previously described (Hämäläinen & Pette, 1996; Putman *et al.*, 2004). Briefly, frozen tibialis anterior muscles were homogenised in an ice cold buffer containing 100 mM NaP_2O_7 (pH 8.5), 5 mM EGTA, 5 mM $MgCl_2$, 0.3 mM KCl, 10 mM DTT (Sigma-Aldrich, Oakville, ON, Canada) and 5 mg ml^{-1} of a protease inhibitor cocktail (Complete™, Roche Diagnostics Corporation). Please refer to Chapter 3, section 3.2.9 for futher details regarding the protease inhibitor cocktail. The supernatants of centrifuged samples were diluted 1:1 with glycerol and stored at -20°C until analysed. Extracts were diluted in modified Laemmli-lysis buffer (Laemmli, 1970) to a concentration of 0.2 μg μl^{-1}, boiled for 6 min and cooled on ice prior to gel loading. MHC isoforms were separated electrophoretically on 7% (w/v) polyacrylamide gels containing glycerol, under denaturing conditions. Samples (1 μg total protein per lane) were electrophoresed in duplicate at 275 V for 24 h at 8°C. Gels were then fixed and MHC isoforms were detected by silver staining and evaluated by integrated densitometry (ChemiGenius, GeneSnap and GeneTools, Syngene, UK).

4.2.9 Myosin Heavy Chain mRNA Analyses by Real-Time Reverse Transcriptase-Polymerase Chain Reaction

Patterns of MHC isoform expression were further analysed at the mRNA level using real-time RT-PCR. The TRIzol® RNA extraction procedure was performed according to an established procedure (Vinsky *et al.*, 2007). For a

detailed description of the extraction procedure, please refer to Chapter 3, section 3.2.10. The concentrations and purity of RNA extracts were evaluated by measuring the absorbance at 260 and 260/280 nm, respectively, using a NanoDrop ND 1000 system (Rose Scientific Ltd, Edmonton, AB, Canada). cDNA synthesis was performed according to an established procedure (Bamford *et al.*, 2003). Briefly, oligo (dT_{15}) primers (Invitrogen, Life Technologies, Burlington, ON, Canada) and M-MLV DNA polymerase (Invitrogen, Life Technologies) were added to diluted samples (1 μg μl^{-1}) and reverse transcription was performed for 1 h at 37°C. Primers (Invitrogen, Life Technologies) and Taqman-MGB probes (Applied Biosystems, Foster City, CA, USA) were designed with EMBL-EBI and aligned using Clustal W for rat MHCIβ (X15939), MHCIIa (L13606), MHCIId(x) (XM 213345) and MHCIIb (L24897) (Table 1). Real-time PCR was performed on 1 μl cDNA samples, in duplicate, using an ABI 7900HT thermocycler (Applied Biosystems). For futher details regarding the specific cycle thresholds and examples of amplification plots of the various MHC isoforms, please refer to Apendix B. 18S RNA (Applied Biosytems) was used as the endogenous control. Relative changes in MHC isoform gene expression were determined using the $2^{-\Delta\Delta Ct}$ method of analysis (Livak & Schmittgen, 2001). Please refer to Apendix C for a detailed list of each MHC isoform and 18S cycle threshold (Ct) value that was obtained for each group. Inter-assay variation was evaluated by repeated analysis of a known sample on each 96-well plate and confirmed to be negligible (data not shown). Additionally, the amplification efficiencies of the MHC- isoforms and 18S were similar (data not shown).

4.2.10 Statistical Analyses

Data are summarised as means ± SEM. Within each group (i.e. Stim or IRR-Stim) differences were assessed compared to Control (i.e. 1d, 2d, 5d or 10d Stim *versus* Control) using a one-way ANOVA. Differences between the IRR-Stim and Stim groups at each time point were assessed using a two-way ANOVA. When a significant *F* ratio was found for the interaction, differences were located using the Newman-Keuls post hoc analysis. Differences were considered

significant at $P < 0.05$. There were no differences between the left and right legs of Control, as determined by the t-test for dependent samples, therefore these data were pooled.

4.3 RESULTS

4.3.1 Animal and Muscle Weights

All animals initially weighed 321 ± 3 g and similarly gained 26 ± 5 g during 10 days of stimulation. Additionally, animal weights did not differ between Stim and IRR-Stim groups of the same number of days of stimulation at all other time points (i.e. 1d, 2d and 5d). Tibialis anterior muscle weights were not different between the left and right legs of all groups.

4.3.2 Satellite Cell Activity

An established method was used to assess satellite cell proliferation (Chapter 3). The number of proliferating and previously proliferating satellite cells was determined by quantifying BrdU staining. Only those stained nuclei that were unambiguously fused to existing muscle fibres were counted, as shown in Fig. 4.1*A*. CLFS first induced an increase in BrdU-positive nuclei at 1 day after the onset of stimulation (i.e. 1d Stim; 3.9-fold increase) up to a maximum of a 13.8-fold increase at 10 days of stimulation (i.e. 10d Stim) compared with Control (Fig. 4.1*B*). In contrast, γ-irradiation plus 1 day (i.e. 1d IRR-Stim; 2.1 ± 0.3 positively stained nuclei mm^{-2}), 2 days (i.e. 2d IRR-Stim; 1.4 ± 0.2), 5 days (i.e. 5d IRR-Stim; 1.6 ± 0.1) or 10 days (i.e. 10d IRR-Stim; 2.0 ± 0.3) of stimulation did not alter the number of proliferating and previously proliferating satellite cells compared with Control (Fig. 4.1*B*; 1.5 ± 0.2).

4.3.3 Myosin Heavy Chain mRNA Expression

CLFS-induced MHC isoform transformations at the mRNA level occurred in the direction of fast-to-slow at 10 days of stimulation [i.e. 10d Stim; MHCIIb

mRNA→MHCIId(x) mRNA→MHCIIa mRNA→MHCI mRNA]. Specifically, 10d Stim MHCI mRNA (Fig. 4.2*A*), MHCIIa mRNA (Fig. 4.2*B*) and MHCIId(x) mRNA (Fig. 4.2*C*) increased compared with Control, with no increase in the expression of MHCIIb mRNA (Fig. 4.2*D*). In 10d IRR-Stim, increases in MHC mRNA levels were observed in 10d IRR-Stim for MHCI (Fig. 4.2*A*) and MHCIIa (Fig. 4.2*B*) compared with Control. Additionally, 10d Stim MHCIId(x) mRNA was 6.9-fold greater compared with 10d IRR-Stim (Fig. 4.2*C*).

4.3.4 Myosin Heavy Chain Isoform Transformations

A representative gel showing the quantitative analytical method used to measure MHC isoform protein content in muscle extracts is illustrated in Fig. 4.3*A*. CLFS-induced fast-to-slow MHC isoform transformations were first observed at 5 days of stimulation [i.e. 5d Stim; MHCIIb→MHCIId(x)→MHCIIa] and continued further at 10 days of stimulation [i.e. 10d Stim; MHCIIb→MHCIId(x)→MHCIIa→MHCI] (Fig. 4.3*B*). Specifically, the slower MHCI and MHCIIa content of 10d Stim both increased 1.9-fold with a concomitant 1.3-fold decrease in MHCIIb content compared with Control. 10d IRR-Stim MHC fast-to-slow transformations only occurred amongst the fast MHC isoforms as shown by a 1.7-fold increase in MHCIIa along with a 1.3-fold decrease in MHCIIb content. Importantly, the relative content of IRR-Stim MHCI was not different from Control and the main effect of MHCI content was significantly greater in Stim compared with IRR-Stim ($P < 0.02$). This finding is consistent with Chapter 3 observations that showed the CLFS-induced fast MHCIIa to slow MHCI transformation did not occur in those muscles previously exposed to γ-irradiation. Interestingly, the relative content of MHCIId(x) in 10d IRR-Stim was significantly larger than in 10d Stim. This, however, likely reflects the restriction of fast-to-slow transformations to the fast MHC isoforms following satellite cell ablation.

4.3.5 Fibre Type Transformations

Detailed fibre type analysis, which included the detection of all pure and hybrid fibre types, were assessed by semi-quantitative immunohistochemical analyses on serial sections (Fig. 4.4) in the deep, middle and superficial regions of each tibialis anterior muscle. CLFS-induced fast-to-slow fibre type transformations were, however, only observed in the deep and middle regions and therefore the analysis was restricted to these areas. As similarly observed in MHC isoform proportions, fast-to-slow fibre type transformations began at 5 days of stimulation [i.e. IID(X)→IIA] and further continued at 10 days of stimulation [i.e. IID(X)→IIA→I] (Fig. 4.5). Specifically, 10d Stim displayed increases in the proportions of the slower type I/IIA (Fig. 4.5*B*), IIA/D(X) (Fig. 4.5*D*) and IIA/D(X)/B (Fig. 4.5*E*) fibres with a concomitant decrease in the proportion of the faster type IID(X) fibres (Fig. 4.5*F*) compared with Control. At 10 days of stimulation in IRR-Stim (i.e. 10d IRR-Stim), however, these fast-to-slow fibre type transformations were limited to the fast fibre population. Specifically, 10d IRR-Stim only displayed increases in the proportions of the hybrid type IIA/D(X)/B fibres (Fig. 4.5*E*) with a concomitant decrease in the proportion of the pure type IID(X) fibres (Fig. 4.5*F*) compared with Control. Most importantly, the emergence of hybrid fibre types that are a hallmark of the response to CLFS (reviewed by Pette, 2002) was not the same in 10d Stim and IRR-Stim. Specifically, the proportion of type IIA/D(X) fibres in 10d IRR-Stim was significantly lower compared with 10d Stim (Fig. 4.5*D*). The proportion of type IIA/D(X)/B fibres was also significantly lower in IRR-Stim compared with Stim (Fig. 4.5*E*; main effect $P < 0.02$). Additionally, consistent with Chapter 3 findings, proportions of the slowest type I (Fig. 4.5*A*) and type I/IIA (Fig. 4.5*B*) fibres in all IRR-Stim groups were not different from Control. Embryonic MHC was not detected in extrafusal fibres (data not shown).

4.4 DISCUSSION

The findings of the present study extend previous works (Delp & Pette, 1994; Putman *et al.*, 1999, 2000; Putman *et al.*, 2001; Chapter 3) by investigating early time points (i.e. 1 to 10 days) of CLFS-induced fast-to-slow fibre type transformations when maximum satellite cell activity and fusion to rapidly transforming fibres are known to occur, especially within the fast IIB and IID(X) fibre populations (Putman *et al.*, 1999). In the present study, the absence of increases in BrdU-positive nuclei in all IRR-Stim groups clearly shows that satellite cell activity was ablated throughout the entire study, thus allowing the early adaptive phase of CLFS-induced fast-to-slow fibre type transformations to be investigated in the absence of a viable satellite cell population. The novel findings of this study are that i) CLFS-induced satellite cell proliferation in vivo begins at 1 day of stimulation and continues throughout the 10 day stimulation period; in those muscles exposed to γ -irradiation, fast-to-slow fibre type transformations during short-term CLFS are ii) attenuated in the fast fibre population and iii) prevented from the final fast-twitch to slow-twitch transformation.

4.4.1 Chronic Low-Frequency Stimulation Model of Muscle Training

CLFS is a model of endurance muscle training resulting in skeletal muscle fast-to-slow fibre type transformations and associated fibre atrophy, which is ideal for studying the effects of increased contractile activity on various skeletal muscle structural, functional, metabolic and molecular properties in the absence of fibre damage in rat (as reviewed by Pette & Staron, 1997, 2000; Pette, 2002). The CLFS-induced decrease in fibre cross-sectional area, specifically in the fast IIB and IID(X) fibre types, is the result of transformation to a slower fibre type, as opposed to fibre degeneration (Delp & Pette, 1994; Chapter 3) or pathological atrophy. CLFS induces rapid and predictable fast-to-slow fibre type transformations by mimicking the electrical discharge pattern of slow motoneurons that innervate slow-twitch muscles. Unlike other rodent exercise models such as voluntary wheel running, however, it causes synchronous

recruitment of all targeted motor units, including those not normally recruited during endurance exercise training (Pette & Staron, 2000). In doing so, the adaptive potential of CLFS-targeted muscles is maximally challenged. Also, the standardised and highly reproducible conditions of CLFS allows for activity-induced fast-to-slow phenotypic changes to occur in a well-defined time-dependent manner (Jaschinski *et al.*, 1998; Pette, 2002). For these reasons, the CLFS model of muscle training was used in the present study.

4.4.2 Fibre Type Transformations in Irradiated Muscles

There are a limited number of studies that have investigated exercise-induced fast-to-slow fibre type transformations in muscles that have also been exposed to ionising radiation (Rosenblatt & Parry, 1992, 1993; Adams *et al.*, 2002; Li *et al.*, 2006). Results from Chapter 3 and the current study are in contrast with those previous investigations, which reported no attenuation of fast-to-slow fibre type transformations in response to overload (Rosenblatt & Parry, 1992, 1993; Adams *et al.*, 2002) or voluntary wheel running (Li *et al.*, 2006) in muscles that were also exposed to ionising radiation. The major differences between those studies (Rosenblatt & Parry, 1992, 1993; Adams *et al.*, 2002; Li *et al.*, 2006) and the present studies (Chapters 3 and 4) were three-fold. First, disruption of satellite cell mitotic activity after a single 25 Gy dose of γ-irradiation has been shown to occur for only 7 days (Mozdziak *et al.*, 1996) with significant recovery taking place 9 and 12 days post-irradiation (Wakeford *et al.*, 1991; McGeachie *et al.*, 1993; Mozdziak *et al.*, 1996). Therefore, weekly 25 Gy doses of γ-irradiation were administered to ensure continuous mitotic disruption of the satellite cell pool while previous studies (Rosenblatt & Parry, 1992, 1993; Adams *et al.*, 2002; Li *et al.*, 2006) only administered a single 25 Gy dose of ionising radiation before the onset of exercise. Consequently, in those studies, a significant amount of satellite cell proliferation was observed in response to 14 days of voluntary wheel running in mouse plantaris muscles (Li *et al.*, 2006) and a greater skeletal muscle DNA content was reported after 15 days of compensatory overload in rat plantaris muscles (Adams *et al.*, 2002). Second, in order to

determine the specific effectiveness of ionising radiation on preventing satellite cell proliferation and subsequent myonuclei contribution, only Li *et al.* (2006) and the present studies (Chapters 3 and 4) directly measured proliferating and previously proliferating satellite cells in vivo. On the other hand, Adams *et al.* (2002) measured DNA content and Rosenblatt & Parry reported myonuclear-to-myoplasmic volume ratio (Rosenblatt & Parry, 1993) or assumed satellite cell sterilisation (Rosenblatt & Parry, 1992). Third, comprehensive and detailed MHC isoform identification methods (i.e. immunohistochemistry, gel electrophoresis and RT-PCR) that detect both pure and hybrid fibre types, were used in Chapters 3 and the present study to assess fast-to-slow fibre type transformations. In contrast, others have only quantified the proportions of MHC protein isoforms (Adams *et al.*, 2002; Li *et al.*, 2006) or restricted their analyses to only adult pure fibre types (Rosenblatt & Parry, 1992, 1993). Taken together, these differences likely accounted for the ability to detect attenuation of fast-to-slow fibre type transformations in the IRR-Stim muscles in Chapter 3 and the present study.

4.4.3 Fast-to-Slow Fibre Type Transformations and Myonuclear Domains

Schultz & Darr (1990) were first to introduce the idea of satellite cell involvement in fast-to-slow fibre type transformations. They hypothesised that since slow-twitch skeletal muscle fibres contain a larger number of myonuclei, smaller cross-sectional areas and cytoplasmic volume (Gibson & Schultz, 1982, 1983) and therefore, smaller myonuclear domain sizes compared with fast-twitch fibres (Cheek, 1985; Schultz *et al.*, 1990; Tseng *et al.*, 1994; Roy *et al.*, 1999), satellite cells play an obligatory role in maintaining the newly fast-to-slow transformed state. Smaller myonuclear domains are presumably a requirement for higher biosynthetic activities and protein turn over in slow-twitch fibres (Goldberg, 1967). For example, the transformation from a fast-twitch to a slower-twitch fibre type would include a decrease in myonuclear domain size by the addition of new myonuclei coupled with a decrease in fibre cross-sectional area and cytoplasmic volume. The results of previous studies (Putman *et al.*, 2000) support this hypothesis, while data from the present study further indicates that

satellite cells may also facilitate fast-to-slow fibre type transformations during the early phase of transformation to CLFS.

It has been previously shown that during short-term CLFS, maximal satellite cell activity and fusion were primarily targeted to the fast IIB and IID(X) fibre types, which preceded fast-to-slow fibre type transformations (Jaschinski *et al.*, 1998; Putman *et al.*, 2000) and preceded decreases in the cross-sectional areas of those fibre types (Delp & Pette, 1994). Therefore, the myonuclear domain sizes of the fast fibre types, which are actively undergoing fast-to-slow transformations, are the first to decrease by the incorporation of satellite cells during short-term CLFS. By comparison, during long-term CLFS, further reductions in myonuclear domain sizes occur via decreases in fibre cross-sectional area of the newly transformed fibres and to a lesser extent by the fusion of satellite cell progeny (Chapter 3). In those muscles exposed to γ-irradiation, results from the present study show that short-term CLFS-induced fast-to-slow fibre type transformations, within the fast fibre population, were attenuated. These findings indicate that satellite cell activity may be important during short-term CLFS to reduce the myonuclear domain sizes of the fast fibre types, thus increasing necessary biosynthetic activity, allowing them to transform without delay. In contrast, satellite cells appear to play an obligatory role in the final transformation from fast type IIA to slow type I fibres (present study; Chapter 3).

4.4.4 Conclusions

Results of the present study show rat tibialis anterior muscles exposed to γ-irradiation, short-term CLFS-induced fast-to-slow fibre type transformations are attenuated in the fast fibre population and prevented from the final type IIA to I transformation. Thus satellite cells appear to play an active role early on in the time course during CLFS-induced fast-to-slow fibre type transformations. Considerable adaptive potential does, however, exist within myonuclei and their domains up to a certain threshold beyond which satellite cells may be required, especially for the final transformation from type IIA to type I fibres.

Table 4.1 Rat specific real-time reverse-transcriptase polymerase chain reaction primers and probes.

Target	Forward Primer	Reverse Primer	Probe
MHCIβ	5'-GCAGTTGGATGAGCGACTCA-3'	5'-TCCTCAATCCTGGCGTTGA-3'	5'-AGAAGGACTTTGAGTTAAAT-3'
MHCIIa	5'-GGCGGCAAGAAGCAGATC-3'	5'-TTCCGCTTCTGCTCACTCTCT-3'	5'-AGGCCAGAGTGCGTG-3'
MHCIId(x)	5'-GGCGGCAAGAAGCAGATC-3'	5'-TTCGTTTTCAACTTCTCCTTCAAGT-3'	5'-AGGCCAGGGTCCG-3'
MHCIIb	5'-GGCGGCAAGAAGCAGATC-3'	5'-TTTTCCACCTCGTTTTCAAGCT-3'	5'-TGGAGGCCAGAGTGA-3'

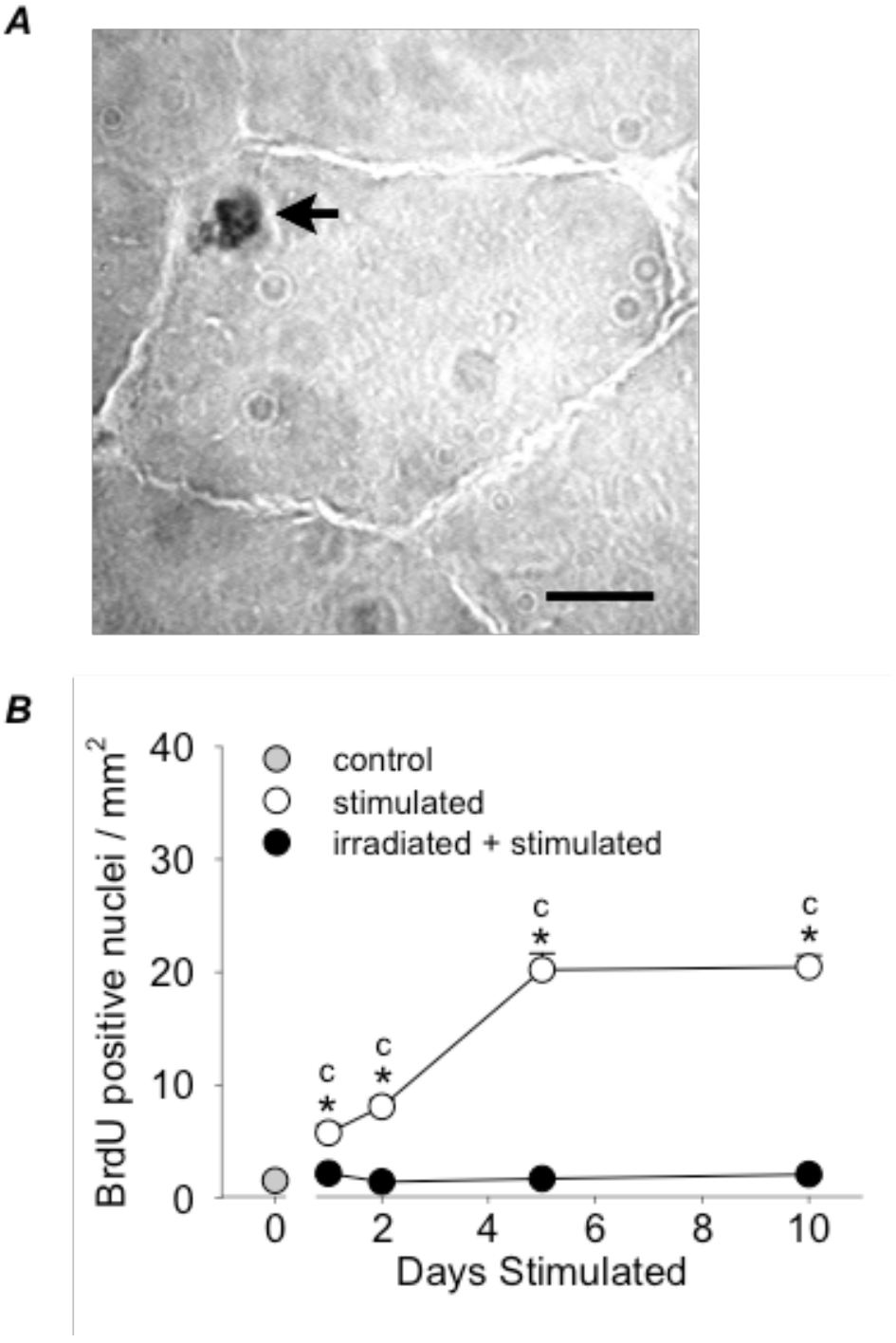

Figure 4.1 Photomicrograph of representative immunohistochemical BrdU stain used to identify proliferating and previously proliferating satellite cells (arrow) in rat tibialis anterior muscles (*A*). Bar represents 10 μm. Number of proliferating and previously proliferating satellite cells per unit area in rat tibialis anterior muscles (*B*). Statistical symbols indicate: ^{c} difference from Control, * difference between Stim and IRR-Stim of the same number of days of stimulation ($P < 0.05$).

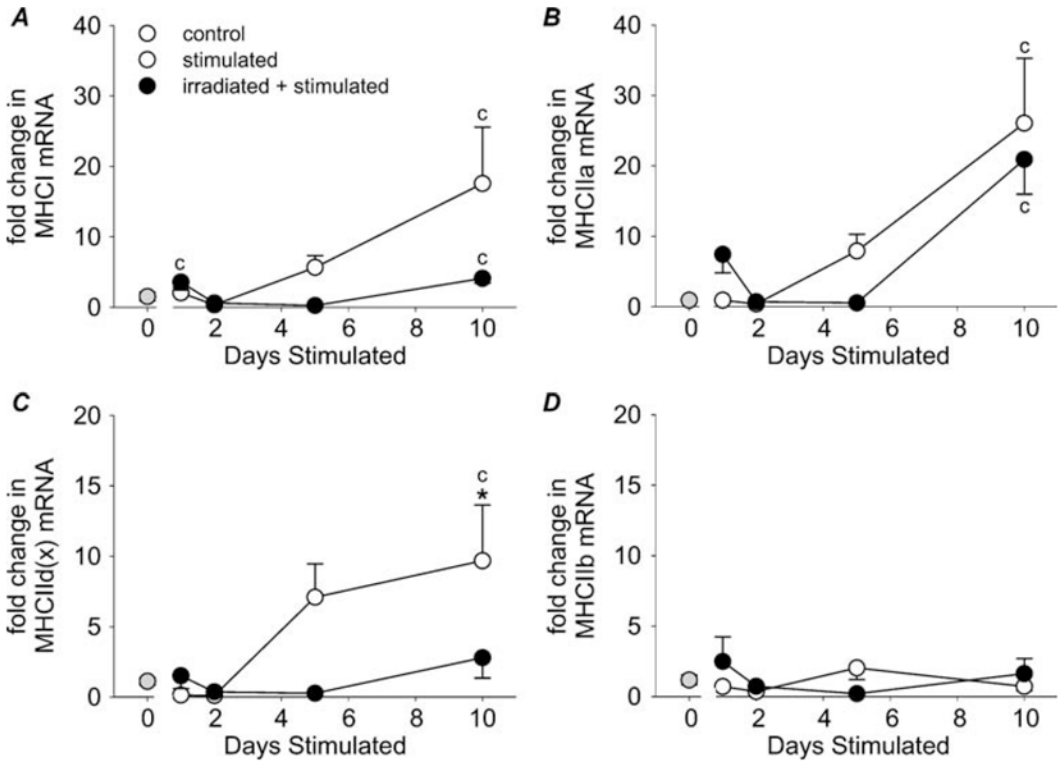

Figure 4.2 Fold changes in MHCI mRNA (*A*), MHCIIa mRNA (*B*), MHCIId(x) mRNA (*C*) and MHCIIb mRNA (*D*) gene expression levels in rat tibialis anterior muscles. Statistical symbols indicate: ^{c} difference from Control, * difference between Stim and IRR-Stim of the same number of days of stimulation ($P < 0.05$).

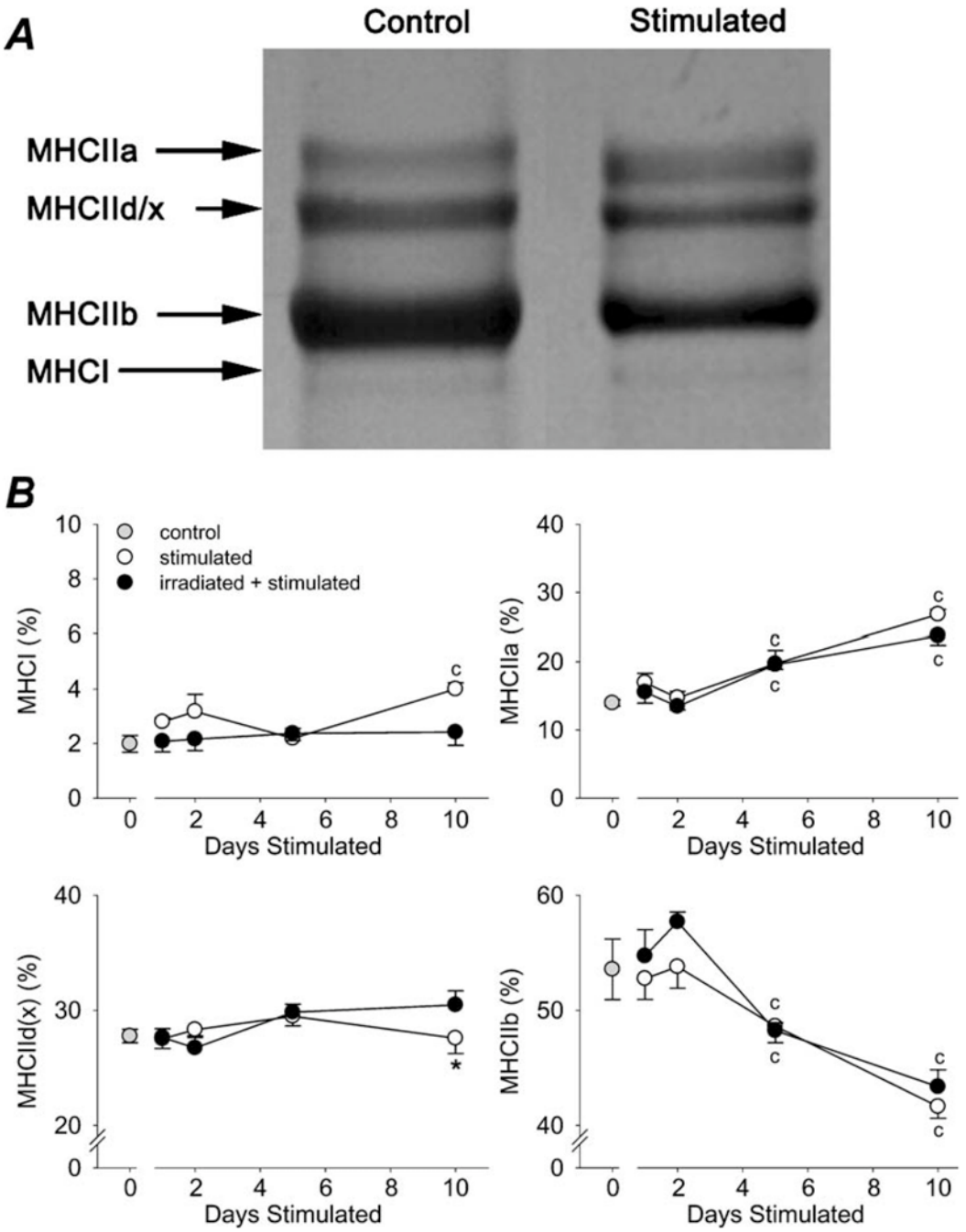

Figure 4.3 Example of the electrophoretic method used to quantify MHC isoform composition of rat tibialis anterior muscles (*A*). Control and stimulated (10d Stim) are shown. Percentage of MHCI, MHCIIa, MHCIId(x) and MHCIIb distribution in rat tibialis anterior muscles as determined by densitometric evaluation of duplicate gels (*B*). Statistical symbols indicate: ^{c} difference from Control, * difference between Stim and IRR-Stim of the same number of days of stimulation ($P < 0.05$).

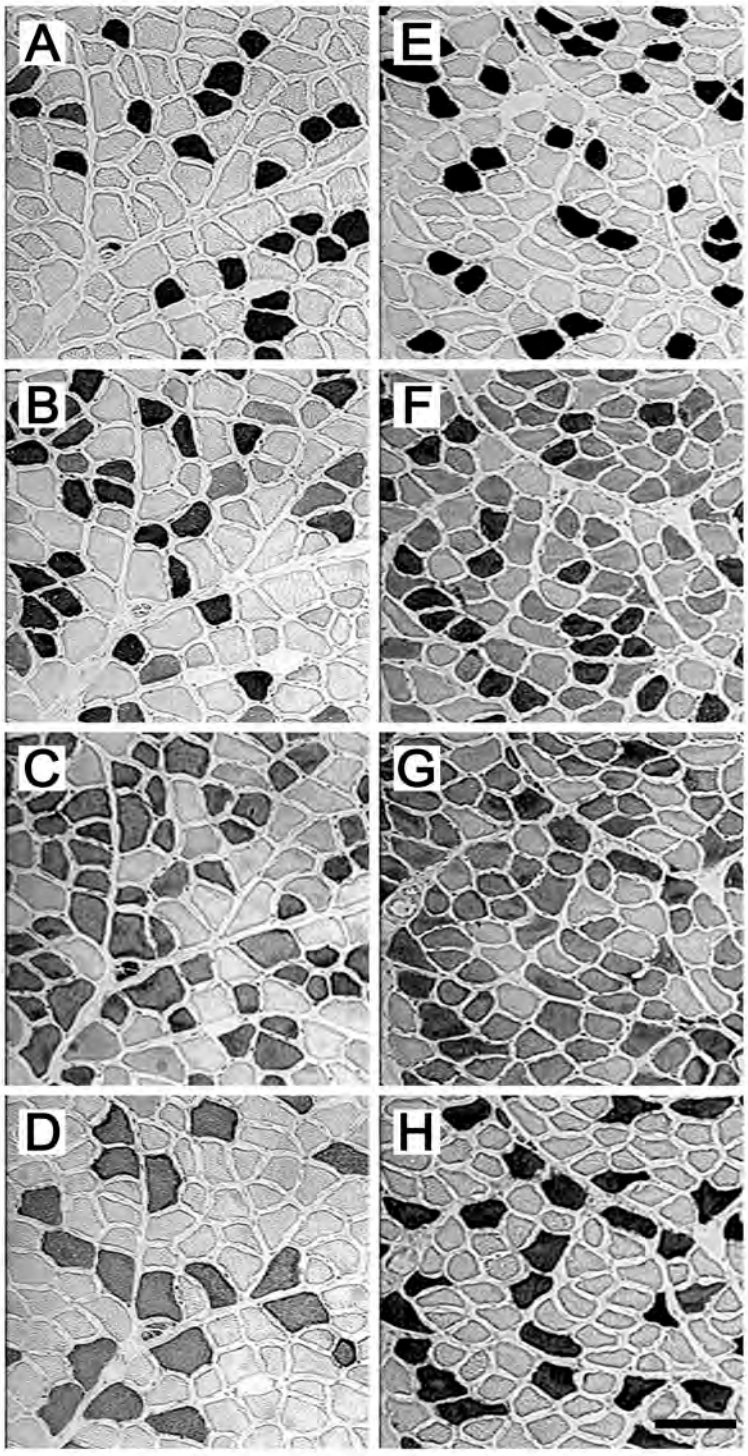

Figure 4.4 Representative photomicrographs of MHC isoform immunohistochemistry of Control (*A*, *B*, *C* and *D*) and 10 day stimulated rat tibialis anterior muscles (*E*, *F*, *G* and *H*). *A* and *E*, immunostains for MHCI (clone BA-D5); *B* and *F*, immunostains for MHCIIa (clone SC-71); *C* and *G*, immunostains for all MHC's except MHCIId(x) (clone BF-35); *D* and *H*, immunostains for MHCIIb (clone BF-F3). Bar represents 100 μm.

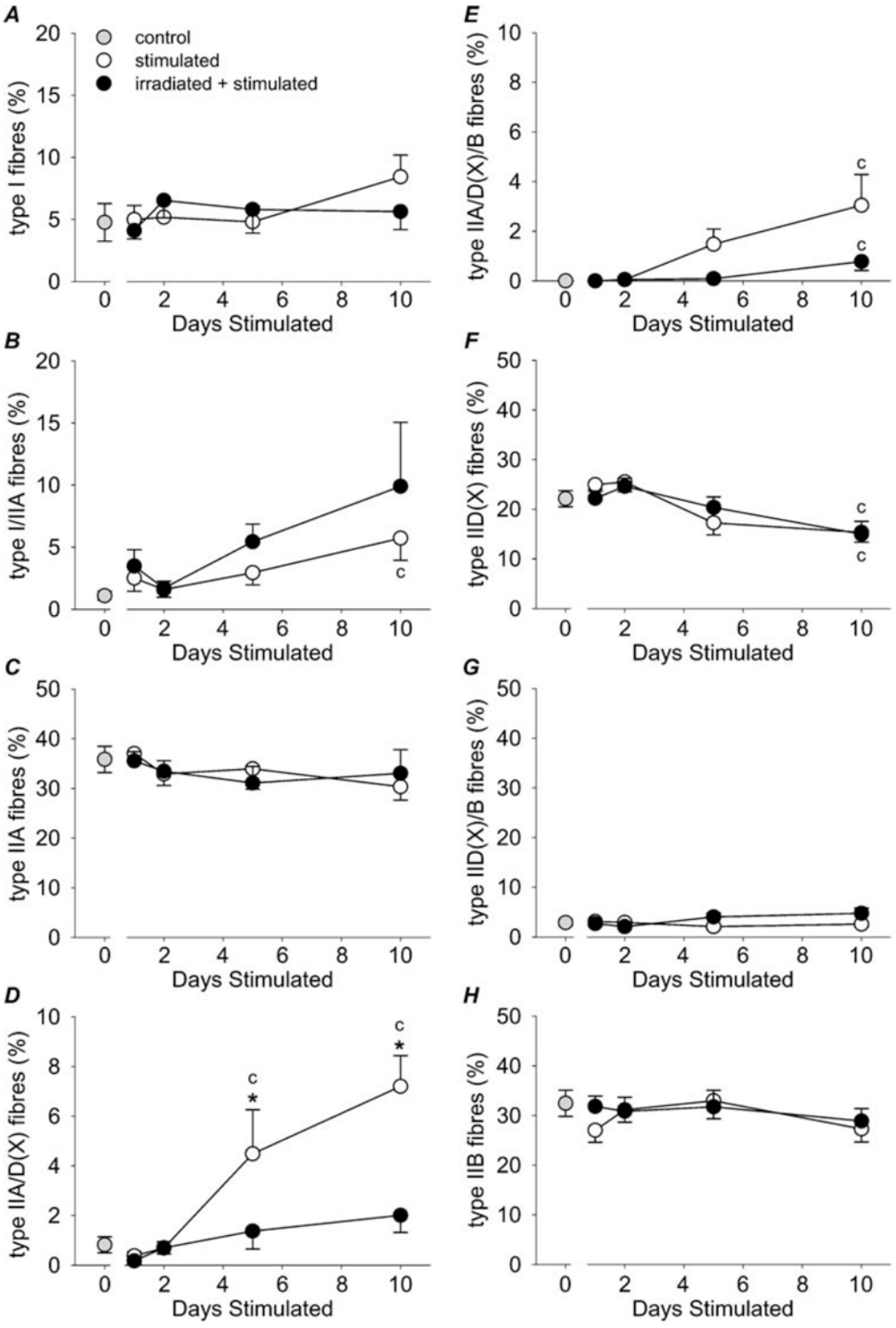

Figure 4.5 The proportion of pure and hybrid fibre types I (*A*), I/IIA (*B*), IIA (*C*), IIA/D(X) (*D*), IIA/D(X)/B (*E*), IID(X) (*F*), IID(X)/B (*G*) and IIB (*H*) in rat tibialis anterior muscles. Fibre types are listed in order from slowest (i.e. type I) to fastest (i.e. type IIB). Statistical symbols indicate: ^{c} difference from Control, * difference between Stim and IRR-Stim of the same number of days of stimulation ($P < 0.05$).

4.5 REFERENCES

Adams GR. (2006). Satellite cell proliferation and skeletal muscle hypertrophy. *Appl Physiol Nutr Metab* **31,** 782-790.

Adams GR, Caiozzo VJ, Haddad F & Baldwin KM. (2002). Cellular and molecular responses to increased skeletal muscle loading after irradiation. *Am J Physiol Cell Physiol* **283,** C1182-C1195.

Bamford JA, Lopaschuk GD, MacLean IM, Reinhart ML, Dixon WT & Putman CT. (2003). Effects of chronic AICAR administration on the metabolic and contractile phenotypes of rat slow- and fast-twitch skeletal muscles. *Can J Physiol Pharmacol* **81,** 1072-1082.

Bamman MM. (2007). Take two NSAIDs and call on your satellite cells in the morning. *J Appl Physiol* **103,** 415-416.

Charge SB & Rudnicki MA. (2004). Cellular and molecular regulation of muscle regeneration. *Physiol Rev* **84,** 209-238.

Cheek DB. (1985). The control of cell mass and replication. The DNA unit--a personal 20-year study. *Early Hum Dev* **12,** 211-239.

Delp MD & Pette D. (1994). Morphological changes during fiber type transitions in low-frequency- stimulated rat fast-twitch muscle. *Cell Tissue Res* **277,** 363-371.

Gibson MC & Schultz E. (1982). The distribution of satellite cells and their relationship to specific fiber types in soleus and extensor digitorum longus muscles. *Anat Rec* **202,** 329-337.

Gibson MC & Schultz E. (1983). Age-related differences in absolute numbers of skeletal muscle satellite cells. *Muscle Nerve* **6,** 574-580.

Goldberg AL. (1967). Protein synthesis in tonic and phasic skeletal muscles. *Nature* **216,** 1219-1220.

Hawke TJ & Garry DJ. (2001). Myogenic satellite cells: physiology to molecular biology. *J Appl Physiol* **91,** 534-551.

Jaschinski F, Schuler MJ, Peuker H & Pette D. (1998). Changes in myosin heavy chain mRNA and protein isoforms of rat muscle during forced contractile activity. *Am J Physiol Cell Physiol* **274,** C365-C370.

Laemmli UK. (1970). Cleavage of structural proteins during the assembly of the head of bacteriophage T4. *Nature* **227,** 680-685.

Lewis RB. (1954). Changes in striated muscle following single intense doses of X-rays. *Lab Invest* **3,** 48-55.

Li P, Akimoto T, Zhang M, Williams RS & Yan Z. (2006). Resident stem cells are not required for exercise-induced fiber-type switching and angiogenesis but are necessary for activity-dependent muscle growth. *Am J Physiol Cell Physiol* **290,** C1461-C1468.

Livak KJ & Schmittgen TD. (2001). Analysis of relative gene expression data using real-time quantitative PCR and the 2(-Delta Delta C(T)) Method. *Methods* **25,** 402-408.

McGeachie JK, Grounds MD, Partridge TA & Morgan JE. (1993). Age-related changes in replication of myogenic cells in mdx mice: quantitative autoradiographic studies. *J Neurol Sci* **119,** 169-179.

Mozdziak PE, Schultz E & Cassens RG. (1996). The effect of in vivo and in vitro irradiation (25 Gy) on the subsequent in vitro growth of satellite cells. *Cell Tissue Res* **283,** 203-208.

O'Connor RS & Pavlath GK. (2007). Point:Counterpoint: Satellite cell addition is/is not obligatory for skeletal muscle hypertrophy. *J Appl Physiol* **103,** 1099-1100.

Pette D. (2002). The adaptive potential of skeletal muscle fibers. *Can J Appl Physiol* **27,** 423-448.

Pette D & Staron RS. (1997). Mammalian skeletal muscle fiber type transitions. *Int Rev Cytol* **170,** 143-223.

Pette D & Staron RS. (2000). Myosin isoforms, muscle fiber types, and transitions. *Microsc Res Tech* **50,** 500-509.

Putman CT, Düsterhöft S & Pette D. (1999). Changes in satellite cell content and myosin isoforms in low-frequency- stimulated fast muscle of hypothyroid rat. *J Appl Physiol* **86,** 40-51.

Putman CT, Düsterhöft S & Pette D. (2000). Satellite cell proliferation in low-frequency stimulated fast muscle of hypothyroid rat. *Am J Physiol Cell Physiol* **279,** C682-C690.

Putman CT, Kiricsi M, Pearcey J, MacLean IM, Bamford JA, Murdoch GK, Dixon WT & Pette D. (2003). AMPK activation increases UCP-3 expression and mitochondrial enzyme activities in rat muscle without fibre type transitions. *J Physiol (Lond)* **551.1,** 169-178.

Putman CT, Sultan KR, Wassmer T, Bamford JA, Skorjanc D & Pette D. (2001). Fiber-type transitions and satellite cell activation in low-frequency-stimulated muscles of young and aging rats. *J Gerontol A Biol Sci Med Sci* **56,** B510-B519.

Rosenblatt DJ & Parry DJ. (1992). Gamma irradiation prevents compensatory hypertrophy of overloaded mouse extensor digitorum longous muscle. *J Appl Physiol* **73,** 2538-2543.

Rosenblatt DJ & Parry DJ. (1993). Adaptation of rat extensor digitorium longous muscle to gamma irradiation and overload. *Pflügers Arch* **423,** 255-264.

Roy RR, Monke SR, Allen DL & Edgerton VR. (1999). Modulation of myonuclear number in functionally overloaded and exercised rat plantaris fibers. *J Appl Physiol* **87,** 634-642.

Schiaffino S, Gorza L, Pitton G, Saggin L, Ausoni S, Sartore S & Lomo T. (1988). Embryonic and neonatal myosin heavy chain in denervated and paralyzed rat skeletal muscle. *Dev Biol* **127,** 1-11.

Schiaffino S, Gorza L, Sartore S, Saggin L, Ausoni S, Vianello M, Gundersen K & Lomo T. (1989). Three myosin heavy chain isoforms in type 2 skeletal muscle fibres. *J Muscle Res Cell Motil* **10,** 197-205.

Schultz E. (1996). Satellite cell proliferative compartments in growing skeletal muscles. *Dev Biol* **175,** 84-94.

Schultz E, Darr KC & Pette D. (1990). The role of satellite cells in adaptive or induced fiber transformations. In *The dynamic state of muscle fibers*, pp. 667-679. Walter de Gruyter, Berlin and New York.

Schultz E & McCormick KM. (1994). Skeletal muscle satellite cells. *Rev Physiol Biochem Pharmacol* **123,** 213-257.

Tseng BS, Kasper CE & Edgerton VR. (1994). Cytoplasm-to-myonucleus ratios and succinate dehydrogenase activities in adult rat slow and fast muscle fibers. *Cell Tissue Res* **275,** 39-49.

Vinsky MD, Murdoch GK, Dixon WT, Dyck MK & Foxcroft GR. (2007). Altered epigenetic variance in surviving litters from nutritionally restricted lactating primiparous sows. *Reprod Fertil Dev* **19,** 430-435.

Wakeford S, Watt DJ & Partridge TA. (1991). X-irradiation improves mdx mouse muscle as a model of myofiber loss in DMD. *Muscle Nerve* **14,** 42-50.

CHAPTER FIVE

NITRIC OXIDE SYNTHASE INHIBITION DELAYS CHRONIC LOW-FREQUENCY STIMULATION-INDUCED SATELLITE CELL ACTIVATION AND PREVENTS SKELETAL MUSCLE ADAPTATION

5.1 INTRODUCTION

Adult skeletal muscle contains heterogeneous, post-mitotic fibres that demonstrate remarkable plasticity in response to altered contractile demands such as exercise. Muscle fibre type diversity is, in part, attributed to the various MHC protein isoforms that largely dictate the rate of force development and maximum shortening velocity of cross-bridge formation (Pette & Staron, 1997). MHC-based fibre types are classified as type I, IIA, IID(X) and IIB that contain the corresponding MHC isoforms listed in increasing order of shortening velocity: MHCI, MHCIIa, MHCIId(x) and MHCIIb (Pette & Staron, 1997). CLFS is a model of endurance exercise training that mimics the tonic firing pattern typical of slow motor neurons and induces satellite cell activation and subsequent fusion to fast-to-slow transforming fibres in the absence of skeletal muscle damage in the rat (Delp & Pette, 1994; Putman *et al.*, 1999, 2000; Putman *et al.*, 2001; Chapter 3). This fast-to-slow fibre type transformation follows the "next nearest-neighbour" rule where fibre types undergo a predictable pattern of transformation in the direction of IIB→IID(X)→IIA→I (Pette & Staron, 2000; Pette, 2002). The mechanisms responsible for initiating satellite cell activation and regulating fast-to-slow fibre type transformations, however, are not yet fully understood. Moreover, the molecular control of CLFS-induced satellite cell activation has yet to be investigated.

Two factors, HGF and NO have been shown to activate quiescent satellite cells. To date, HGF, which is localised in the extracellular matrix of uninjured skeletal muscle, is the only growth factor shown to activate satellite cells from quiescence in primary culture and in vivo (Allen *et al.*, 1995; Tatsumi *et al.*, 1998). In response to mechanical stretch (Tatsumi *et al.*, 2001; Anderson &

Pilipowicz, 2002; Tatsumi *et al.*, 2002) or injury (Tatsumi *et al.*, 1998; Anderson, 2000), HGF colocalises with the c-met receptor on satellite cells and initiates activation. The second factor, NO, is a short-lived ubiquitous signaling molecule that is controlled at the synthesis level by NOS, which in turn is regulated by Ca^{2+}-calmodulin binding (Stamler & Meissner, 2001). Initially demonstrated by Anderson *et al*. (2000), the release of HGF, HGF/c-met colocalisation and immediate satellite cell activation are blocked if NOS is inhibited (Anderson & Pilipowicz, 2002; Tatsumi *et al.*, 2002). Additionally, satellite cell activation can be augmented in response to supplemental NO administration (Anderson & Pilipowicz, 2002; Tatsumi *et al.*, 2002; Betters *et al.*, 2008a; Betters *et al.*, 2008b). Collectively, these studies show that NO is released upstream of HGF and influences HGF-mediated satellite cell activation. Interestingly, nNOS, which is the primary isoform expressed in normal skeletal muscle, is upregulated in response to CLFS in rat (Reiser *et al.*, 1997). Therefore, it seems possible that CLFS-induced satellite cell activation may occur via a NO-dependent pathway.

The pathway by which tonic firing of slow motor neurons induces transcription of slower-fibre-specific genes involves sustained elevations in intracellular Ca^{2+} levels sufficient to stimulate calcineurin signaling activity (Liu *et al.*, 2001; Tothova *et al.*, 2006). Calcineurin is a Ca^{2+}/calmodulin-dependent serine/threonine protein phosphatase that dephosphorylates cytoplasmic nuclear factors of activated T-cells (NFAT), resulting in its nuclear translocation and activation of a slow muscle gene program (Chin *et al.*, 1998). Low-frequency stimulation has been shown to cause calcineurin-dependent NFAT nuclear translocation in vitro (Liu *et al.*, 2001) and in vivo (Tothova *et al.*, 2006). NFAT transcriptional activity, however, is subject to a dynamic cycle of activation (i.e. dephosphorylation) and deactivation (i.e. phosphorylation) resulting in nucleocytoplasmic shuttling. Skeletal muscle NFAT rephosporylation can occur by several protein kinases, such as glycogen synthase kinase-3β (GSK-3β), which has been identified as an important regulator of NFAT-mediated increases in slow MHC gene expression (Jiang *et al.*, 2006) and nuclear export after prior electrical

stimulation (Shen *et al.*, 2007). Recently, Drenning *et al.* (2008) have shown that NO facilitates NFAT nuclear accumulation and increased MHCI mRNA expression via GSK-3β inhibition in C_2C_{12} myotubes. Collectively, these observations suggest that CLFS-induced satellite cell activation and subsequent fast-to-slow fibre type transformations may be regulated, at least in part, by NO signaling.

The purpose of the present study was therefore to test the hypotheses that in vivo pharmacological inhibition of NOS activity in the rat would prevent i) immediate CLFS-induced satellite cell activation and ii) subsequent fast-to-slow fibre type transformations. Endogenous NO production was blocked by administering a pharmacological inhibitor of NOS activity, L-NAME. Satellite cell activity was assessed by continuous DNA labeling with BrdU followed by immunolocalisation (Schultz, 1996). MHC-based fibre type transformations were evaluated at the mRNA level by real-time RT-PCR (Vinsky *et al.*, 2007), and at the protein level by SDS-PAGE (Hämäläinen & Pette, 1996; Putman *et al.*, 2004) and immunohistochemistry (Putman *et al.*, 2001; Putman *et al.*, 2003).

5.2 METHODS

5.2.1 Animal Care and Treatment

Sixty adult male Wistar rats were used in this study (Charles River Laboratories, Montreal, PQ, Canada). Animals were individually housed under controlled environmental conditions (22°C with 12:12-h light-dark cycle) and received standard rat chow and water or L-NAME solution *ad libitum*, which was measured and replaced daily. Body mass was also recorded daily throughout the experimental period and the dose of L-NAME, per kilogram of body mass, was calculated for each rat in the treatment groups. All animal procedures were carried out in accordance with the guidelines of the CCAC and received ethical approval from the University of Alberta. Animals were randomly assigned to one of the following ten groups: sham operation of the left leg only (Control); L-

NAME plus Control (L-Control), 1 day (1d L-Stim), 2 days (2d L-Stim), 5 days (5d L-Stim) or 10 days (10d L-Stim) of CLFS of the left leg only; 1 day (1d Stim), 2 days (2d Stim), 5 days (5d Stim) or 10 days (10d Stim) of CLFS only (n = 6, animals each group). The application of CLFS has been shown to elicit a compensatory effect in the contralateral control muscles due to increased weight bearing (Putman *et al.*, 2000; Chapter 3; [5]Martins *et al.*, 2009), therefore comparisons were made to Control or L-Control. Animals in the Control, 1d Stim, 2d Stim, 5d Stim and 10d Stim groups were also part of another study (Chapter 4) that was conducted in parallel with the present study.

5.2.2 Systemic Inhibition of Nitric Oxide Synthase Activity

The pharmacological inhibition of NOS was achieved by administering the competitive non-isoform specific NOS inhibitor L-NAME (Sigma-Aldrich, Oakville, ON, Canada) daily in the drinking water of animals starting 2 days prior to the onset of stimulation and continuing until euthanisation. A L-NAME concentration of 0.75 mg ml^{-1} was used that resulted in a dose of ~100 mg (kg body $mass^{-1}$) day^{-1}. A dose of 90-100 mg (kg body $mass^{-1}$) day^{-1} has previously been shown to effectively inhibit NOS activity in the rat (Smith *et al.*, 2002; Sellman *et al.*, 2006; Soltow *et al.*, 2006).

5.2.3 Chronic Low-frequency Stimulation and BrdU Labeling

CLFS (10 Hz, impulse width 380 μs, 12 h day^{-1}) was applied across the left common peroneal nerve as previously described (Simoneau & Pette, 1988; Putman *et al.*, 2004; Chapter 3; Chapter 4). Briefly, bipolar electrodes were implanted under anesthesia [75 mg (kg body wt)$^{-1}$ ketamine, 10 mg (kg body wt)$^{-1}$ xylezine and 0.5 mg (kg body wt)$^{-1}$ acepromazine maleate] lateral to the common peroneal nerve of the left hindlimb, externalised at the dorsal intrascapular region, and connected to a small, portable stimulator. Animals were allowed to recover for 7 days before the onset of 0, 1, 2, 5 or 10 consecutive days of stimulation.

[5] Martins *et al*. 2009, which is a published version of Chapter 4, will hereafter be referred to as Chapter 4.

Animals received a continuous infusion of the thymidine analogue BrdU (10 mg ml^{-1}) via subcutaneously implanted Alzet® mini-osmotic pumps (model 2ML1, 10 μl hr^{-1} release rate and 2 ml volume) (Schultz, 1996), which were replaced 1 wk later in those animals receiving 10 days of stimulation.

5.2.4 Muscle Sampling

Upon completion of the stimulation period, animals were anesthetised and the tibialis anterior muscles were excised from both hindlimbs, quickly fixed in a slightly longitudinally stretched position and frozen in melting isopentane (-159°C). Muscles were stored in liquid nitrogen (-196°C). The anesthetised animals were euthanised after all muscles were collected with an overdose of Euthanyl [100 mg (kg body wt)$^{-1}$] (Bimedia-MTC Animal Health Inc., Cambridge, ON, Canada), followed by exsanguination.

5.2.5 Antibodies for Immunohistochemistry

Monoclonal antibodies directed against adult and embryonic MHC isoforms (Schiaffino *et al.*, 1988; Schiaffino *et al.*, 1989) were harvested from the supernatant of hybridoma cell lines obtained from the American Type Culture Collection (Manassas, VA, USA): BA-D5 (IgG, anti-MHCI), SC-71 (IgG, anti-MHCIIa), BF-F3 (IgM, anti-MHCIIb) and BF-45 (IgG, anti-MHC-embryonic). Clone BF-35 (purified IgG, not MHCIIx) (also known as MHCIId) was a generous gift from Prof. S. Schiaffino (Padova, Italy). Mouse monoclonal anti-BrdU (clone BMC 9318) was obtained from Roche Diagnostics Corporation (Indianapolis, IN, USA). Biotinylated horse anti-mouse IgG (rat-absorbed, affinity-purified) and biotinylated goat anti-mouse IgM were obtained from Vector Laboratories, Inc. (Burlingame, CA, USA).

5.2.6 Immunohistochemistry for Myosin and BrdU

Tibialis anterior muscles were mounted in embedding medium (Tissue-Tek O.C.T. Compound, Miles Scientific, USA) and 10 μm-thick transverse frozen

sections were collected from the mid-belly of each tibialis anterior muscle at -20°C. Immunostaining was completed according to established protocols for MHC isoforms (Putman *et al.*, 2001; Putman *et al.*, 2003) and BrdU (Schultz, 1996). Briefly, air-dried sections stained for BrdU were fixed at room temperature for 15 min in 70% (v/v) ethanol, washed in PBS-T and then with PBS. All sections were then incubated for 15 minutes in 3% (v/v) H_2O_2 in methanol and washed as before. Sections stained for BrdU were permealised for 1 h in 2N HCl and washed. Serial sections stained for BA-D5, SC-71, BF-35, BF-45 and BrdU were incubated at room temperature for 1 h in BS-1 containing avidin-D blocking reagent (Vector Laboratories Inc.). Sections stained for BF-F3 were incubated in BS-2. Sections were incubated overnight at 4°C with a primary antibody that was diluted in its corresponding blocking solution containing a biotin blocking reagent (Vector Laboratories Inc.). Antibodies were diluted as follows: BA-D5 at 1:400, SC-71 at 1:100, BF-35 at 1:10,000, BF-45 at 1:50 and anti-BrdU at 1:10 in BS-1; BF-F3 at 1:400 in BS-2. After several washings, a biotinylated horse-anti-mouse-IgG (BA-D5; SC-71; BF-35; BF-45; anti-BrdU) or biotinylated goat-anti-mouse-IgM (BF-F3) was applied for 1 hour at a dilution of 1:200. Sections were then washed again and incubated with Vectastain ABC Reagent according to the manufacturer's instructions (Vector Laboratories Inc.), washed and reacted with 0.07% (w/v) diaminobenzidine, 0.05% (v/v) H_2O_2 and 0.03% (w/v) $NiCl_2$ in 50 mM Tris-HCl (pH 7.5). Control samples were run in parallel in which the primary IgM antibody was omitted, or a non-specific mouse IgG antibody was substituted (Santa Cruz). All sections were subsequently dehydrated, cleared, and mounted in Entellan (Merck, Darmstadt, Germany).

5.2.7 Immunohistochemical Analyses

MHC isoform semi-quantitative analyses were completed with a Leitz Diaplan microscope (Ernst Leitz Wetzlar GmbH, Germany) fitted with a Pro-Series High Performance Charge-Coupled Digital camera (Cohu Inc., San Diego, CA, USA), Image-Pro Plus imaging software (Media Cybernetics Inc., Bethesda, MD, USA) and a custom-designed analytical program (Putman *et al.*, 2000).

MHC isoforms from three representative cross-sectional areas of tibialis anterior muscles (i.e. deep, middle and superficial regions) were examined from each group. Type I, IIA, IIB and embryonic fibres were identified by positive staining and type IID(X) fibres were identified by the absence of staining with all antibodies directed against the various MHC isoforms. A similar number of fibres were examined across all groups, totaling 80,726. BrdU semi-quantitative analysis was completed with a Leka DMRBE microscope (Leica Microsystems GmbH Wetzal, Germany) at 640x magnification. BrdU positive nuclei were enumerated on cross-sections of all tibialis anterior muscles. An average of 521 ± 12 (mean ± SEM) fibres were examined for each muscle.

5.2.8 Myosin Heavy Chain mRNA Analyses by Real-Time Reverse Transcriptase-Polymerase Chain Reaction

Patterns of MHC isoform expression were analysed at the mRNA level using real-time RT-PCR (Vinsky *et al.*, 2007; Chapter 4). Please refer to Chapter 3, section 3.2.10 for further details regarding the RNA extraction procedure. The concentrations and purity of RNA extracts were evaluated by measuring the absorbance at 260 and 260/280 nm, respectively, using a NanoDrop ND 1000 system (Rose Scientific Ltd, Edmonton, AB, Canada). cDNA synthesis was performed according to an established procedure (Bamford *et al.*, 2003). Samples were diluted to 1 μg μl^{-1} and reverse transcription was performed for 1h at 37°C with oligo (dT_{15}) primers (Invitrogen, Life Technologies, Burlington, ON, Canada) and M-MLV DNA polymerase (Invitrogen, Life Technologies). Primers (Invitrogen, Life Technologies) and Taqman-MGB probes (Applied Biosystems, Foster City, CA, USA) were designed with EMBL-EBI and aligned using Clustal W for rat MHCIβ (X15939), MHCIIa (L13606), MHCIId(x) (XM 213345) and MHCIIb (L24897) (Table 5.1). Real-time PCR was performed on 1 μl cDNA samples, in duplicate, using an ABI 7900HT thermocycler (Applied Biosystems). For futher details regarding the specific cycle thresholds and examples of amplification plots of the various MHC isoforms, please refer to Apendix B. 18S RNA (Applied Biosytems) was used as the endogenous control. Relative changes

in MHC isoform gene expression were determined using the $2^{-\Delta\Delta Ct}$ method of analysis (Livak & Schmittgen, 2001). Please refer to Apendix C for a detailed list of each MHC isoform and 18S Ct value that was obtained for each group. Inter-assay variation was evaluated by repeated analysis of a known sample on each 96-well plate and confirmed to be negligible (data not shown). Additionally, the amplification efficiencies of the MHC isoforms and 18S were similar (data not shown).

5.2.9 Electrophoretic Analyses of Myosin Heavy Chain Protein Isoforms

Relative contents of the various adult MHC isoforms were analysed as previously described (Hämäläinen & Pette, 1996; Putman *et al.*, 2004). Briefly, frozen powdered tibialis anterior muscles were stirred on ice for 30 min in a buffer containing 100 mM NaP_2O_7 (pH 8.5), 5 mM EGTA, 5 mM $MgCl_2$, 0.3 mM KCl, 10 mM DTT (Sigma-Aldrich, Oakville, ON, Canada) and 5 mg ml^{-1} of a protease inhibitor cocktail (Complete™, Roche Diagnostics Corporation). Please refer to Chapter 3, section 3.2.9 for futher details regarding the protease inhibitor cocktail. Samples were then centrifuged at 12,000x*g* for 5 min at 4°C; supernatants were diluted 1:1 with glycerol and stored at -20°C until analysed. Prior to gel loading, muscle extracts were diluted in modified Laemmli lysis buffer to a concentration of 0.2 μg μl^{-1} and boiled for 6 min (Leammli, 1970). Samples (1 μg total protein per lane) were electrophoresed (275 V for 24 h at 8°C) in duplicate on 7% (w/v) polyacrylamide gels containing glycerol, under denaturing conditions. Gels were then fixed and MHC isoforms were detected by silver staining and evaluated by integrated densitometry (ChemiGenius, GeneSnap and GeneTools, Syngene, UK).

5.2.10 Statistical Analyses

Data are summarised as means ± SEM. Differences between group means were assessed using a two-way ANOVA [i.e. treatment (stimulation or L-NAME plus stimulation X days of stimulation (0, 1, 2, 5 or 10 days)]. When a significant *F* ratio was found for the interaction, differences were located using the Newman-

Keuls post hoc analysis. Differences were considered significant at $P < 0.05$. There were no differences between the left and right legs of Control or L-Control, as determined by the t-test for dependent samples, therefore these data were pooled.

5.3 RESULTS

5.3.1 Animal and Muscle Weights

Animals initially weighed 318 ± 3 g and similarly gained 29 ± 6 g during 10 days of stimulation. Additionally, animal weights did not differ between Stim and L-Stim groups of the same number of days of stimulation at all other time points (i.e. 0d, 1d, 2d and 5d).

5.3.2 Satellite Cell Activation/Proliferation

An established method was used to assess BrdU positive nuclei (Chapter 3). Activated and previously activated satellite cells were determined by quantifying BrdU staining. Only those stained nuclei that were unambiguously fused to existing muscle fibres were counted, as shown in Fig. 5.1*A*. CLFS first induced an increase in BrdU-positive nuclei at 1 day of stimulation (i.e. 1d Stim; 3.9-fold increase) up to a maximum of a 21.3-fold increase at 10 days of stimulation (i.e. 10d Stim) compared with Control (Fig. 5.1*B*). Interestingly, L-Stim BrdU-positive nuclei only remained at control levels for the first two days (i.e. 1d L-Stim, 2d L-Stim), and then increased to the same extent as Stim (i.e. 5d Stim and 10d Stim; Fig. 5.1*B*).

5.3.3 Myosin Heavy Chain mRNA Expression

Control and L-Control were not different from each other (Fig. 5.2). CLFS-induced fast-to-slow MHC isoform transformations at the mRNA level began at 5 days of stimulation [i.e. 5d Stim; MHCIIb mRNA→MHCIId(x) mRNA] and continued at 10 days of stimulation [i.e. 10d Stim; MHCIIb

mRNA→MHCIId(x) mRNA→MHCIIa mRNA→MHCI mRNA]. Specifically, 10d Stim MHCI mRNA (Fig. 5.2*A*), MHCIIa mRNA (Fig. 5.2*B*) and MHCIId(x) mRNA (Fig. 5.2*C*) increased compared with Control, with no increase in the expression of MHCIIb mRNA (Fig. 5.2*D*). In contrast, all L-Stim MHC mRNA isoforms remained at control levels throughout 10 days of stimulation (Fig. 5.2). Additionally, 10d Stim MHCI mRNA, MHCIIa mRNA and MHCIId(x) mRNA were 17-fold (Fig. 5.2*A*), 26-fold (Fig. 5.2*B*) and 9-fold (Fig. 5.2*C*) greater compared with 10d L-Stim, respectively.

5.3.4 Myosin Heavy Chain Isoform Transformations

A representative gel showing the quantitative analytical method used to measure MHC isoform protein content in muscle extracts is illustrated in Fig. 5.3*A*. Control and L-Control were not different from each other (Fig. 5.3). CLFS-induced fast-to-slow MHC isoform transformations were first observed at 10 days of stimulation (Fig. 5.3*B*). Specifically, the relative content of 10d Stim MHCI increased 2.0- and 2.6-fold compared with Control and 10d L-Stim, respectively, which were not different from each other (Fig. 5.3*B*). As observed at the mRNA level, MHC isoform protein content in L-Stim remained at control levels throughout 10 days of stimulation (Fig. 5.3*B*).

5.3.5 Fibre Type Transformations

Detailed fibre type analysis, which included the detection of all pure and hybrid fibre types, was assessed by semi-quantitative immunohistochemical analyses on serial sections in the deep, middle and superficial regions of each tibialis anterior muscle (Fig. 5.4). As observed in Chapter 4, CLFS-induced fast-to-slow fibre type transformations were only observed in the deep and middle regions and therefore the analysis was restricted to these areas. Consistent with the observations in MHC isoform protein content, CLFS first induced fast-to-slow fibre type transformations at 10 days of stimulation (i.e. 10d Stim), while L-Stim remained at control levels. Specifically, increases in the proportion of fibres expressing the slowest MHCI were observed in 10d Stim compared with Control

and 10d L-Stim, which were not different (Fig. 5.5*A*). Additionally, the emergence of hybrid fibre types that are a hallmark of the adaptive response to CLFS (Pette, 2002) was not the same in Stim and L-Stim. Overall, the proportion of fibres expressing multiple MHC isoforms (i.e. hybrid fibres) in 10d Stim was 1.8- and 3.1-fold greater compared with Control and 10d L-Stim, respectively, which were not different from each other (Fig. 5.5*E*). Embryonic MHC was not detected in extrafusal fibres (data not shown).

5.4 DISCUSSION

Nitric oxide has been established as an important signaling molecule in skeletal muscle (Stamler & Meissner, 2001). Therefore, the effect of blocking NOS activity on CLFS-induced satellite cell activation and fast-to-slow MHC-based fibre type transformations were examined. Multiple early time points of CLFS were chosen because CLFS-induced satellite cell activation has been shown to occur as early as 1 day after the onset of stimulation with maximum proliferation occurring by 5 to 10 days (Putman *et al.*, 1999; Chapter 4). Additionally, CLFS-induced fast-to-slow MHC isoform transformations have been shown to begin at the mRNA level after 3 days and at the protein level after 5 days that rapidly continued to change through 10 days (Jaschinski *et al.*, 1998). This delayed adaptation at the protein level likely reflects the more advanced state of change at the mRNA level compared with the much slower rate of MHC protein turnover. Results of the current study support these findings, while the main findings of this study were that blocking NOS activity with L-NAME delayed CLFS-induced satellite cell activation and prevented fast-to-slow fibre type transformations in rat fast-twitch muscle.

5.4.1 Nitric Oxide and Satellite Cell Activity

It appears that this is the first study to investigate the underlying signaling mechanisms involved in CLFS-induced satellite cell activation. As reviewed by Wozniak *et al*. (2005), the NO/HGF-dependent satellite cell activation pathway

has been well defined, but signaling mechanisms involved in satellite cell activation may also function in a NO-independent manner. This idea was first supported by results from nNOS$^{-/-}$ mice that showed only delayed satellite cell activation after muscle injury and were capable of full regeneration (Anderson, 2000). The possibility of alternative NO production sources from eNOS and/or iNOS, however, could not be ruled out. More recently, stretch-induced increases in satellite cell activity have been observed as early as 2 days after hindlimb suspension in rats treated with L-NAME (Tatsumi *et al.*, 2006). Additionally, in 7 and 12 day overloaded plantaris muscles of rats whose NOS activity was blocked, satellite cell activity (Sellman *et al.*, 2006) and subsequent myonuclear addition (Gordon *et al.*, 2007), respectively, were similar to normal overloaded muscles. Collectively, it appears that both NO-dependent and NO-independent mechanisms may play a role in satellite cell activation. Results from the present study suggest that the immediate and/or preferred CLFS-induced satellite cell activation pathway occurs in a NO-dependent fashion as shown by the lack of increase in satellite cell activity for the first 2 days of stimulation in L-NAME treated rats. However, findings from recent studies (Sellman *et al.*, 2006; Tatsumi *et al.*, 2006; Gordon *et al.*, 2007) and the present study also indicate that an alternative satellite cell activation pathway, which has yet to be identified, exists that can fully compensate in the absence of prolonged NOS activity.

5.4.2 Nitric Oxide and Fast-to-Slow Fibre Type Transformations

In order to elicit a pronounced stimulus for fast-to-slow fibre type transformations in the absence of muscle fibre regeneration, CLFS was employed, which is a model of muscle training that mimics the electrical discharge pattern of slow motor neurons innervating slow-twitch muscles. Unlike other rodent exercise models, however, it causes synchronous recruitment of all targeted motor units, including those not normally recruited during exercise training (Pette & Staron, 2000). In doing so, the adaptive potential of CLFS-targeted muscles is maximally challenged. Also, the standardised and highly reproducible conditions

of CLFS allows for activity-induced fast-to-slow phenotypic changes to occur in a well-defined time-dependent manner (Jaschinski *et al.*, 1998; Pette, 2002).

To date, there are very few studies that have investigated the involvement of NO in fast-to-slow fibre type transformations (Smith *et al.*, 2002; Sellman *et al.*, 2006; Drenning *et al.*, 2008). Sellman *et al.* (2006) reported that L-NAME-induced NOS inhibition prevented the up-regulation of MHCI mRNA in rat plantairs muscles following 5 days of functional overload, which was also confirmed in vitro (Drenning *et al.*, 2008). Present results not only support, but extend these recent observations by indicating that NO may also play a critical role in the expression of fast MHC mRNAs involved in CLFS-induced fast-to-slow transformations within rat fast-twitch muscle [i.e. MHCIIb mRNA→MHCIId(x) mRNA→MHCIIa mRNA]. Whether L-NAME is preventing this fast-to-slow MHC-based transformation via the same pathway proposed by Drenning *et al.* (2008) requires further investigation. At the protein level, Smith *et al.* (2002) found that NO was required for chronic overload-induced fast-to-slow MHC isoform transformations in rat. They also reported, however, that type IID(X)/B fibre types significantly increased in response to L-NAME treatment; this effect was not observed at the MHC isoform protein level in that study (Smith *et al.,* 2002). Results from the present study show that indeed, L-NAME prevented CLFS-induced fast-to-slow MHC isoform protein and fibre type transformations, but did not significantly affect basal expression levels. This difference in findings between Smith *et al.,* (2002) and the current study may have been due to the different analytical methods employed to detect fibre types. In the present study, immunohistochemical fibre type analysis was performed that utilised monoclonal antibodies directed against the four adult MHC isoforms expressed in rat, as well as detecting all pure and hybrid fibre types. On the other hand, Smith *et al.,* (2002) performed histochemical myofibril ATPase analysis that only detects type I, IIA and the combination of IID(X) and IIB, and restricted their analysis only to these fibre types. Taken together, these differences likely accounted for the discrepancy in findings.

5.4.3 Conclusions

Results of the present study indicate that NOS activity is important for CLFS-induced satellite cell activation, but an unknown alternative mechanism exists that is able to fully compensate under conditions where NO levels are suppressed within rat tibialis anterior muscles. Additionally, NO appears to be a key mediator of MHC expression during CLFS-induced fast-to-slow fibre type transformation.

Table 5.1 Rat specific real-time reverse-transcriptase polymerase chain reaction primers and probes.

Target	Forward Primer	Reverse Primer	Probe
MHCIβ	5'-GCAGTTGGATGAGCGACTCA-3'	5'-TCCTCAATCCTGGCGTTGA-3'	5'-AGAAGGACTTTGAGTTAAAT-3'
MHCIIa	5'-GGCGGCAAGAAGCAGATC-3'	5'-TTCCGCTTCTGCTCACTCTCT-3'	5'-AGGCCAGAGTGCGTG-3'
MHCIId(x)	5'-GGCGGCAAGAAGCAGATC-3'	5'-TTCGTTTTCAACTTCTCCTTCAAGT-3'	5'-AGGCCAGGGTCCG-3'
MHCIIb	5'-GGCGGCAAGAAGCAGATC-3'	5'-TTTTCCACCTCGTTTTCAAGCT-3'	5'-TGGAGGCCAGAGTGA-3'

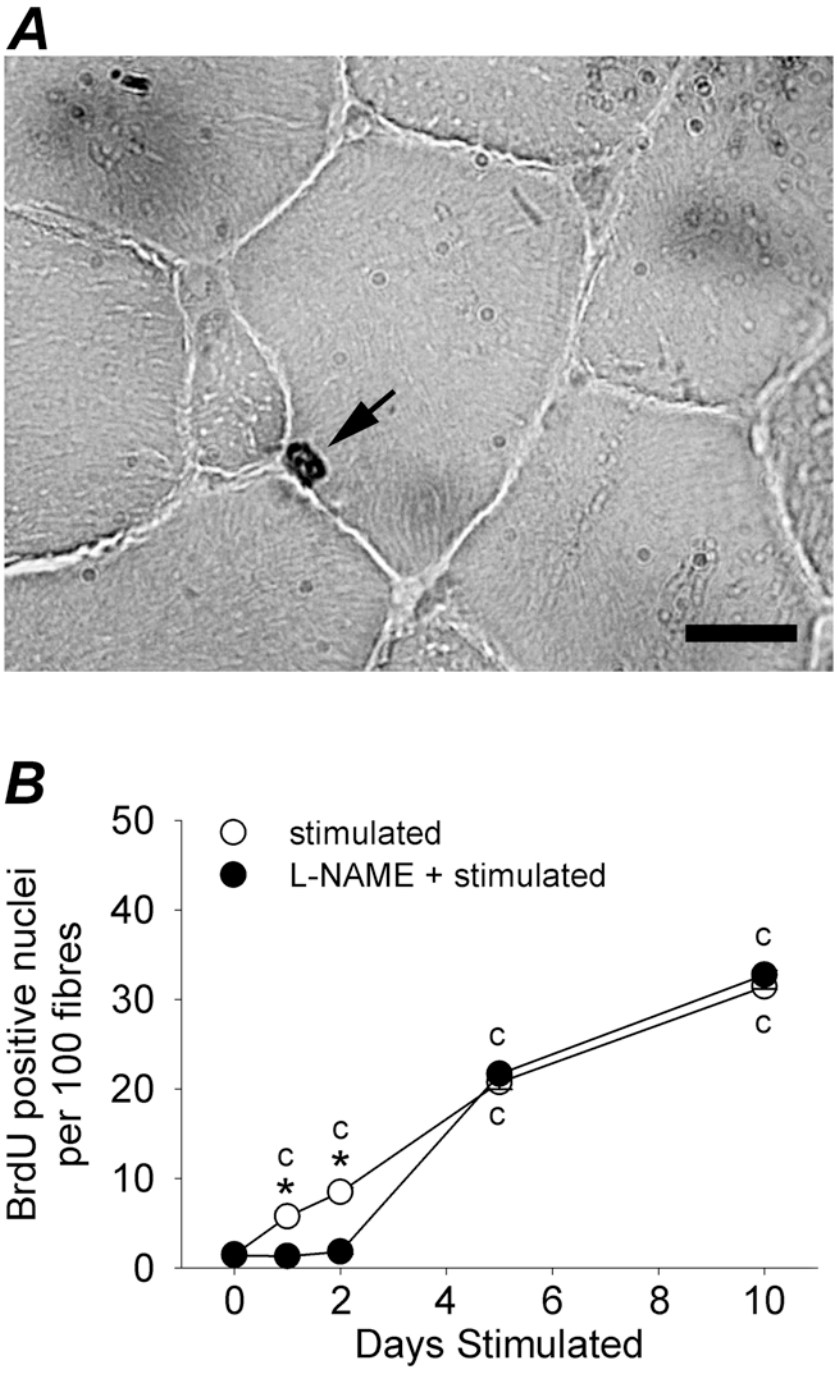

Figure 5.1 Photomicrograph of representative immunohistochemical BrdU stain used to identify activated satellite cells (arrow) in rat tibialis anterior muscles (*A*). Bar represents 10 μm. Number of BrdU positive nuclei per 100 fibres in rat tibialis anterior muscles (*B*). Statistical symbols indicate: ^{c} difference from respective control group (Control or L-Control), * difference between Stim and L-Stim of the same number of days of stimulation ($P < 0.05$).

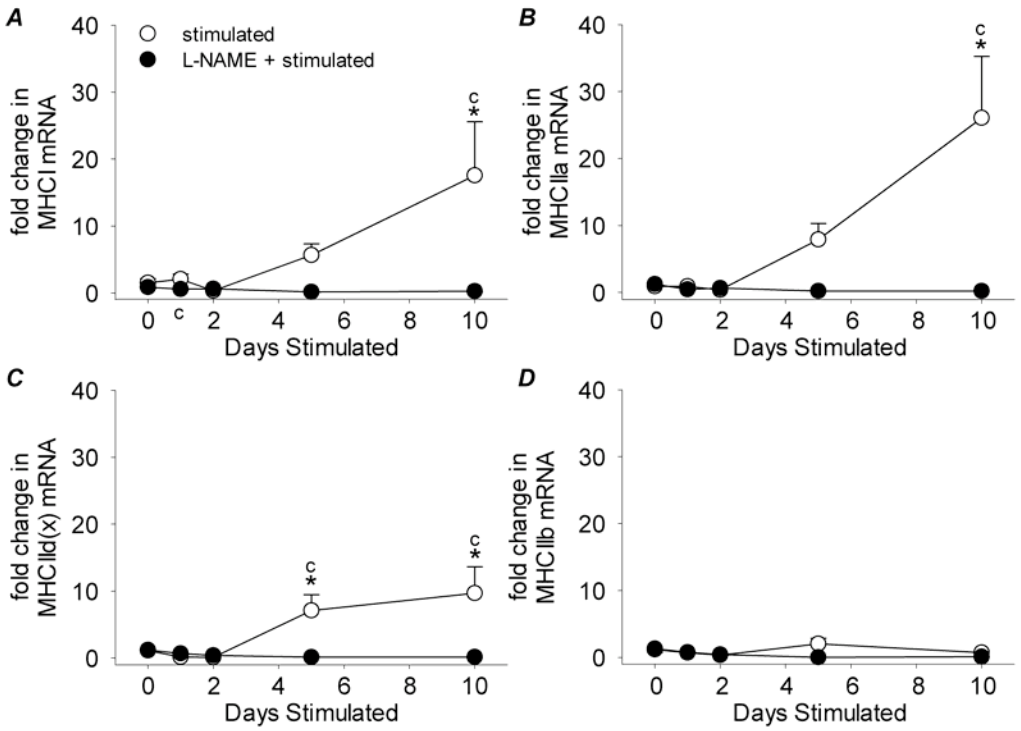

Figure 5.2 Fold changes in MHCI mRNA (*A*), MHCIIa mRNA (*B*), MHCIId(x) mRNA (*C*) and MHCIIb mRNA (*D*) gene expression levels in rat tibialis anterior muscles. Statistical symbols indicate: ^{c} difference from respective control group (Control or L-Control), * difference between Stim and L-Stim of the same number of days of stimulation ($P < 0.05$).

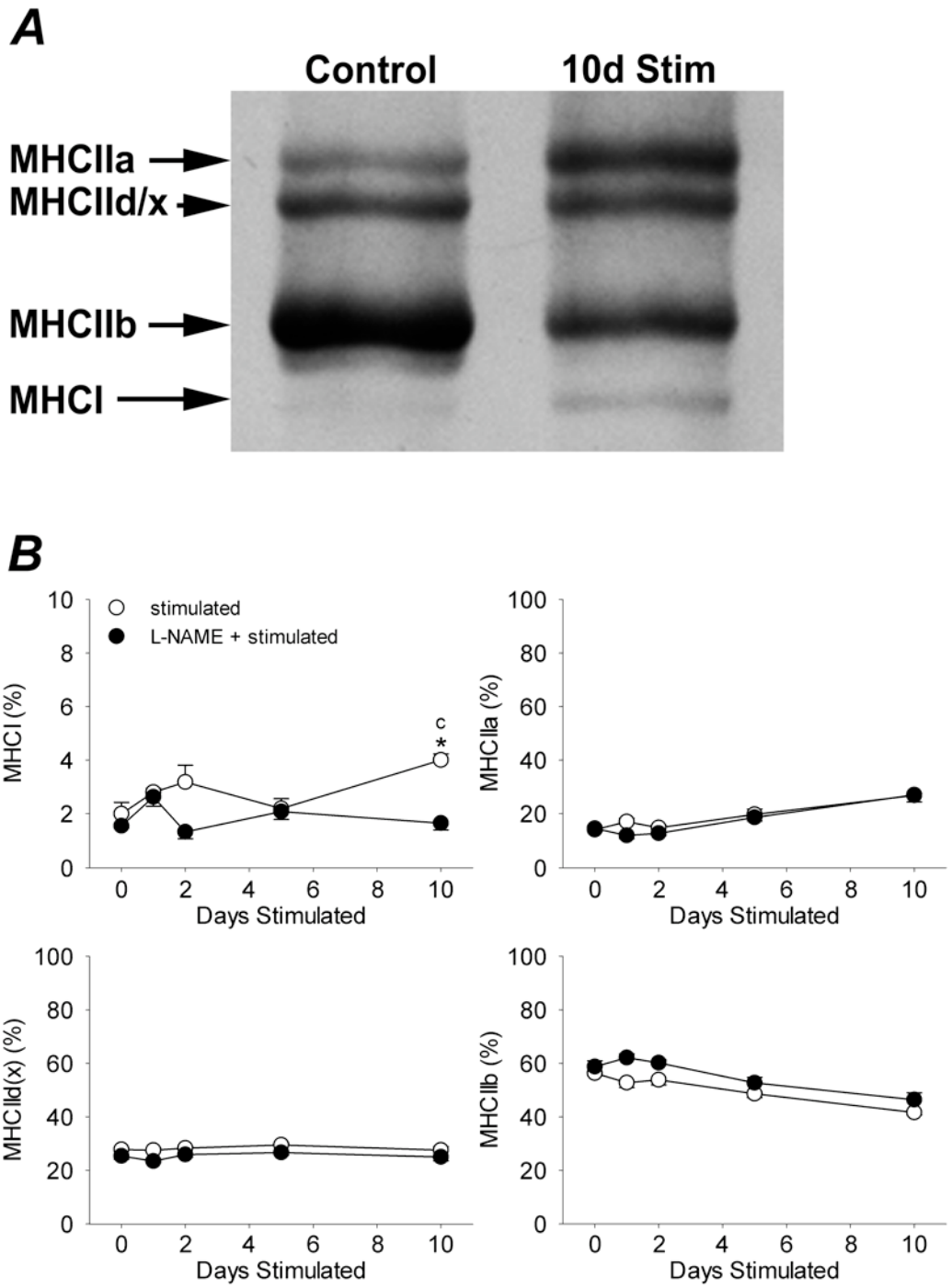

Figure 5.3 Example of the electrophoretic method used to quantify MHC isoform composition of Control and 10 day stimulated (10d Stim) rat tibialis anterior muscles (*A*). Percentage of MHCI, MHCIIa, MHCIId(x) and MHCIIb distribution in rat tibialis anterior muscles as determined by densitometric evaluation of duplicate gels (*B*). Statistical symbols indicate: ^{c} difference from respective control group (Control or L-Control), * difference between Stim and L-Stim of the same number of days of stimulation ($P < 0.05$).

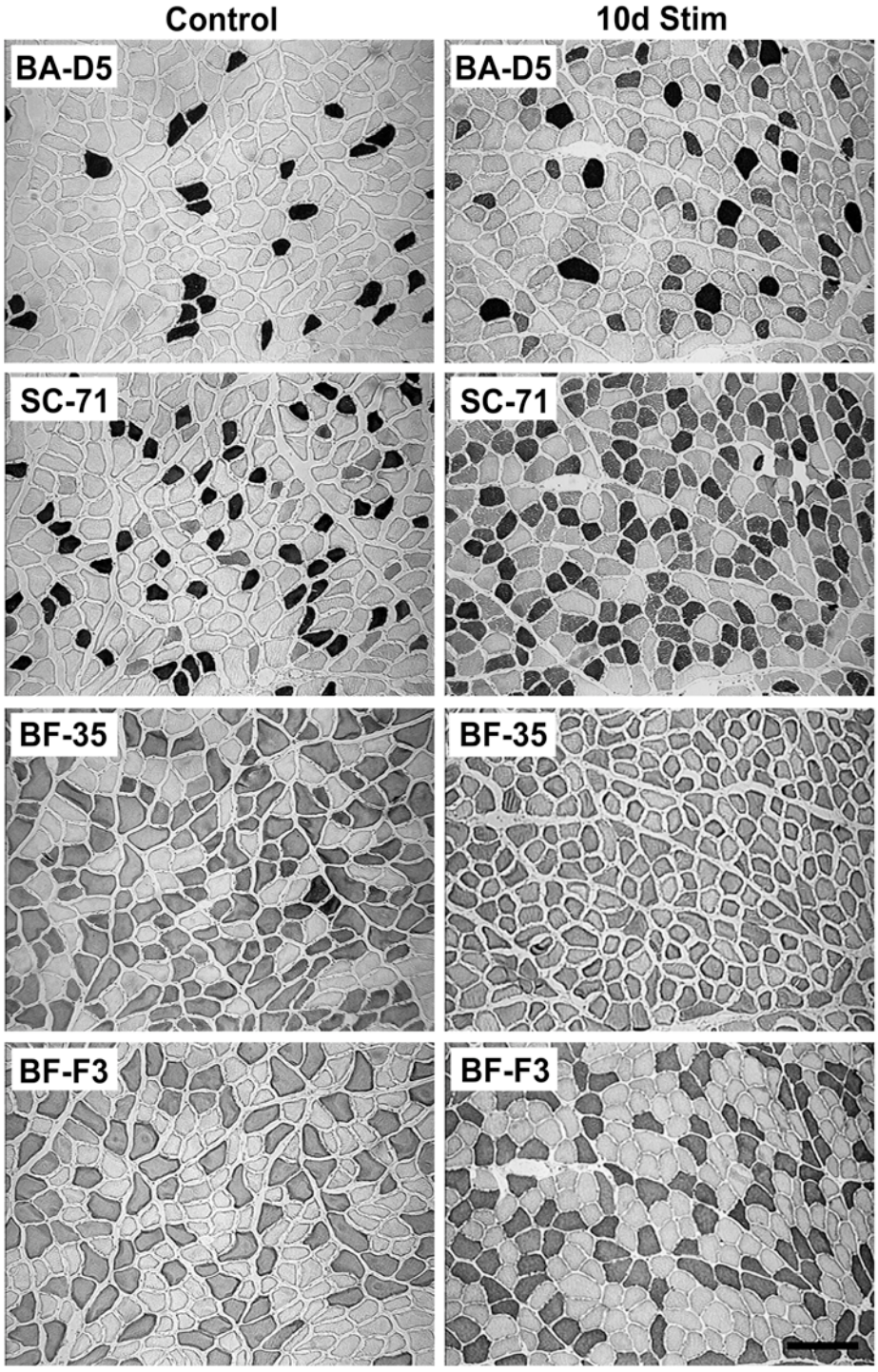

Figure 5.4 Representative MHC isoform immunohistochemistry photomicrographs of Control and 10 day stimulated (10d Stim) rat tibialis anterior muscles. Immunostains for MHCI (clone BA-D5), MHCIIa (clone SC-71), all MHC's except MHCIId(x) (clone BF-35) and MHCIIb (clone BF-F3) are shown. Bar represents 100 μm.

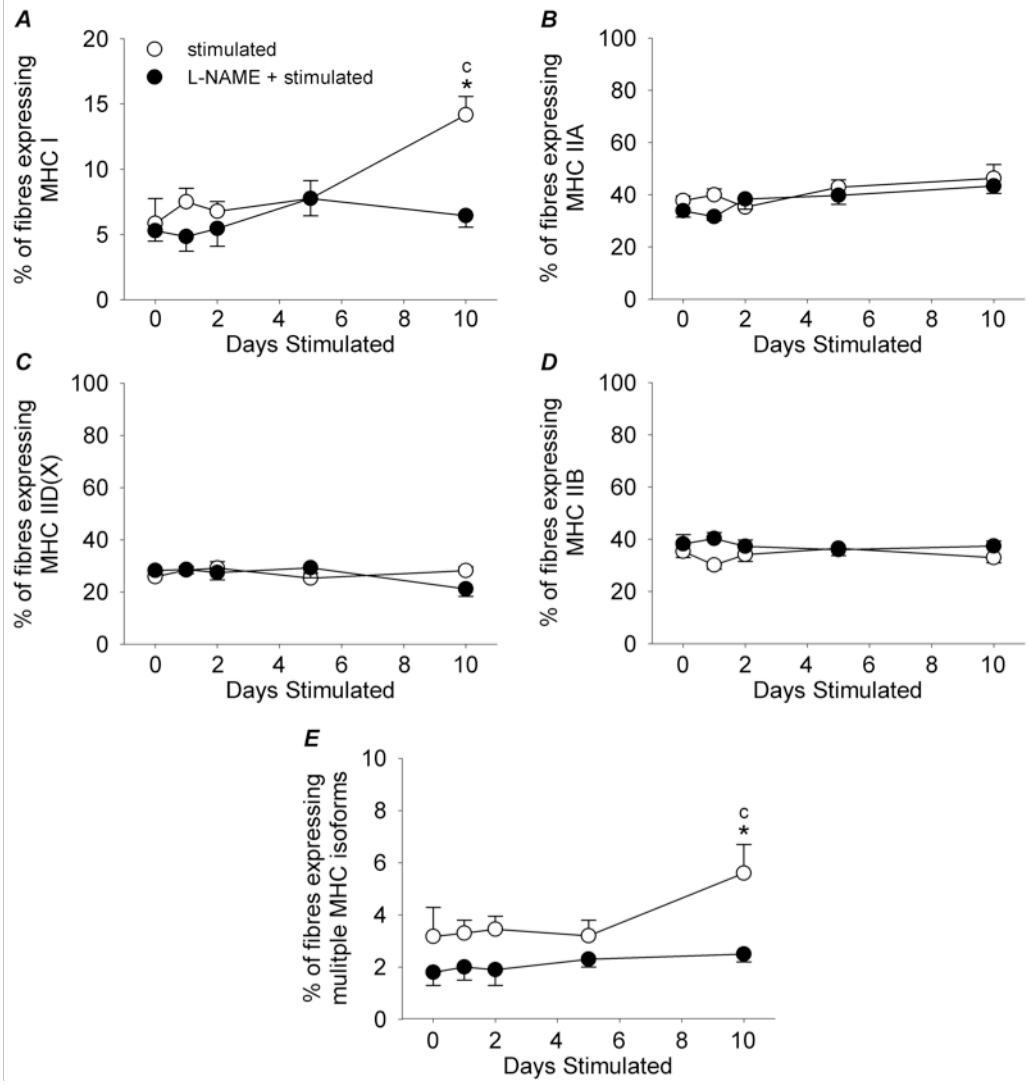

Figure 5.5 The percentage of fibres expressing MHCI (*A*), MHCIIa (*B*), MHCIId(x) (*C*), MHCIIb (*D*) and multiple MHC isoforms (*E*). Statistical symbols indicate: ^{c} difference from respective control group (Control or L-Control), * difference between Stim and L-Stim of the same number of days of stimulation ($P < 0.05$).

5.5 REFERENCES

Allen RE, Sheehan SM, Taylor RG, Kendall TL & Rice GM. (1995). Hepatocyte growth factor activates quiescent skeletal muscle satellite cells in vitro. *J Cell Physiol* **165,** 307-312.

Anderson J & Pilipowicz O. (2002). Activation of muscle satellite cells in single-fiber cultures. *Nitric Oxide* **7,** 36-41.

Anderson JE. (2000). A role for nitric oxide in muscle repair: nitric oxide-mediated activation of muscle satellite cells. *Mol Biol Cell* **11,** 1859-1874.

Bamford JA, Lopaschuk GD, MacLean IM, Reinhart ML, Dixon WT & Putman CT. (2003). Effects of chronic AICAR administration on the metabolic and contractile phenotypes of rat slow- and fast-twitch skeletal muscles. *Can J Physiol Pharmacol* **81,** 1072-1082.

Betters JL, Lira VA, Soltow QA, Drenning JA & Criswell DS. (2008a). Supplemental nitric oxide augments satellite cell activity on cultured myofibers from aged mice. *Exp Gerontol* **43,** 1094-1101.

Betters JL, Long JH, Howe KS, Braith RW, Soltow QA, Lira VA & Criswell DS. (2008b). Nitric oxide reverses prednisolone-induced inactivation of muscle satellite cells. *Muscle Nerve* **37,** 203-209.

Chin ER, Olson EN, Richardson JA, Yang Q, Humphries C, Shelton JM, Wu H, Zhu W, Bassel-Duby R & Williams RS. (1998). A calcineurin-dependent transcriptional pathway controls skeletal muscle fiber type. *Genes Dev* **12,** 2499-2509.

Delp MD & Pette D. (1994). Morphological changes during fiber type transitions in low-frequency- stimulated rat fast-twitch muscle. *Cell Tissue Res* **277,** 363-371.

Drenning JA, Lira VA, Simmons CG, Soltow QA, Sellman JE & Criswell DS. (2008). Nitric oxide facilitates NFAT-dependent transcription in mouse myotubes. *Am J Physiol Cell Physiol* **294,** C1088-1095.

Gordon SE, Westerkamp CM, Savage KJ, Hickner RC, George SC, Fick CA & McCormick KM. (2007). Basal, but not overload-induced, myonuclear addition is attenuated by NG-nitro-L-arginine methyl ester (L-NAME) administration. *Can J Physiol Pharmacol* **85,** 646-651.

Hämäläinen N & Pette D. (1996). Slow-to-fast transitions in myosin expression of rat soleus muscle by phasic high-frequency stimulation. *FEBS Lett* **399,** 220-222.

Jaschinski F, Schuler MJ, Peuker H & Pette D. (1998). Changes in myosin heavy chain mRNA and protein isoforms of rat muscle during forced contractile activity. *Am J Physiol Cell Physiol* **274,** C365-C370.

Jiang H, Li H & DiMario JX. (2006). Control of slow myosin heavy chain 2 gene expression by glycogen synthase kinase activity in skeletal muscle fibers. *Cell Tissue Res* **323,** 489-494.

Liu Y, Cseresnyes Z, Randall WR & Schneider MF. (2001). Activity-dependent nuclear translocation and intranuclear distribution of NFATc in adult skeletal muscle fibers. *J Cell Biol* **155,** 27-39.

Laemmli UK. (1970). Cleavage of structural proteins during the assembly of the head of bacteriophage T4. *Nature* **227,** 680-685.

Livak KJ & Schmittgen TD. (2001). Analysis of relative gene expression data using real-time quantitative PCR and the 2(-Delta Delta C(T)) Method. *Methods* **25,** 402-408.

Martins KJ, Gordon T, Pette D, Dixon WT, Foxcroft GR, MacLean IM & Putman CT. (2006). Effect of satellite cell ablation on low-frequency-stimulated fast-to-slow fibre-type transitions in rat skeletal muscle. *J Physiol* **572,** 281-294.

Martins KJ, Murdoch GK, Shu Y, Harris RL, Gallo M, Dixon WT, Foxcroft GR, Gordon T & Putman CT. (2009). Satellite cell ablation attenuates short-term fast-to-slow fibre type transformations in rat fast-twitch skeletal muscle. *Pflügers Arch*.

Pette D. (2002). The adaptive potential of skeletal muscle fibers. *Can J Appl Physiol* **27,** 423-448.

Pette D & Staron RS. (1997). Mammalian skeletal muscle fiber type transitions. *Int Rev Cytol* **170,** 143-223.

Pette D & Staron RS. (2000). Myosin isoforms, muscle fiber types, and transitions. *Microsc Res Tech* **50,** 500-509.

Putman CT, Dixon WT, Pearcey J, MacLean IM, Jendral MJ, Kiricsi M, Murdoch GK & Pette D. (2004). Chronic low-frequency stimulation up-regulates uncoupling protein-3 in transforming rat fast-twitch skeletal muscle *Am J Physiol Regul Integr Comp Physiol* **287,** R1419-R1426.

Putman CT, Düsterhöft S & Pette D. (1999). Changes in satellite cell content and myosin isoforms in low-frequency- stimulated fast muscle of hypothyroid rat. *J Appl Physiol* **86,** 40-51.

Putman CT, Düsterhöft S & Pette D. (2000). Satellite cell proliferation in low-frequency stimulated fast muscle of hypothyroid rat. *Am J Physiol Cell Physiol* **279,** C682-C690.

Putman CT, Kiricsi M, Pearcey J, MacLean IM, Bamford JA, Murdoch GK, Dixon WT & Pette D. (2003). AMPK activation increases UCP-3 expression and mitochondrial enzyme activities in rat muscle without fibre type transitions. *J Physiol (Lond)* **551.1,** 169-178.

Putman CT, Sultan KR, Wassmer T, Bamford JA, Skorjanc D & Pette D. (2001). Fiber-type transitions and satellite cell activation in low-frequency-stimulated muscles of young and aging rats. *J Gerontol A Biol Sci Med Sci* **56,** B510-B519.

Reiser PJ, Kline WO & Vaghy PL. (1997). Induction of neuronal type nitric oxide synthase in skeletal muscle by chronic electrical stimulation in vivo. *J Appl Physiol* **82,** 1250-1255.

Schiaffino S, Gorza L, Pitton G, Saggin L, Ausoni S, Sartore S & Lomo T. (1988). Embryonic and neonatal myosin heavy chain in denervated and paralyzed rat skeletal muscle. *Dev Biol* **127,** 1-11.

Schiaffino S, Gorza L, Sartore S, Saggin L, Ausoni S, Vianello M, Gundersen K & Lomo T. (1989). Three myosin heavy chain isoforms in type 2 skeletal muscle fibres. *J Muscle Res Cell Motil* **10,** 197-205.

Schultz E. (1996). Satellite cell proliferative compartments in growing skeletal muscles. *Dev Biol* **175,** 84-94.

Sellman JE, DeRuisseau KC, Betters JL, Lira VA, Soltow QA, Selsby JT & Criswell DS. (2006). In vivo inhibition of nitric oxide synthase impairs upregulation of contractile protein mRNA in overloaded plantaris muscle. *J Appl Physiol* **100,** 258-265.

Shen T, Cseresnyes Z, Liu Y, Randall WR & Schneider MF. (2007). Regulation of the nuclear export of the transcription factor NFATc1 by protein kinases after slow fibre type electrical stimulation of adult mouse skeletal muscle fibres. *J Physiol* **579,** 535-551.

Simoneau JA & Pette D. (1988). Species-specific effects of chronic nerve stimulation upon tibialis anterior muscle in mouse, rat, guinea pig and rabbit. *Pflügers Arch* **412,** 86-92.

Smith LW, Smith JD & Criswell DS. (2002). Involvement of nitric oxide synthase in skeletal muscle adaptation to chronic overload. *J Appl Physiol* **92,** 2005-2011.

Soltow QA, Betters JL, Sellman JE, Lira VA, Long JH & Criswell DS. (2006). Ibuprofen inhibits skeletal muscle hypertrophy in rats. *Med Sci Sports Exerc* **38,** 840-846.

Stamler JS & Meissner G. (2001). Physiology of nitric oxide in skeletal muscle. *Physiol Rev* **81,** 209-237.

Tatsumi R, Anderson JE, Nevoret CJ, Halevy O & Allen RE. (1998). HGF/SF is present in normal adult skeletal muscle and is capable of activating satellite cells. *Dev Biol* **194,** 114-128.

Tatsumi R, Hattori A, Ikeuchi Y, Anderson JE & Allen RE. (2002). Release of hepatocyte growth factor from mechanically stretched skeletal muscle satellite cells and role of pH and nitric oxide. *Mol Biol Cell* **13,** 2909-2918.

Tatsumi R, Liu X, Pulido A, Morales M, Sakata T, Dial S, Hattori A, Ikeuchi Y & Allen RE. (2006). Satellite cell activation in stretched skeletal muscle and the role of nitric oxide and hepatocyte growth factor. *Am J Physiol Cell Physiol* **290,** C1487-1494.

Tatsumi R, Sheehan SM, Iwasaki H, Hattori A & Allen RE. (2001). Mechanical stretch induces activation of skeletal muscle satellite cells in vitro. *Exp Cell Res* **267,** 107-114.

Tothova J, Blaauw B, Pallafacchina G, Rudolf R, Argentini C, Reggiani C & Schiaffino S. (2006). NFATc1 nucleocytoplasmic shuttling is controlled by nerve activity in skeletal muscle. *J Cell Sci* **119,** 1604-1611.

Vinsky MD, Murdoch GK, Dixon WT, Dyck MK & Foxcroft GR. (2007). Altered epigenetic variance in surviving litters from nutritionally restricted lactating primiparous sows. *Reprod Fertil Dev* **19,** 430-435.

Wozniak AC, Kong J, Bock E, Pilipowicz O & Anderson JE. (2005). Signaling satellite-cell activation in skeletal muscle: markers, models, stretch, and potential alternate pathways. *Muscle Nerve* **31,** 283-300.

CHAPTER SIX

GENERAL DISCUSSION AND INTERPRETATIONS

6.1 SUMMARY OF RESULTS

The purpose of the preceeding experiments was to investigate the activity-induced activating signaling mechanisms and subsequent contributions of satellite cells to skeletal muscle adaptations in rat.

Chapter 3 tested the specific hypothesis that long-term (21 days) CLFS-induced fast-to-slow fibre type transformations would be attenuated in rat fast-twitch tibialis anterior muscles exposed to γ-irradiation. Chapter 4 investigated earlier time points of stimulation and tested the specific hypothesis that in those muscles exposed to γ-irradiation, short-term (1 to 10 days) CLFS-induced fast-to-slow fibre type transformations would be i) attenuated in the fast fibre population and ii) prevented from the final fast-twitch to slow-twitch transformation. In response to weekly focal 25 Gy doses of γ-irradiation, the disruption of satellite cell mitotic activity was successfully maintained throughout 21 days of stimulation while not causing any skeletal muscle damage, morphology abnormalities, or interfering with baseline muscle gene and protein expression. Therefore, the following outcomes are described in rat tibialis anterior muscles exposed to γ-irradiation: i) short-term CLFS-induced fast-to-slow MHC isoform protein and fibre type transformations are attenuated in the fast fibre population and prevented from the final fast-twitch to slow-twitch transformation, ii) long-term CLFS-induced fast-to-slow MHC isoform protein and fibre type transformations are also prevented from the final fast type IIA to slow type I transformation, and iii) CLFS-induced fast-to-slow MHC isoform transformations at the mRNA level are initially delayed, specifically in MHCIId(x) mRNA, but at 21 days of stimulation, expression levels of all MHC isoforms are not different from normal stimulated muscles. In summary, CLFS-induced fast-to-slow MHC isoform protein and fibre type transformations are attenuated in the fast fibre population during short-term stimulation and prevented from the final fast-twitch

to slow-twitch transformation throughout 21 days of stimulation in those muscles exposed to γ-irradiation. At the MHC mRNA level, however, CLFS-induced fast-to-slow transformations are only initially slightly delayed.

In Chapter 5, it was hypothesised that in vivo pharmacological inhibition of NOS activity in the rat would prevent i) immediate CLFS-induced satellite cell activation and ii) subsequent fast-to-slow fibre type transformations. The inhibition of NOS activity during short-term CLFS in rat tibialis anterior muscles, produced the following observations: i) satellite cell activity was initially blocked but, subsequently able to proliferate to the same extent as normally stimulated muscles, and ii) MHC-based fast-to-slow transformations at the mRNA, protein and fibre type levels were not different from control non-stimulated muscles. In summary, NO appears to be required for immediate CLFS-induced satellite cell activity but, an unknown alternative mechanism appears to exist that is able to fully compensate under conditions where NO levels are suppressed within rat tibialis anterior muscles. Additionally, NO appears to be a key mediator of MHC isoform expression during CLFS-induced fast-to-slow fibre type transformations.

6.2 SATELLITE CELLS ARE INVOLVED IN CLFS-INDUCED FAST-TO-SLOW FIBRE TYPE TRANSFORMATIONS

6.2.1 Fast-to-Slow Fibre Type Transformations and Myonuclear Domain Threshold

A myonuclear domain is defined as the theoretical volume of cytoplasm surrounding and controlled by the gene products of a single myonucleus (Cheek, 1985). This concept originates from the finding that mRNA produced by a single myonucleus is restricted to the area immediately surrounding that particular myonucleus (Pavlath *et al.*, 1989; Ralston & Hall, 1992). The causal link between satellite cell-derived myonuclear accretion, increased fibre size and a constant myonuclear domain size during skeletal muscle hypertrophy has been well recognised (reviewed by Schultz, 1989; Adams, 2006; O'Connor & Pavlath,

2007). However, small increases in myofibre cross-sectional area and cytoplasmic volume can be supported by existing myonuclei up to a certain threshold or myonuclear domain ceiling above which myonuclear accretion from satellite cells is required to support continued hypertrophy (Chin, 2004; Kadi *et al.*, 2004; Petrella *et al.*, 2006; O'Connor & Pavlath, 2007). Interestingly, it appears that a myonuclear domain threshold may also exist in CLFS-induced fast-to-slow fibre type transformations.

As discussed in Chapter 4, Schultz & Darr (1990) first hypothesised that since slow-twitch skeletal muscle fibres contain a larger number of myonuclei, smaller cross-sectional areas and cytoplasmic volume (Gibson & Schultz, 1982, 1983) and therefore, smaller myonuclear domain sizes compared with fast-twitch fibres (Cheek, 1985; Schultz *et al.*, 1990; Tseng *et al.*, 1994; Roy *et al.*, 1999), satellite cells play an obligatory role in maintaining the newly fast-to-slow transformed state. For example, the transformation from a faster to a slower fibre type would include a decrease in myonuclear domain size first by the addition of new myonuclei then coupled with a decrease in fibre cross-sectional area and cytoplasmic volume (Putman *et al.,* 1999). Expanding upon this hypothesis, based on results from Chapters 3 and 4, it also appears that existing myonuclei can support fast-to-slow fibre type transformations up to certain threshold, beyond which, myonuclear accretion from satellite cells is necessary for continued transformation. For example, the final CLFS-induced fast-twitch to slow-twitch MHC isoform protein and fibre type transformation did not occur at any time point in those muscles that had been exposed to γ-irradiation. Thus, it appears that CLFS-induced fast-to-slow transformations within the fast fibre population can be supported by existing myonuclei but, beyond this threshold, myonuclear accretion from satellite cells may be required to support the final transformation from the fast type IIA to the slow type I fibre population. It should be noted that within the fast fibre population of those muscles that had been exposed to γ-irradiation, fast-to-slow fibre type transformations were initially attenuated during CLFS. These results indicate that satellite cell activity may also important during

short-term CLFS to reduce the myonuclear domain sizes of the fast fibre types, allowing them to transform without delay. Collectively, results from previous studies (Jaschinski *et al.*, 1998; Putman *et al.*, 1999) and Chapters 3 and 4 support the following hypotheses, which is currently being investigated: i) myonuclear domain sizes of the fast fibre types are first to decrease by the incorporation of satellite cells during short-term CLFS, ii) further reductions in myonuclear domain sizes occur via decreases in fibre cross-sectional area of the newly transformed fibres and to a lesser extent by the fusion of satellite cell progeny during long-term CLFS, and iii) a myonuclear domain threshold exists in CLFS-induced fast-to-slow fibre type transformations.

6.2.2 Satellite Cells and Translational Capacity

Adams *et al.* (2002) investigated the underlying cellular and molecular mechanisms responsible for preventing compensatory muscle hypertrophy to occur beyond the myonuclear domain threshold in those muscles lacking a viable satellite cell population. Results of that study indicate γ -irradiation-induced inhibition of the hypertrophy response is not related to the ability of existing myonuclei to produce mRNA, but to intracellular signaling pathways associated with the regulation of protein translation. They found that the phosphorylation states of ribosomal protein S6 kinase-1 (S6K1) and eukaryotic initiation factor 4E-binding protein-1 (4E-BP1) returned to baseline after 3 days of overload in γ-irradiation exposed rat plantaris muscles, which remained elevated throughout 15 days in normal overloaded muscles. Outlined in Figure 6.1, signaling in the Akt-mammalian target of rapamycin (mTOR) pathway, of which S6K1 and 4E-BP1 are downstream targets, promotes increased protein synthesis in a number of ways (reviewed by Adams, 2006; Coffey & Hawley, 2007; Miyazaki & Esser, 2009). For example, phosphorylated S6K1 appears to be involved in facilitating the translation of components of the translational apparatus itself via recruitment and promotion of translation of specific mRNA's that encode several ribosomal proteins and translation elongation factors. On the other hand, hyperphosphorylation of 4E-BP1 removes its inhibitory effects on eukaryotic

initiation factor 4E, which is involved in formation of the initiation complex by binding to the 5' end of mRNA and aiding in binding it to the ribosome. Adams *et al.* (2002) also found that total RNA retuned to baseline in those overloaded rat plantaris muscles exposed to γ-irradiation, which remained elevated in normal overloaded muscles. Total RNA is generally accepted as being indicative of alterations in rRNA and therefore, translational capacity of the tissue, because approximately 85% of bulk RNA is rRNA. Since rRNA is a final gene product (i.e. can not be amplified like mRNA via polyribosomes), increasing rRNA requires more DNA templates, which in skeletal muscle, comes from incrased satellite cell-derived myonucelar accreation.

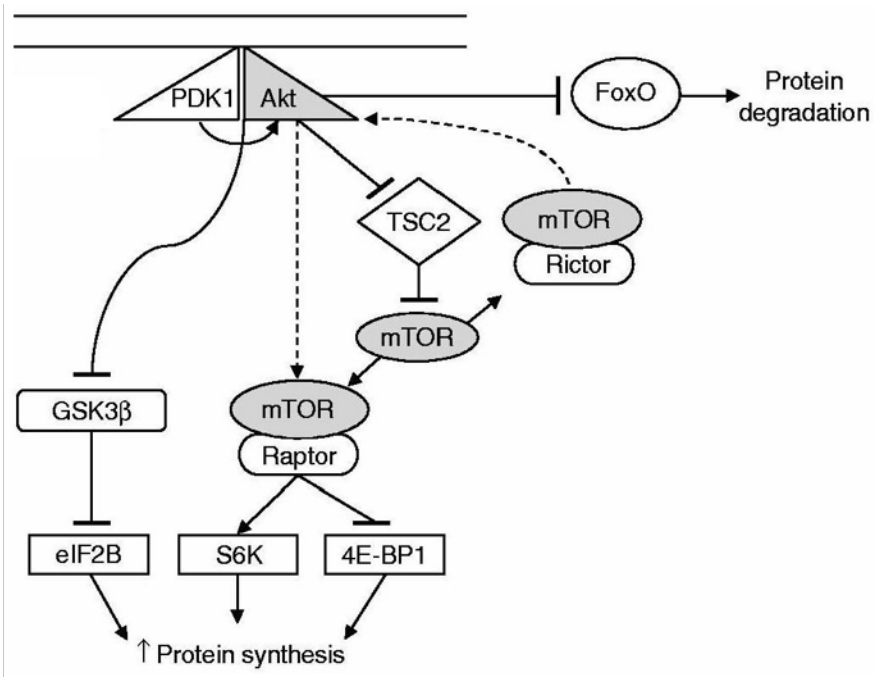

Figure 6.1 Akt signaling. Arrows=activation, bars=inhibition, dashed line=direct activation. 4E-BP1=eukaryotic initiation factor 4E-binding protein-1; eIF2B=eukaryotic initiation factor 2B; FoxO=forkhead box O; GSK3β=glycogen synthase kinase 3β; mTOR=mammalian target of rapamycin; PDK1= 3'-phosphoinositide-dependent protein kinase-1; S6K=ribosomal protein S6 kinase; TSC2=tuberous sclerosis complex-2; ↑=increase. With permission from Coffey & Hawley (2007).

Stimulation of fast-twitch muscles with slow-patterned activity causes a fast-to-slow fibre type transformation that requires both the up-regulation of slower and repression of faster contractile proteins. Additionally, the smaller myonuclear domains of slow-twitch fibres are presumably a requirement for the higher biosynthetic activities and protein turnover rates that occurs in these fibres (Goldberg, 1967; Edgerton & Roy, 1991; Tseng *et al.*, 1994). Interestingly, Nader & Esser (2001) found that a single bout of low-frequency stimulation caused a significant increase in Akt and S6K1 phosphorylation immediately and 3 hours post-exercise, respectively, in rat tibialis anterior musles. Based on the findings of Adams *et al* (2002) and Nader & Esser (2001), it is therefore attractive to hypothesise that myonuclear accretion from satellite cells is necessary to increase traslational capacity for CLFS-induced fast-to-slow transformation to occur without delay in the fast fibre types and for the final type IIA to type I transformation.

Results from Chapters 3 and 4 show that CLFS-induced MHC-based fast-to-slow transformations at the mRNA level were not different, for the most part (see section 6.2.3), between normal stimulated muscles and those also exposed to γ-irradiation, while at the protein level, transformation within the fast fibres were delayed and the final transformation to type I fibres did not occur. Therefore, in those muscles that lack a viable satellite cell populaiton, the limiting factor in CLFS-induced fast-to-slow fibre type transformation does not appear to be the ability to produce MHC mRNA, but perhaps the signaling pathways associated with translational and/or post-translational regulation. Hence, a natural progression in the investigation of satellite cell involvement in fast-to-slow fibre type transformations would be to determine the specific underlying cellular and molecular mechanisms responsible for impairing MHC-based fast-to-slow transformations at the protein level in those muscles exposed to γ-irradiation. While it is appealing to propose that this regulation may occur via the Akt-mTOR patway, there are conflicting data regarding this pathways response to low-frequency stimulation. As opposed to the findings reported by Nader & Esser

(2001), Atherton *et al.* (2005) found that in isolated rat extensor digitorum longus muscles exposed to 3 hours of low-frequency stimulation, the Akt-mTOR-related signaling cascade was deactivated. Additional contradictory data also exists regarding the Akt-mTOR response to treadmill and wheel running in rodents (Coffey & Hawley, 2007).

6.2.3 Default Satellite Cell Progeny Expression

Throughout 21 days of stimulation, CLFS-induced MHC-based fast-to-slow transformations at the mRNA level were not different between normal stimulated muscles and those also exposed to γ-irradiation, with one exception (Fig's. 3.6 and 4.2). At 10 days of stimulation, MHCIId(x) mRNA expression was significantly greater in normal stimulated muscles compared to previously irradiated muscles (Fig. 4.2*C*). This difference, however, may be due to a lack of initial default MHC mRNA expression from satellite cell progeny as opposed to an indication of delayed fast-to-slow MHC mRNA transformation in those muscles where satellite cell activity was inhibited.

It appears that the default MHC isoform program of satellite cell progeny from adult skeletal muscle may be MHCIId(x) (Pin & Merrifield, 1997; Conway *et al.*, 2004). It was demonstrated that satellite cells of the L6 myoblast lineage (Yaffe, 1968) only expresses embryonic and adult MHCIId(x) in vitro (Conway *et al.*, 2004). Additionally, injection of L6 myoblasts into regenerating adult rat hindlimb muscles caused formation of MHCIId(x) fibres in vivo (Pin & Merrifield, 1997). Therefore, since the default program of satellite cell progeny appears to be MHCIId(x) (Pin & Merrifield, 1997; Conway *et al.*, 2004) and maximum satellite cell activity and fusion have been shown to occur between 5 and 10 days of stimulation (Putman *et al.*, 1999; Chapter 4), it seems possible that the significant increase seen in MHCIId(x) mRNA at 10 days in normal stimulated tibialis anterior muscles may be due, at least in part, to the initial default MHC isoform expression of satellite cell progeny. It should be noted that this initial default expression is not fixed but, can be influenced by slow patterns

of innervation (Pin & Merrifield, 1997; Kalhovde *et al.*, 2005). For example, Pin & Merrifield (1997) found that those L6 myoblasts that fused with type I fibres only initially expressed MHCIId(x) mRNA. Furthermore, it has been found that deinnervated regenerating soleus muscles, which form new fibres from satellite cells, only display the fastest fibre types (Whalen *et al.*, 1990; Kalhovde *et al.*, 2005), which is in contrast to its phenotypic profile under normal conditions. Interestingly, when a slow stimulus pattern was subsequently imposed, a significant fast-to-slow transformation occurred (Kalhovde *et al.*, 2005). Results from Chapter 3 support these findings because MHCIId(x) mRNA levels returned to baseline at 21 days of stimulation, indicating that the default MHCIId(x) mRNA expression of satellite cell progeny observed at 10 days of stimulation had been overridden by a prolonged pattern of slow motoneuron activity.

6.3 NITRIC OXIDE-DEPENDENT SATELLITE CELL ACTIVATION IS THE PREFERRED PATHWAY IN RESPONSE TO CLFS

As discussed in Chapters 2 and 5, the NO-dependent satellite cell activation pathway has been well defined, but signaling mechanisms involved in satellite cell activation may also function in a NO-independent manner (Wozniak *et al.*, 2005). To date, NOS inhibition has been utilised in a number of studies including in vitro, in vivo and single fibre cultures employing injury-, crushed muscle extract-, stretch- and overload-induced satellite cell activation models to investigate the involvement of NO in this process (Table 6.1). Interestingly, studies that have demonstrated a dependence on NO for satellite cell activation have focused on early time points of measurement post-activation initiation (immediate to 48 hours) (Anderson, 2000; Anderson & Pilipowicz, 2002; Tatsumi *et al.*, 2002; Sakata *et al.*, 2006; Tatsumi *et al.*, 2006), while those results supporting a NO-independent pathway have focused on later time points (50 hours and 7 to 12 days) (Sellman *et al.*, 2006; Tatsumi *et al.*, 2006; Gordon *et al.*, 2007). Collectively, these studies and results from Chapter 5, suggest that the primary and/or immediate satellite cell activation pathway is NO-dependent while

an alternative pathway, which has yet to be identified, exists that can fully compensate in the absence of optimal NO availability.

Table 6.1 Summary of research investigating the involvement of NO in satellite cell activation.

Study	Model	Activation Method	Time of Measurement Post-Activation Initiation	Result: Presence of NO	Result: NOS inhibition
Anderson (2000)	Rat	3 s crush injury	3 s post-crush	Immediate indicators of satellite cell activation	No indication of satellite cell activation
Sakata *et al.* (2006)	Rat	2 h hind limb stretch via suspension	18 h post-stretch	Increase in BrdU+ nuclei	No increase in BrdU+ nuclei
Tatsumi *et al.* (2006)	Rat	2 h hind limb stretch via suspension	32 and 38 h post-stretch	Increase in BrdU+ nuclei	No increase in BrdU+ nuclei
Tatsumi *et al.* (2002)	Cultured adult rat muscle	36 h mechanical stretch	36 h post-plating	Increase in BrdU+ nuclei	No increase in BrdU+ nuclei
Anderson *et al.* (2002)	Cultured single fibres	48 h in crushed muscle extract medium	48 h post-plating	Increase in BrdU+ nuclei	No increase in BrdU+ nuclei
Tatsumi *et al.* (2006)	Rat	2 h hind limb stretch via suspension	50 h post-stretch	Increase in BrdU+ nuclei	Increase in BrdU+ nuclei, but not to same extent as normal stretch
Gordon *et al.* (2007)	Rat	7 d hindlimb overload	7d post-overload	Increase in BrdU+ nuclei	Increase in BrdU+ nuclei to same extent as normal overload
Sellman *et al.* (2006)	Rat	12 d hindlimb overload	12 d post-overload	Increase in BrdU+ subsarcolemmal nuclei	Increase in BrdU+ nuclei to same extent as normal overload

As outlined in Figure 6.2A, the current model of skeletal muscle satellite cell activation involves the stimulation of nitric oxide production via Ca^{2+}-calmodulin-dependent NOS activity in satellite cells and/or muscle fibres, followed by MMP-2 activation, which in turn, cleaves the proteoglycan tether attached to HGF localised in the extracellular matrix, and finally the presentation of HGF to the c-met receptor (Tatsumi & Allen, 2008). Therefore, it is possible that the NO-independent pathway could stimulate satellite cell activation via involvement in one or more of the following steps: i) MMP-2 activation from an alternative source (Fig. 6.2B), or ii) presentation of extracellular matrix-independent HGF to c-met (Fig. 6.2C).

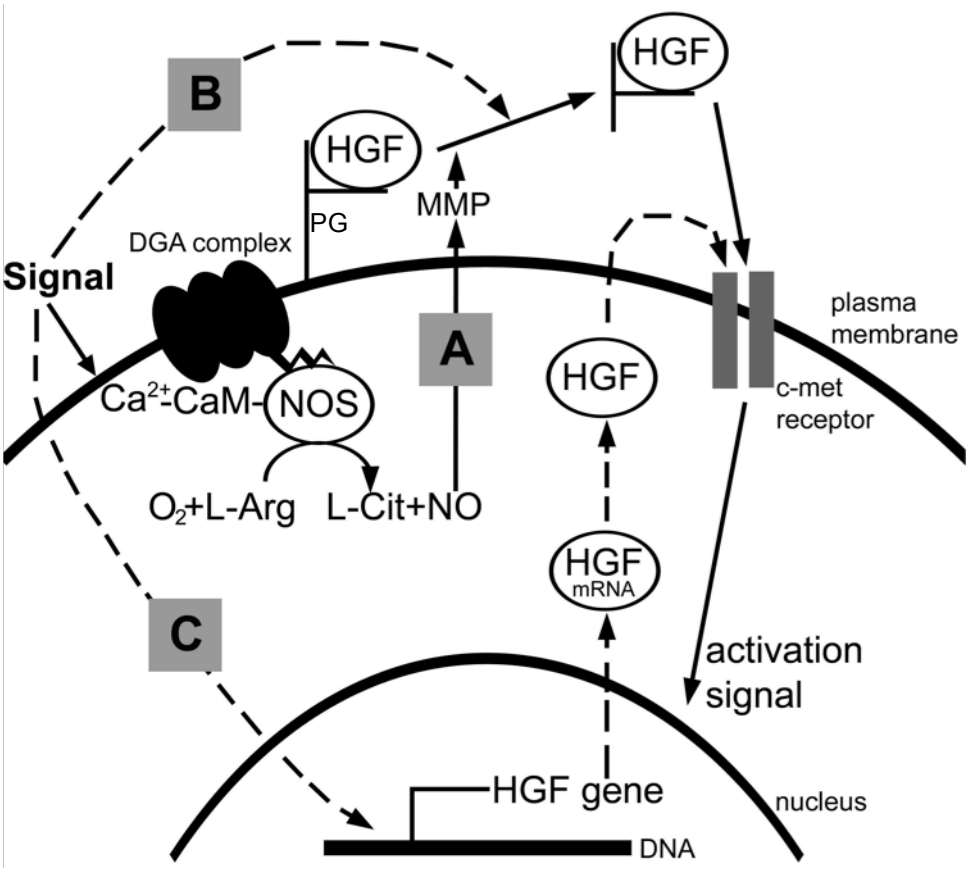

Figure 6.2 Schematic representation of the possible mechanisms of satellite cell activation. Ca^{2+}-CaM=calcium-calmodulin complex; DGA=dystrophin-glycogen associated; HGF=hepatocyte growth factor protein (active form); L-Arg=L-arginine; L-Cit=L-citruline; MMP=matrix metalloproteinase; NO=nitric oxide; NOS=nitric oxide synthase; PG=proteoglycans; straight arrows=NO-dependent satellite cell activation pathway (A); dashed arrows=potential NO-independent activation pathways (B and C).

6.3.1 Hepatocyte Growth Factor Liberation from the Extracellular Matrix

MMPs are a major group of proteolytic enzymes that are best know for their ability to cleave several different extracellular matrix proteins, although relatively little is known regarding their role in skeletal muscle (reviewed by Carmeli *et al.*, 2004; Haas, 2005). Thus far, several MMPs have been identified in skeletal muscle, including MMP-2, -3, -7 and -9 of which, MMP-2, -3 and -9 can cleave heparin sulfate proteoglycans (VanSaun & Werle, 2000; Carmeli *et al.*, 2004). MMP-3 appears to be specifically associated with argin, a basal lamina component that plays a key role in the formation and maintenance of the neuromuscular junction (VanSaun & Werle, 2000), while MMP-2 and -9 are thought to play important roles in skeletal muscle adaptation to exercise and regeneration (Carmeli *et al.*, 2004). Additionally, satellite cells and myoblasts have been shown to constitutively synthesise and secrete MMP-2, but not MMP-9 (Guerin & Holland, 1995; Kherif *et al.*, 1999; Yamada *et al.*, 2008), which has been shown to be localised in inflammatory cells and activated satellite cells in injured skeletal muscle (Kherif *et al.*, 1999; Fukushima *et al.*, 2007). Therefore, the potential involvement of NO-independent cleavage of HGF with its associated proteoglycan would likely appear to specifically involve MMP-2, which will be the focus of the following paragraphs.

In addition to the possibility that NO may directly activate MMP-2 (Chakraborti *et al.*, 2003; Yamada *et al.* 2008), cyclooxygenase (COX) and mitogen-activated protein kinase (MAPK) signaling have also been shown to regulate MMP-2. For example, production and secretion of MMP-2 protein have been shown to occur through a prostaglandin-dependent pathway (Kranenburg *et al.*, 2004; Husain & Crosson, 2008). Reviewed by Funk (2001), signaling through this pathway involves the COX enzymes that induce the conversion of arachidonic acid to prostaglandins, which subsequently bind to G-protein coupled receptors. Two isoforms of COX have been identified and are present in skeletal muscle, the constitutively expressed COX-1 that serves basal physiological functions and the inducibly expressed COX-2 that increases primarily in response

to inflammatory stimuli. Although COX signaling has not been specifically investigated in satellite cell activation, COX-1 and 2 have been shown to be important for skeletal muscle myoblast proliferation, differentiation and fusion in vitro (Mendias *et al.*, 2004; Bondesen *et al.*, 2007) and COX-2 appears to play a role in skeletal muscle regeneration in vivo (Bondesen *et al.*, 2004). Specifically, Mendias *et al.* (2004) reported that inhibition of COX-2 resulted in decreased satellite cell proliferation, differentiation and fusion, while inhibition of COX-1 resulted in decreased differentiation and fusion in cultured rat satellite cells. Additionally, Mackey *et al*. (2007) demonstrated that the administration of indomethacin, a nonsteroidal anti-inflammatory drug that nonselectively blocks COX activity, abolished a non-injury endurance training-induced increase in satellite cell activity in humans. Collectively, these studies indicate that COX signaling, which can be induced in the absence of fibre injury, influences satellite cell activity that may be mediated in part through MMP-2 activity.

The MAPK family plays an important role in relaying extracellular signals to intracellular responses (Roux & Blenis, 2004). The most extensively studied subfamilies of MAPKs are extracellular signal-regulated kinase (ERK1/2), c-jun N-terminal kinase (JNK) and p38 MAPK. Specifically, ERK1/2, which increases in response to low intensity exercise (Kramer & Goodyear, 2007), has been shown to enhance production of MMP-2 and its activator membrane type I (MT1)-MMP (Haas, 2005) as well as playing an important role in the regulation of satellite cell activity (Jones *et al.*, 2001; Roux & Blenis, 2004). Moreover, in response to the application of CLFS in rat, ERK1/2 activity is markedly increased (Murgia *et al.*, 2000; Altherton *et al*, 2005) along with mRNA levels of MMP-2 and MT1-MMP, and protein levels of active MMP-2 and MT1-MMP (Haas *et al.*, 2000). Interestingly, G protein-coupled receptors transmit activating signals to the Raf/MEK/ERK cascade (Roux & Blenis, 2004), thus leading to the possibility that COX may lie upstream of ERK1/2 mediated MMP-2 regulation. Husain & Crosson (2008) provide evidence in ciliary muscle cells, where they show COX-dependent prostaglandin-induced secretion of MMP-2 requires the involvement of

ERK1/2. This signaling pathway appears to be likely involved in CLFS-induced satellite cell activity but, whether it is regulated by NO must be considered. In this regard, administration of the NOS inhibitor L-NAME was shown to inhibit increases in COX-2 mRNA in 14 day overloaded rat plantaris muscles (Soltow *et al.*, 2006). Additionally, chronic NO deficiency has been shown to inhibit ERK1/2 and MMP-2 activation in rat hearts (Spanikova *et al.*, 2008). Collectively, these results suggest that MMP-2 regulation by COX-ERK1/2 signaling may occur in a NO-dependent fashion and therefore, HGF liberation from the extracellular matrix may not be involved in NO-independent satellite cell activation.

An additional reason why the above proposed pathway may not be involved in extracellular matrix HGF liberation has to do with the time line of satellite cell and COX activation. For example, in response to overload in rat plantaris muscles, satellite cell proliferation has been detected as early as 2 days after the onset of stimulus (Sakuma *et al.*, 2003), while inducible COX-2 mRNA does not increase until 14 days; (COX-1 mRNA does not increase in response to overload) (Soltow *et al.*, 2006). Although it appears that NO-dependent COX-ERK1/2 signaling promotes MMP-2 production and activation and therefore, may play a role in satellite cell activation, based on the time line of overload-induced satellite cell proliferation and induction of COX-2 production, it seems that COX-ERK1/2 signaling may play a larger role in the regulation of satellite cells after activation. In support of this idea, COX signaling is known to be important for satellite cell proliferation, differentiation and fusion (Mendias *et al.*, 2004; Bondesen *et al.*, 2007), while ERK1/2 has been implicated as a key regulator of cell proliferation in a number of tissues (Roux & Blenis, 2004) including skeletal muscle satellite cells (Jones *et al.*, 2001).

6.3.2 Extracellular Matrix-Independent Source of HGF

Since NO-independent liberation of HGF from the extracellular matrix does not seem likely (Fig. 6.2B), this raises the possibility that HGF from another

source may colocalise with the c-met receptor to initiate activation of quiescent satellite cells. Although HGF associated with heparin sulfate proteoglycans appears to have a greater affinity for the c-met receptor (Derksen *et al.*, 2002), HGF alone can also stimulate satellite cell activation as shown in vitro (Tatsumi *et al.*, 1998). In vivo, it has been demonstrated that overloaded rat skeletal muscle is associated with increased HGF mRNA and protein content, and increased BrdU positive satellite cells, all of which are unaffected by long-term L-NAME administration (Sellman *et al.*, 2006; Gordon *et al.*, 2007). While it appears that NO is required for HGF release from the extracellular matrix (Anderson & Pilipowicz, 2002; Tatsumi *et al.*, 2002; Tatsumi *et al.*, 2006), the lack of L-NAME effect on overload-induced HGF mRNA or protein abundance in skeletal muscle indicates that de novo HGF production may not be dependent on NO. Therefore, it appears that the NO-dependent release of HGF from the extracellular matrix may represent an immediate response pathway for satellite cell activation, while HGF production, which does not seem to require NO signaling, may be necessary for continued activation, restocking extracellular matrix stores, and/or play a pivotal role in the NO-independent satellite cell activation pathway (Fig. 6.2C). This potential NO-independent patway is currently under investigation.

6.4 NITRIC OXIDE IS A KEY MEDIATOR OF CLFS-INDUCED FAST-TO-SLOW MHC-BASED TRANSFORMATIONS

Thus far, only the Criswell laboratory has investigated the involvement of NO in fast-to-slow MHC-based transformations (Smith *et al.*, 2002; Sellman *et al.*, 2006; Drenning *et al.*, 2008). They initially reported that NOS inhibition prevented the up-regulation of MHCI mRNA and protein during functional overload of the rat plantairs muscle (Smith *et al.*, 2002; Sellman *et al.*, 2006). More recently, their laboratory has demonstrated that NO facilitates Ca^{2+}-ionophore-induced NFAT nuclear accumulation and increased MHCI mRNA expression via GSK-3β inhibition in C_2C_{12} myotubes; Figure 6.3 illustrates their proposed model of slow gene regulation (Drenning *et al.*, 2008). Through Ca^{2+}-

calmodulin binding, NOS catalyses the production of NO. Subsequently, soluble guanylate cyclase (sGC), the principle receptor for NO, catalyses the formation of the second messenger cyclic guanosine monophosphate (cGMP) from guanosine triphosphate. cGMP-dependent kinases then inhibit GSK-3β, allowing NFAT to accumulate in the nucleus.

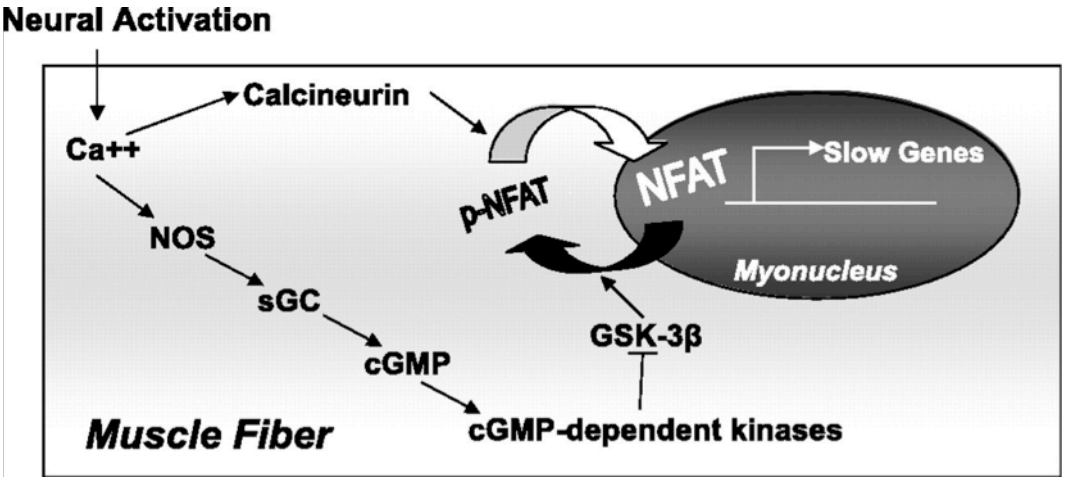

Figure 6.3 Proposed model. Nitric oxide facilitates calcium-induced NFAT nuclear accumulation and subsequent expression of slow-type mRNAs by inhibiting GSK-3β and reducing export of NFAT from the nucleus. Ca++=calcium; cGMP=cyclic guanosine monophosphate; GSK-3β=glycogen synthase kinase-3β; NFAT=nuclear factor of activated T cells; NOS=nitric oxide synthase; p-NFAT=phosphorylated NFAT; sGC=soluble guanylate cyclase. With permission from Drenning *et al.* (2008).

6.4.1 Slow Myosin Heavy Chain Regulation

Based on the findings in Chapter 5, this proposed pathway (Fig. 6.3) might be extended to include control of CLFS-induced up-regulation of MHCI in vivo. This, however, would require further investigation. Additionally, NFAT appears to act synergistically with myocyte enhancing factor (MEF)2 in turning on slow muscle-specific genes (Chin *et al.*, 1998; Wu *et al,* 2000). Moreover, both NFAT and MEF2 consensus binding sequences are present within the transcriptional control regions of multiple slow-fibre specific genes (Chin *et al*, 1998). The

currently known signaling pathways that are involved in activity-induced regulation of slow muscle specific genes (Liu *et al.*, 2005b) including MHCI (Meissner *et al.*, 2007; Drenning *et al.*, 2008) are depicted in Figure 6.4; these include the calcineurin/NO-NFAT, calcineurin-MEF2 and calmodulin-dependent protein kinase (CaMK)/histone deacetylase (HDAC)-MEF2 pathways. Therefore, in addition to regulating MHCI gene expression by potentially facilitating NFAT nuclear accumulation in vivo, NO may also be involved in promoting other transcription factors associated with slow fibre type gene expression during fast-to-slow transformations.

Within the nucleus, MEF2 transcriptional activity is controlled through association with class II HDACs that when dephosphorylated, bind to and represses MEF2 (reviewed by Bertos *et al.*, 2001). In response to various signals, HDAC becomes phosphorylated, which allows binding to occur with intracellular chaperone protein 14-3-3, causing nucleocytoplasmic shuttling of HDAC and thus, the removal of MEF2 inhibition (Bertos *et al.*, 2001). Exercise such as voluntary wheel running and low-frequency stimulation have been shown to cause HDAC4 translocation from the nucleus to the cytoplasm and increase MEF2 activity (Dunn *et al.*, 2001; Wu *et al.*, 2001; Liu *et al.*, 2005a; Liu *et al.*, 2005b), which in turn, promotes expression of slow muscle-specific genes (Chin *et al.*, 1998; Wu *et al.*, 2000; Meissner *et al.*, 2007). Therefore, it seems possible that NO may also influence activity-induced MEF2/HDAC regulation. This interaction, however, has not yet been studied in skeletal muscle, but in endothelial cells NO appears to enhance HDAC activity (Illi *et al.*, 2008). Specifically, Illi *et al.* (2008) found that NO induced HDAC4 nuclear translocation in human endothelial cells. Whether NO exerts the same effect in activity-induced fast-to-slow transformations in skeletal muscle, however, remains to be investigated. Additionally, the potential that NO may enhance both HDAC4 and NFAT nuclear accumulation in activity-induced skeletal muscle adaptation appears contradictory. It is possible, however, that the activation of MEF2 via synergistic stimulation by CaMK and calcineurin (Wu *et al.*, 2000),

may override the potential negative influence of NO-induced HDAC nuclear translocation on slow gene expression. Collectively, it is apparent that the mechanisms underlying the key regulatory influence of NO on slow MHC gene expression requires further investigation, which is currently in its infancy.

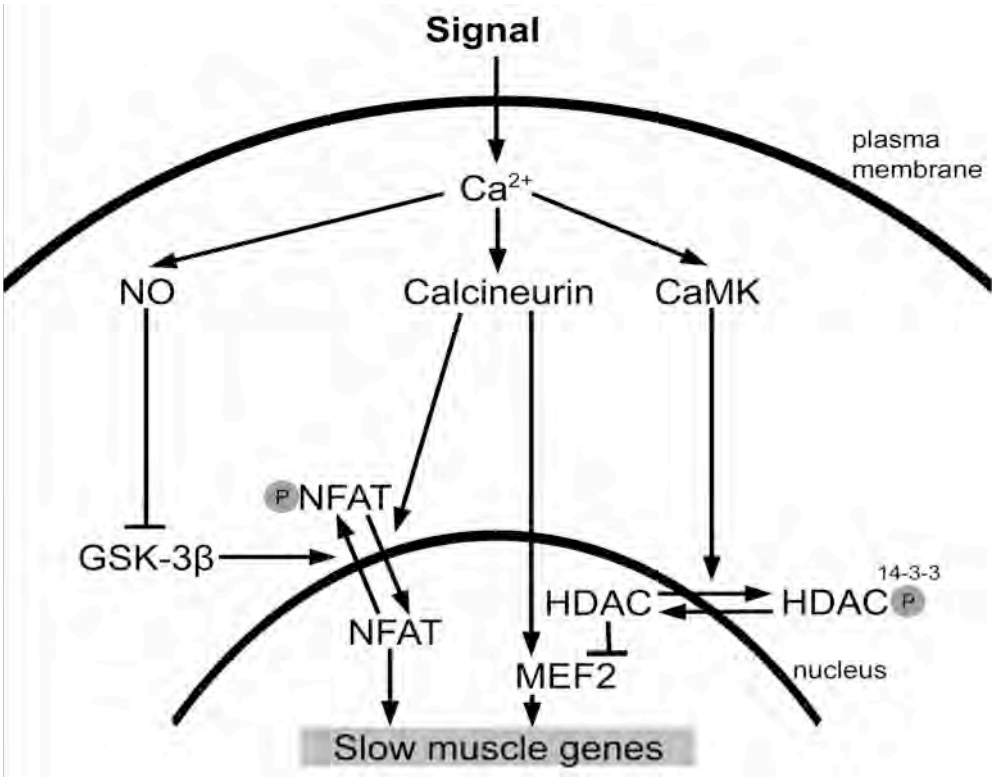

Figure 6.4 Simplified scheme of the signaling pathways involved in activity-dependent up-regulation of slow muscle gene expression. Ca^{2+}=calcium; CaMK=calmodulin-dependent protein kinase; GSK-3β=glycogen synthase kinase-3β; HDAC=histone deacetylase; MEF2=myocyte enhancing factor-2; NFAT=nuclear factor of activated T cells; NO=nitric oxide; P=phosphorylated.

6.4.2 Fast Myosin Heavy Chain Regulation

To date, NO regulation of activity-induced MHC-based adaptations has only been investigated at the mRNA and protein levels of the slowest MHC isoform (Smith *et al.*, 2002; Sellman *et al.*, 2006; Drenning *et al.*, 2008). Therefore, the current proposed pathway of NO regulation (Fig. 6.3) does not

fully explain the requirement of NOS activity for the up-regulation of all MHC isoforms involved in CLFS-induced fast-to-slow fibre type transformations [i.e. MHCI, MHCIIa and MHCIId(x)] as observed for the first time in Chapter 5. Similar to slow gene regulation, calcineurin and CaMK signaling have also been implicated in the shift from type IIB and IID(X) fibres to the slower type IIA fibres (Dunn *et al.*, 1999; Allen *et al.*, 2001; Dunn *et al.*, 2001; Allen & Leinwand, 2002; Miyazaki *et al.*, 2004). In response to overload or low-frequency stimulation, downstream effectors of calcineurin are most readily increased in the fastest IIB and IID(X) fibres, while administration of cyclosporine, at a dose sufficient to inhibit calcineurin activity, prevented overload-induced increases in NFAT and MEF2 activity, as well as preventing type IIB→IID(X)→IIA fibre transformations in mice (Dunn *et al.*, 1999; Dunn *et al.*, 2001; Miyazaki *et al.*, 2004). Moreover, when more potent inhbitors of calcineurin (i.e. FK506 and CAIN) were used in rats, the slower MHCI and IIa mRNAs were downregulated with concomitant increases in the fastest MHCIId(x) and IIb mRNAs (Serrano *et al.*, 2001). Further evidense supporting a role for calcineurin in mediating fast MHC regulation comes from Allen *et al.* (2001, 2002), who demonstrated that Ca^{2+}-ionophore treated C_2C_{12} myoblasts preferentially activated the MHCIIa promoter and protein content to a greater extent than the other two fast MHC promoters by calcineurin- and CaMK-dependent MEF2 and NFAT signaling. Collectively, it appears that in addition to regulating slow muscle specific genes, both MEF2 and NFAT transcriptional activity play a role in activity-induced fast-to-slow fibre type transformations within the fast fibre population. Therefore, the slow MHC gene regulatory pathway proposed by Drenning *et al*. (2008) that involves the synergistic regulatory mechanisms of calcineurin and NO on NFAT, may also apply to fast MHC gene regulation during fast-to-slow fibre type transformations. Again, the potential regulation of NO on MEF2 transcriptional activity has yet to be investigated in skeletal muscle. The influence of NO on NFAT nuclear accumulation in vivo is currently under investigation. Prelimary results show that CLFS-induced increases in NFAT nuclear localisation, as detected by

immunofluorescence in rat tibialis anterior muscles, does not occur in L-NAME treated animals. Quantitative confirmation is being performed by western blot analysis of NFAT phosphorylation states in the rat extensor digitorum longus.

6.5 CONCLUSIONS

Results from Chapters 3 and 4 reveal that satellite cells may play a role in the fast fibre population during short-term CLFS-induced fast-to-slow fibre type transformations and the final fast type IIA to slow type I transformation. It is possible that satellite cells may be required to increase translational capacity during CLFS-induced fast-to-slow transformations. As discovered in Chapter 5, NO appears to be required for immediate CLFS-induced satellite cell activation but, a yet to be defined pathway exists that can fully compensate in the absence of NOS activity. It seems that this alternative pathway may involve NO-independent production of HGF. Additionally, NO appears to be a key regulator of MHC gene expression during fast-to-slow fibre type transformations. It is possible that NO regulates CLFS-induced MHC gene expression by promoting NFAT nuclear accumulation via GSK-3β inhibition. This and other potential regulatory pathways, however, require further investigation.

6.6 REFERENCES

Adams GR. (2006). Satellite cell proliferation and skeletal muscle hypertrophy. *Appl Physiol Nutr Metab* **31,** 782-790.

Allen DL & Leinwand LA. (2002). Intracellular calcium and myosin isoform transitions. Calcineurin and calcium-calmodulin kinase pathways regulated preferential activation of the IIa myosin heavy chain promoter. *J Biol Chem* **277,** 45323-45330.

Allen DL, Sartorius CA, Sycuro LK & Leinwand LA. (2001). Different pathways regulate expression of the skeletal myosin heavy chain genes. *J Biol Chem* **276,** 43524-43533.

Anderson J & Pilipowicz O. (2002). Activation of muscle satellite cells in single-fiber cultures. *Nitric Oxide* **7,** 36-41.

Anderson JE. (2000). A role for nitric oxide in muscle repair: nitric oxide-mediated activation of muscle satellite cells. *Mol Biol Cell* **11,** 1859-1874.

Atherton PJ, Babraj J, Smith K, Singh J, Rennie MJ & Wackerhage H. (2005). Selective activation of AMPK-PGC-1alpha or PKB-TSC2-mTOR signaling can explain specific adaptive responses to endurance or resistance training-like electrical muscle stimulation. *FASEB J* **19,** 786-788.

Bertos NR, Wang AH & Yang XJ. (2001). Class II histone deacetylases: structure, function, and regulation. *Biochem Cell Biol* **79,** 243-252.

Bondesen BA, Jones KA, Glasgow WC & Pavlath GK. (2007). Inhibition of myoblast migration by prostacyclin is associated with enhanced cell fusion. *FASEB J* **21,** 3338-3345.

Bondesen BA, Mills ST, Kegley KM & Pavlath GK. (2004). The COX-2 pathway is essential during early stages of skeletal muscle regeneration. *Am J Physiol Cell Physiol* **287,** C475-483.

Carmeli E, Moas M, Reznick AZ & Coleman R. (2004). Matrix metalloproteinases and skeletal muscle: a brief review. *Muscle Nerve* **29,** 191-197.

Chakraborti S, Mandal M, Das S, Mandal A & Chakraborti T. (2003). Regulation of matrix metalloproteinases: an overview. *Mol Cell Biochem* **253,** 269-285.

Cheek DB. (1985). The control of cell mass and replication. The DNA unit--a personal 20-year study. *Early HumDev* **12,** 211-239.

Chin ER. (2004). The role of calcium and calcium/calmodulin-dependent kinases in skeletal muscle plasticity and mitochondrial biogenesis. *Proc Nutr Soc* **63,** 279-286.

Chin ER, Olson EN, Richardson JA, Yang Q, Humphries C, Shelton JM, Wu H, Zhu W, Bassel-Duby R & Williams RS. (1998). A calcineurin-dependent transcriptional pathway controls skeletal muscle fiber type. *Genes Dev* **12,** 2499-2509.

Coffey VG & Hawley JA. (2007). The molecular bases of training adaptation. *Sports Med* **37,** 737-763.

Conway K, Pin C, Kiernan JA & Merrifield P. (2004). The E protein HEB is preferentially expressed in developing muscle. *Differentiation* **72,** 327-340.

Derksen PW, Keehnen RM, Evers LM, van Oers MH, Spaargaren M & Pals ST. (2002). Cell surface proteoglycan syndecan-1 mediates hepatocyte growth factor binding and promotes Met signaling in multiple myeloma. *Blood* **99,** 1405-1410.

Drenning JA, Lira VA, Simmons CG, Soltow QA, Sellman JE & Criswell DS. (2008). Nitric oxide facilitates NFAT-dependent transcription in mouse myotubes. *Am J Physiol Cell Physiol* **294,** C1088-1095.

Dunn SE, Burns JL & Michel RN. (1999). Calcineurin is required for skeletal muscle hypertrophy. *JBiolChem* **274,** 21908-21912.

Dunn SE, Simard AR, Bassel-Duby R, Williams RS & Michel RN. (2001). Nerve activity-dependent modulation of calcineurin signaling in adult fast and slow skeletal muscle fibers. *J Biol Chem* **276,** 45243-45254.

Edgerton VR & Roy RR. (1991). Regulation of skeletal muscle fiber size, shape and function. *J Biomech* **24 Suppl 1,** 123-133.

Fukushima K, Nakamura A, Ueda H, Yuasa K, Yoshida K, Takeda Si & Ikeda S-i. (2007). Activation and localization of matrix metalloproteinase-2 and -9 in the skeletal muscle of the muscular dystrophy dog (CXMDJ). *BMC Musculoskeletal Disorders* **8,** 54.

Funk CD. (2001). Prostaglandins and leukotrienes: advances in eicosanoid biology. *Science* **294,** 1871-1875.

Gibson MC & Schultz E. (1982). The distribution of satellite cells and their relationship to specific fiber types in soleus and extensor digitorum longus muscles. *AnatRec* **202,** 329-337.

Gibson MC & Schultz E. (1983). Age-related differences in absolute numbers of skeletal muscle satellite cells. *Muscle Nerve* **6,** 574-580.

Goldberg AL. (1967). Protein synthesis in tonic and phasic skeletal muscles. *Nature* **216,** 1219-1220.

Gordon SE, Westerkamp CM, Savage KJ, Hickner RC, George SC, Fick CA & McCormick KM. (2007). Basal, but not overload-induced, myonuclear addition is attenuated by NG-nitro-L-arginine methyl ester (L-NAME) administration. *Can J Physiol Pharmacol* **85,** 646-651.

Guerin C & Holland PC. (1995). Synthesis and secretion of matrix-degrading metalloproteases by human skeletal muscle satellite cells. *Developmental Dynamics* **202,** 91-99.

Haas TL. (2005). Endothelial cell regulation of matrix metalloproteinases. *Can J Physiol Pharmacol* **83,** 1-7.

Haas TL, Milkiewicz M, Davis SJ, Zhou AL, Egginton S, Brown MD, Madri JA & Hudlicka O. (2000). Matrix metalloproteinase activity is required for activity-induced angiogenesis in rat skeletal muscle. *Am J Physiol Heart Circ Physiol* **279,** H1540-1547.

Hall ZW & Ralston E. (1989). Nuclear domains in muscle cells. *Cell* **59,** 771-772.

Husain S & Crosson CE. (2008). Role of PKCε in PGF2α-stimulated MMP-2 secretion from human ciliary muscle cells. *J Ocul Pharmacol Ther* **24,** 268-277.

Illi B, Dello Russo C, Colussi C, Rosati J, Pallaoro M, Spallotta F, Rotili D, Valente S, Ragone G, Martelli F, Biglioli P, Steinkuhler C, Gallinari P, Mai A, Capogrossi MC & Gaetano C. (2008). Nitric oxide modulates chromatin folding in human endothelial cells via protein phosphatase 2A activation and class II histone deacetylases nuclear shuttling. *Circ Res* **102,** 51-58.

Jaschinski F, Schuler MJ, Peuker H & Pette D. (1998). Changes in myosin heavy chain mRNA and protein isoforms of rat muscle during forced contractile activity. *Am J Physiol Cell Physiol* **274,** C365-C370.

Jones NC, Fedorov YV, Rosenthal RS & Olwin BB. (2001). ERK1/2 is required for myoblast proliferation but is dispensable for muscle gene expression and cell fusion. *J Cell Physiol* **186,** 104-115.

Kadi F, Schjerling P, Andersen LL, Charifi N, Madsen JL, Christensen LR & Andersen JL. (2004). The effects of heavy resistance training and detraining on satellite cells in human skeletal muscles. *J Physiol* **558,** 1005-1012.

Kalhovde JM, Jerkovic R, Sefland I, Cordonnier C, Calabria E, Schiaffino S & Lomo T. (2005). "Fast" and "slow" muscle fibres in hindlimb muscles of adult rats regenerate from intrinsically different satellite cells. *J Physiol* **562,** 847-857.

Kherif S, Lafuma C, Dehaupas M, Lachkar S, Fournier JG, Verdiere-Sahuque M, Fardeau M & Alameddine HS. (1999). Expression of matrix metalloproteinases 2 and 9 in regenerating skeletal muscle: a study in experimentally injured and mdx muscles. *Dev Biol* **205,** 158-170.

Kramer HF & Goodyear LJ. (2007). Exercise, MAPK, and NF-kappaB signaling in skeletal muscle. *J Appl Physiol* **103,** 388-395.

Kranenburg O, Gebbink MF & Voest EE. (2004). Stimulation of angiogenesis by Ras proteins. *Biochim Biophys Acta* **1654,** 23-37.

Liu Y, Randall WR & Schneider MF. (2005a). Activity-dependent and -independent nuclear fluxes of HDAC4 mediated by different kinases in adult skeletal muscle. *J Cell Biol* **168,** 887-897.

Liu Y, Shen T, Randall WR & Schneider MF. (2005b). Signaling pathways in activity-dependent fiber type plasticity in adult skeletal muscle. *J Muscle Res Cell Motil* **26,** 13-21.

Mackey AL, Kjaer M, Dandanell S, Mikkelsen KH, Holm L, Dossing S, Kadi F, Koskinen SO, Jensen CH, Schroder HD & Langberg H. (2007). The influence of anti-inflammatory medication on exercise-induced myogenic precursor cell responses in humans. *J Appl Physiol* **103,** 425-431.

Meissner JD, Umeda PK, Chang KC, Gros G & Scheibe RJ. (2007). Activation of the beta myosin heavy chain promoter by MEF-2D, MyoD, p300, and the calcineurin/NFATc1 pathway. *J Cell Physiol* **211,** 138-148.

Mendias CL, Tatsumi R & Allen RE. (2004). Role of cyclooxygenase-1 and -2 in satellite cell proliferation, differentiation, and fusion. *Muscle Nerve* **30,** 497-500.

Miyazaki M & Esser KA. (2009). Cellular mechanisms regulating protein synthesis and skeletal muscle hypertrophy in animals. *J Appl Physiol* **106,** 1367-1373.

Miyazaki M, Hitomi Y, Kizaki T, Ohno H, Haga S & Takemasa T. (2004). Contribution of the calcineurin signaling pathway to overload-induced skeletal muscle fiber-type transition. *J Physiol Pharmacol* **55,** 751-764.

Murgia M, Serrano AL, Calabria E, Pallafacchina G, Lomo T & Schiaffino S. (2000). Ras is involved in nerve-activity-dependent regulation of muscle genes. *Nat Cell Biol* **2,** 142-147.

Nader GA & Esser KA. (2001). Intracellular signaling specificity in skeletal muscle in response to different modes of exercise. *J Appl Physiol* **90,** 1936-1942.

O'Connor RS & Pavlath GK. (2007). Point:Counterpoint: Satellite cell addition is/is not obligatory for skeletal muscle hypertrophy. *J Appl Physiol* **103,** 1099-1100.

Pavlath GK, Rich K, Webster SG & Blau HM. (1989). Localization of muscle gene products in nuclear domains. *Nature* **337,** 570-573.

Petrella JK, Kim JS, Cross JM, Kosek DJ & Bamman MM. (2006). Efficacy of myonuclear addition may explain differential myofiber growth among resistance-trained young and older men and women. *Am J Physiol Endocrinol Metab* **291,** E937-E946.

Pin CL & Merrifield PA. (1997). Developmental potential of rat L6 myoblasts in vivo following injection into regenerating muscles. *Dev Biol* **188,** 147-166.

Putman CT, Düsterhöft S & Pette D. (1999). Changes in satellite cell content and myosin isoforms in low-frequency- stimulated fast muscle of hypothyroid rat. *J Appl Physiol* **86,** 40-51.

Ralston E & Hall ZW. (1992). Restricted distribution of mRNA produced from a single nucleus in hybrid myotubes. *J Cell Biol* **119,** 1063-1068.

Roux PP & Blenis J. (2004). ERK and p38 MAPK-activated protein kinases: a family of protein kinases with diverse biological functions. *Microbiol Mol Biol Rev* **68,** 320-344.

Roy RR, Monke SR, Allen DL & Edgerton VR. (1999). Modulation of myonuclear number in functionally overloaded and exercised rat plantaris fibers. *J Appl Physiol* **87,** 634-642.

Sakata T, Tatsumi R, Yamada M, Shiratsuchi S, Okamoto S, Mizunoya W, Hattori A & Ikeuchi Y. (2006). Preliminary experiments on mechanical stretch-induced activation of skeletal muscle satellite cells *in vivo*. *Animal Science Journal* **77,** 518-525.

Schultz E. (1989). Satellite cell behaviour during skeletal muscle growth and regeneration. *Med Sci Sports Exerc* **21,** S181-S186.

Schultz E, Darr KC & Pette D. (1990). The role of satellite cells in adaptive or induced fiber transformations. In *The dynamic state of muscle fibers*, pp. 667-679. Walter de Gruyter, Berlin and New York.

Sellman JE, DeRuisseau KC, Betters JL, Lira VA, Soltow QA, Selsby JT & Criswell DS. (2006). In vivo inhibition of nitric oxide synthase impairs upregulation of contractile protein mRNA in overloaded plantaris muscle. *J Appl Physiol* **100,** 258-265.

Serrano AL, Murgia M, Pallafacchina G, Calabria E, Coniglio P, Lomo T & Schiaffino S. (2001). Calcineurin controls nerve activity-dependent specification of slow skeletal muscle fibers but not muscle growth. *Proc Natl Acad Sci U S A* **98,** 13108-13113.

Smith LW, Smith JD & Criswell DS. (2002). Involvement of nitric oxide synthase in skeletal muscle adaptation to chronic overload. *J Appl Physiol* **92,** 2005-2011.

Soltow QA, Betters JL, Sellman JE, Lira VA, Long JH & Criswell DS. (2006). Ibuprofen inhibits skeletal muscle hypertrophy in rats. *Med Sci Sports Exerc* **38,** 840-846.

Spanikova A, Simoncikova P, Ravingerova T, Pechanova O & Barancik M. (2008). The effect of chronic nitric oxide synthases inhibition on regulatory proteins in rat hearts. *Mol Cell Biochem* **312,** 113-120.

Tatsumi R & Allen RE. (2008). Mechano-biology of resident myogenic stem cells: Molecular mechanism of stretch-induced activation of satellite cells. *Animal Science Journal* **79,** 279-290.

Tatsumi R, Anderson JE, Nevoret CJ, Halevy O & Allen RE. (1998). HGF/SF is present in normal adult skeletal muscle and is capable of activating satellite cells. *Dev Biol* **194,** 114-128.

Tatsumi R, Hattori A, Ikeuchi Y, Anderson JE & Allen RE. (2002). Release of hepatocyte growth factor from mechanically stretched skeletal muscle satellite cells and role of pH and nitric oxide. *Mol Biol Cell* **13,** 2909-2918.

Tatsumi R, Liu X, Pulido A, Morales M, Sakata T, Dial S, Hattori A, Ikeuchi Y & Allen RE. (2006). Satellite cell activation in stretched skeletal muscle and the role of nitric oxide and hepatocyte growth factor. *Am J Physiol Cell Physiol* **290,** C1487-1494.

Tseng BS, Kasper CE & Edgerton VR. (1994). Cytoplasm-to-myonucleus ratios and succinate dehydrogenase activities in adult rat slow and fast muscle fibers. *Cell Tissue Res* **275,** 39-49.

VanSaun M & Werle MJ. (2000). Matrix metalloproteinase-3 removes agrin from synaptic basal lamina. *J Neurobiol* **43,** 140-149.

Whalen RG, Harris JB, Butler-Browne GS & Sesodia S. (1990). Expression of myosin isoforms during notexin-induced regeneration of rat soleus muscles. *Dev Biol* **141,** 24-40.

Wozniak AC, Kong J, Bock E, Pilipowicz O & Anderson JE. (2005). Signaling satellite-cell activation in skeletal muscle: markers, models, stretch, and potential alternate pathways. *Muscle Nerve* **31,** 283-300.

Wu H, Naya FJ, McKinsey TA, Mercer B, Shelton JM, Chin ER, Simard AR, Michel RN, Bassel-Duby R, Olson EN & Williams RS. (2000). MEF2 responds to multiple calcium-regulated signals in the control of skeletal muscle fiber type. *EMBO J* **19,** 1963-1973.

Wu H, Rothermel B, Kanatous S, Rosenberg P, Naya FJ, Shelton JM, Hutcheson KA, DiMaio JM, Olson EN, Bassel-Duby R & Williams RS. (2001). Activation of MEF2 by muscle activity is mediated through a calcineurin-dependent pathway. *EMBO J* **20,** 6414-6423.

Yaffe D. (1968). Retention of differentiation potentialities during prolonged cultivation of myogenic cells. *Proc Natl Acad Sci USA* **61,** 477-483.

Yamada M, Sankoda Y, Tatsumi R, Mizunoya W, Ikeuchi Y, Sunagawa K & Allen RE. (2008). Matrix metalloproteinase-2 mediates stretch-induced activation of skeletal muscle satellite cells in a nitric oxide-dependent manner. *Int J Biochem Cell Biol* **40,** 2183-2191.

APPENDIX A

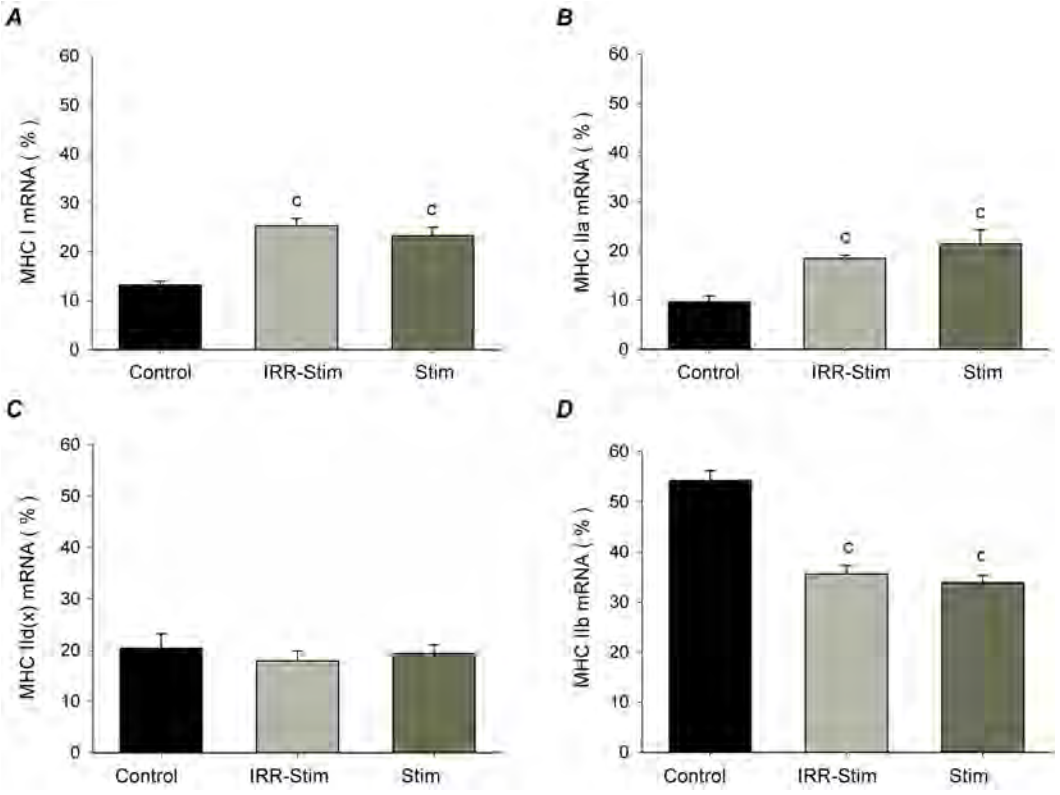

Figure 1 MHCI mRNA (*A*), MHCIIa mRNA (*B*), MHCIId(x) mRNA (*C*) and MHCIIb mRNA (*D*) expression levels expressed as a percent of total MHC mRNA content in rat tibialis anterior muscles of sham-operated (Control) and the contralateral right legs of γ -irradiated plus 21 day stimulated (IRR-Stim) or stimulated only (Stim). Statistical symbol indicates: ^{c} difference from Control ($P < 0.05$).

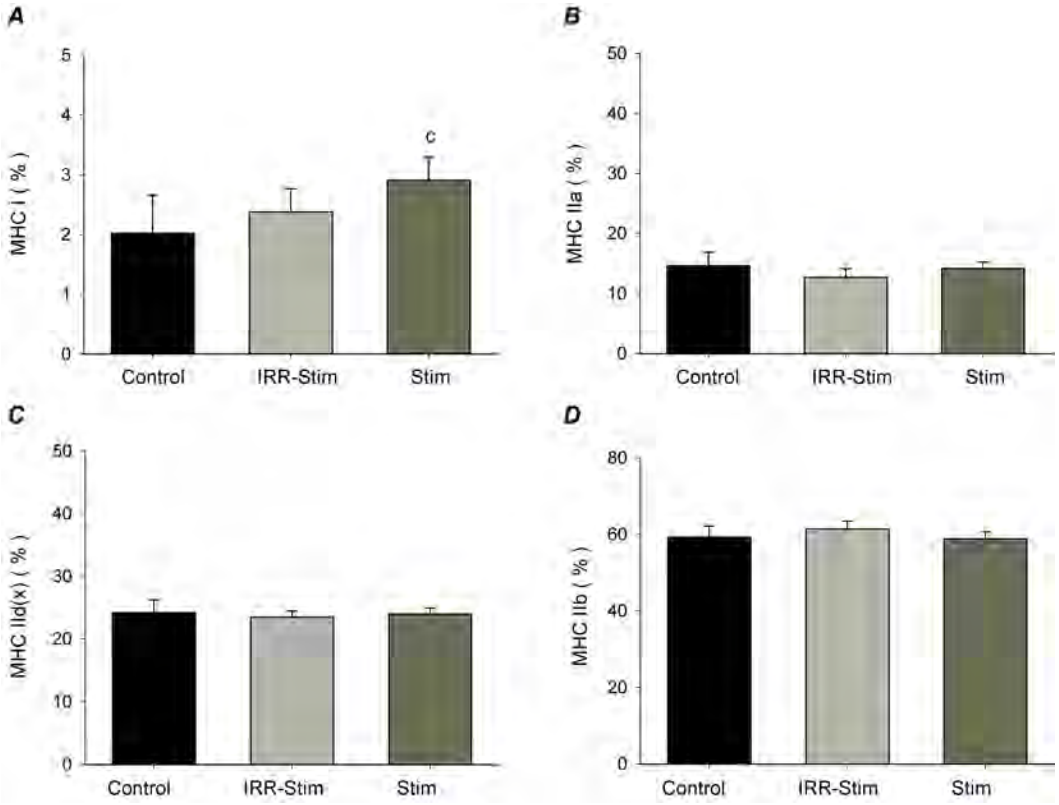

Figure 2 Percentage of MHCI (*A*), MHCIIa (*B*), MHCIId(x) (*C*) and MHCIIb (*D*) distribution in rat tibialis anterior muscles of sham-operated (Control) and the contralateral right legs of γ -irradiated plus 21 day stimulated (IRR-Stim) or stimulated only (Stim). Statistical symbol indicates: ^{c} difference from Control ($P < 0.05$).

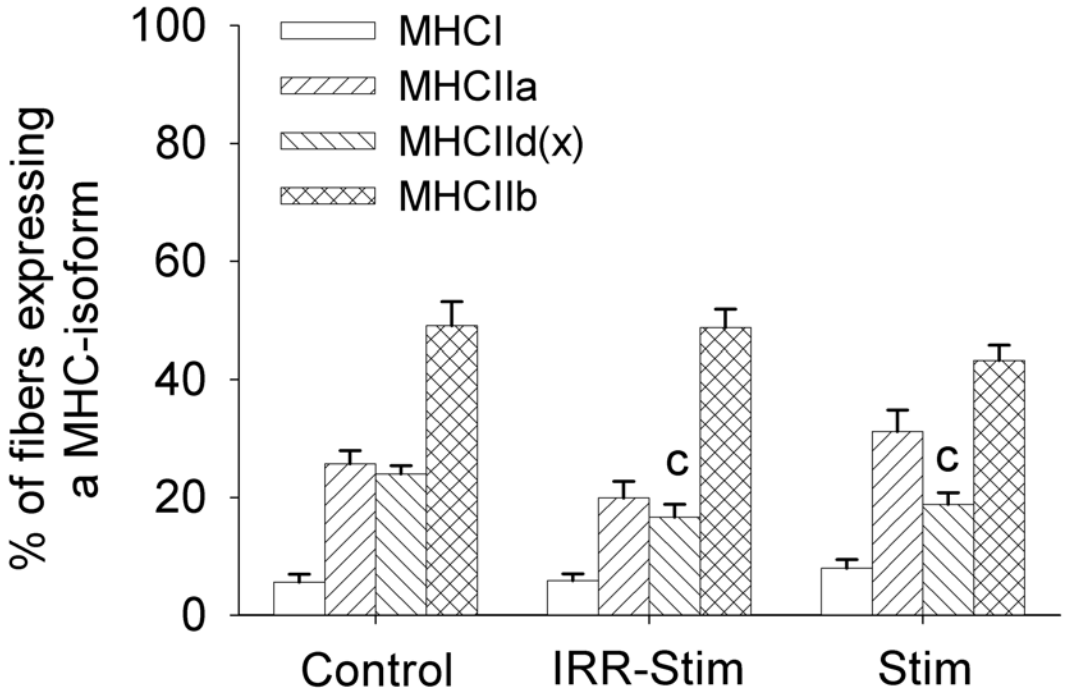

Figure 3 The percentage of fibres expressing a particular MHC isoform in rat tibialis anterior muscles of sham-operated (Control) and the contralateral right legs of γ-irradiated plus 21 day stimulated (IRR-Stim) or stimulated only (Stim). Statistical symbol indicates: [c] difference from Control ($P < 0.05$).Control ($P < 0.05$).

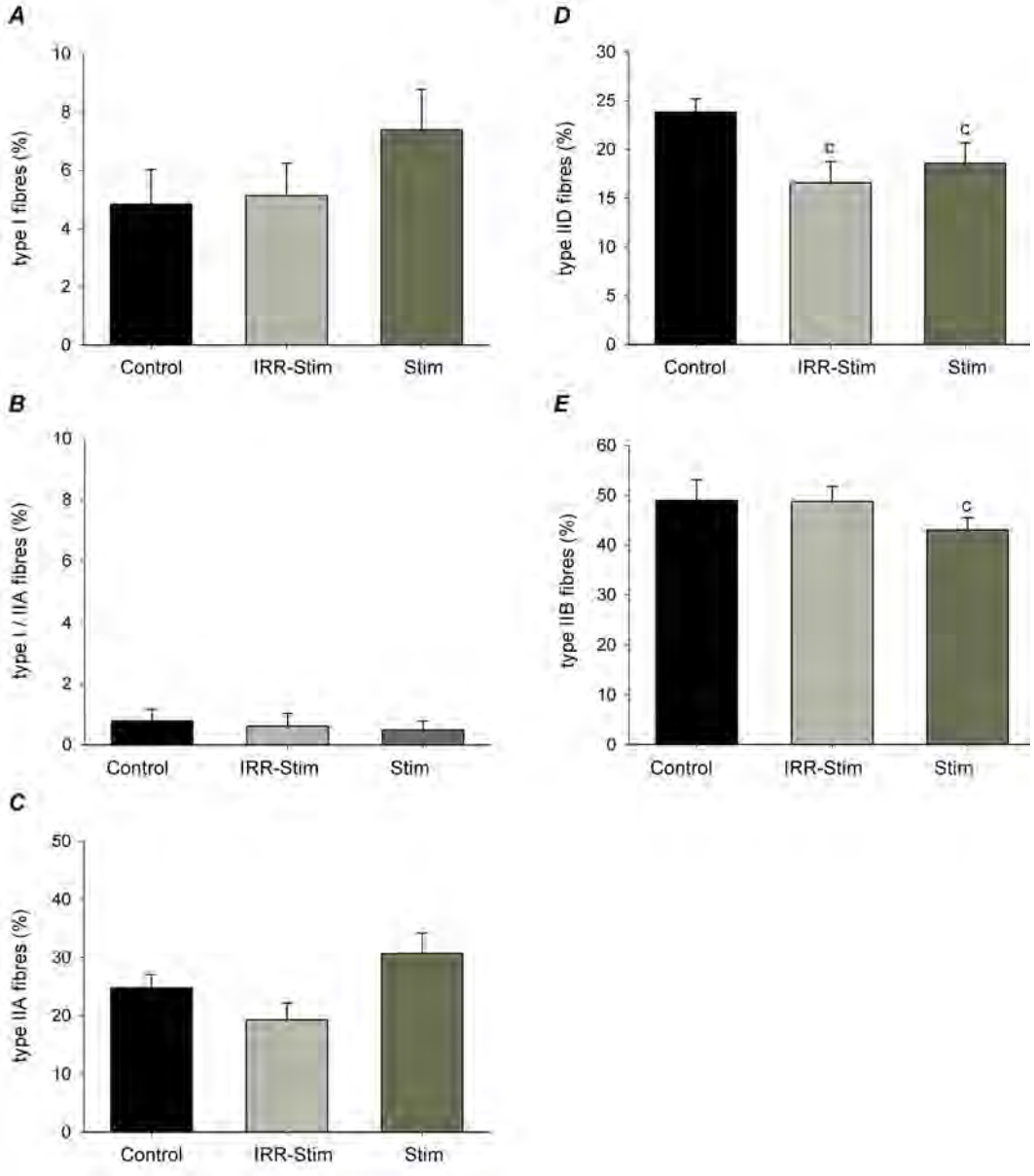

Figure 4 The proportion of pure and hybrid fibre types I (*A*), I/IIA (*B*), IIA (*C*), IID (*D*) and IIB (*E*) in rat tibialis anterior muscles of sham-operated (Control) and the contralateral right legs of γ-irradiated plus 21 day stimulated (IRR-Stim) or stimulated only (Stim). Statistical symbol indicates: ^{c} difference from Control ($P < 0.05$).

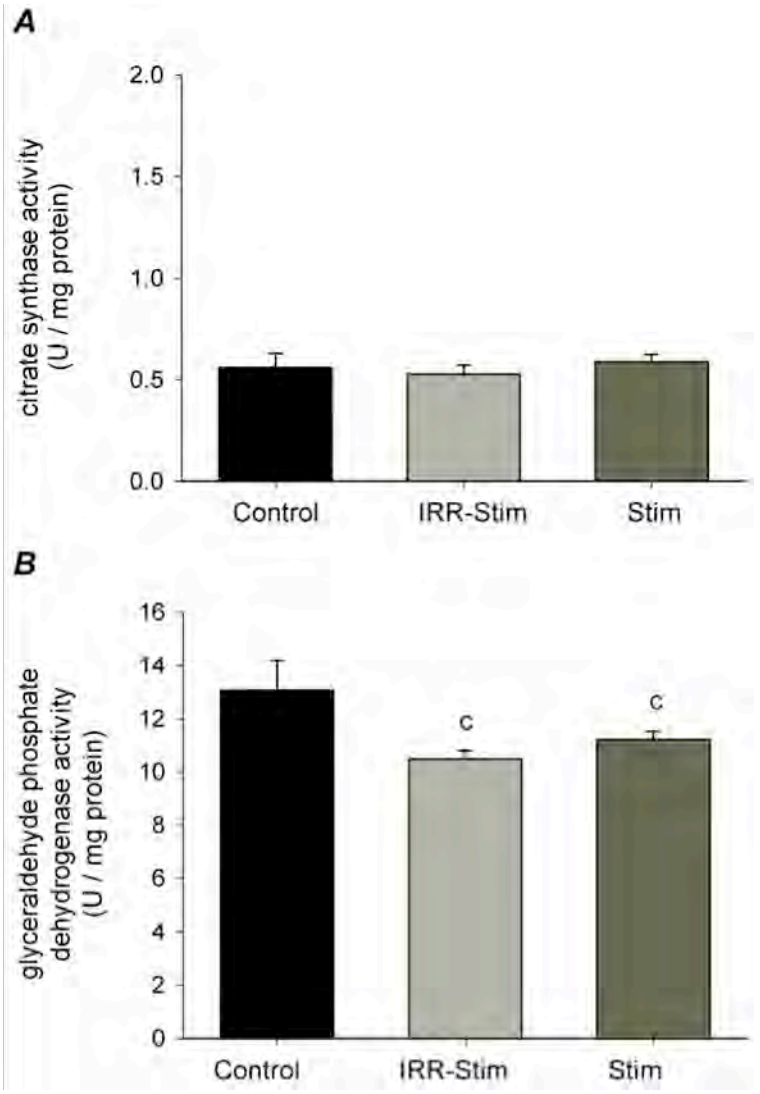

Figure 5 Citrate synthase (*A*) and glyceraldehyde phosphate dehydrogenase (*B*) activities in rat tibialis anterior muscles of sham-operated (Control) and the contralateral right legs of γ -irradiated plus 21 day stimulated (IRR-Stim) or stimulated only (Stim). Statistical symbol indicates: ^{c} difference from Control ($P < 0.05$).

APPENDIX B

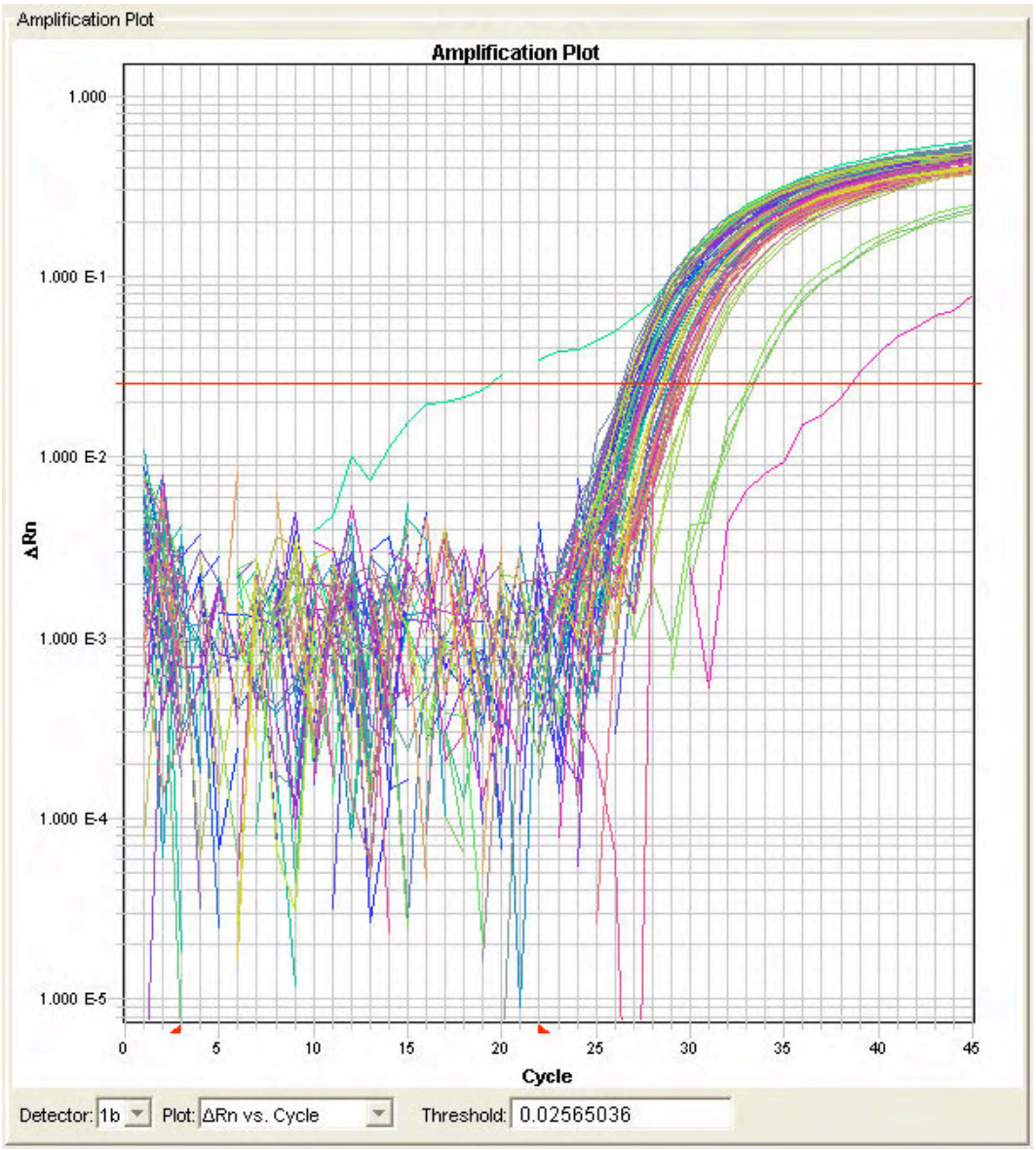

Figure 1 Representative real-time polymerase chain reaction amplification plot of MHCI mRNA that had a cycle threshold (horizontal red line) of 0.0257.

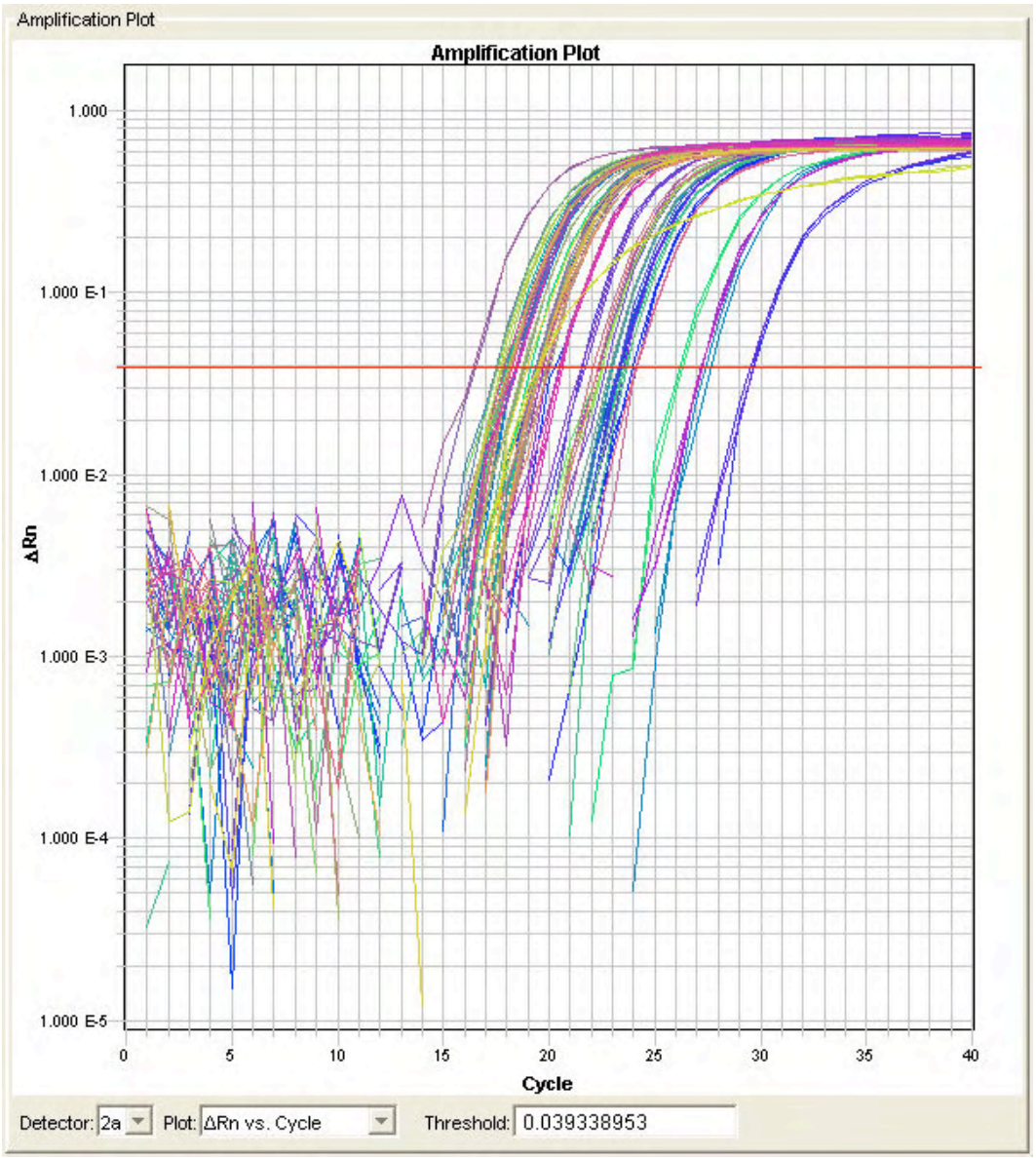

Figure 2 Representative real-time polymerase chain reaction amplification plot of MHCIIa mRNA that had a cycle threshold (horizontal red line) of 0.0393.

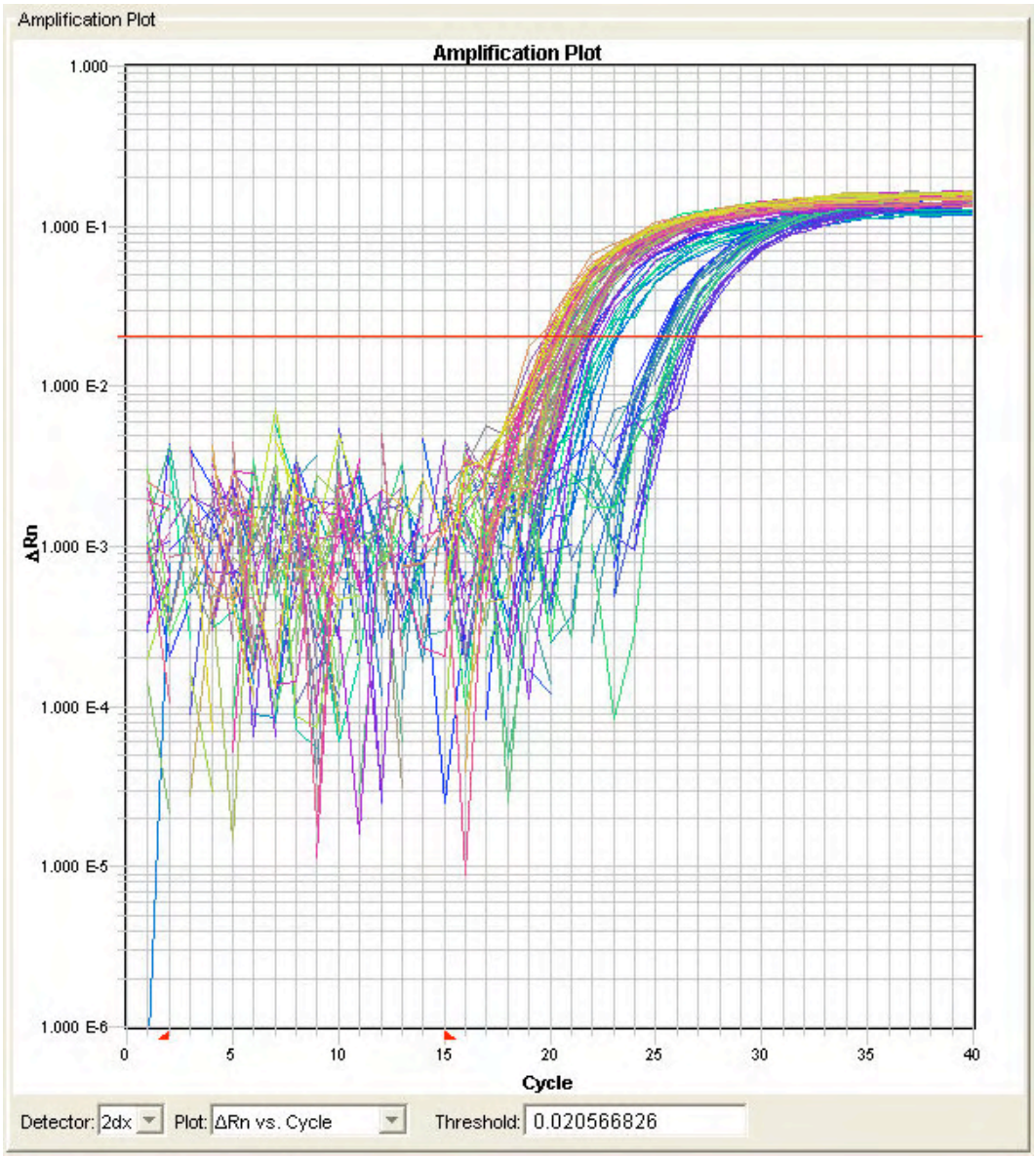

Figure 3 Representative real-time polymerase chain reaction amplification plot of MHCIId(x) mRNA that had a cycle threshold (horizontal red line) of 0.0206.

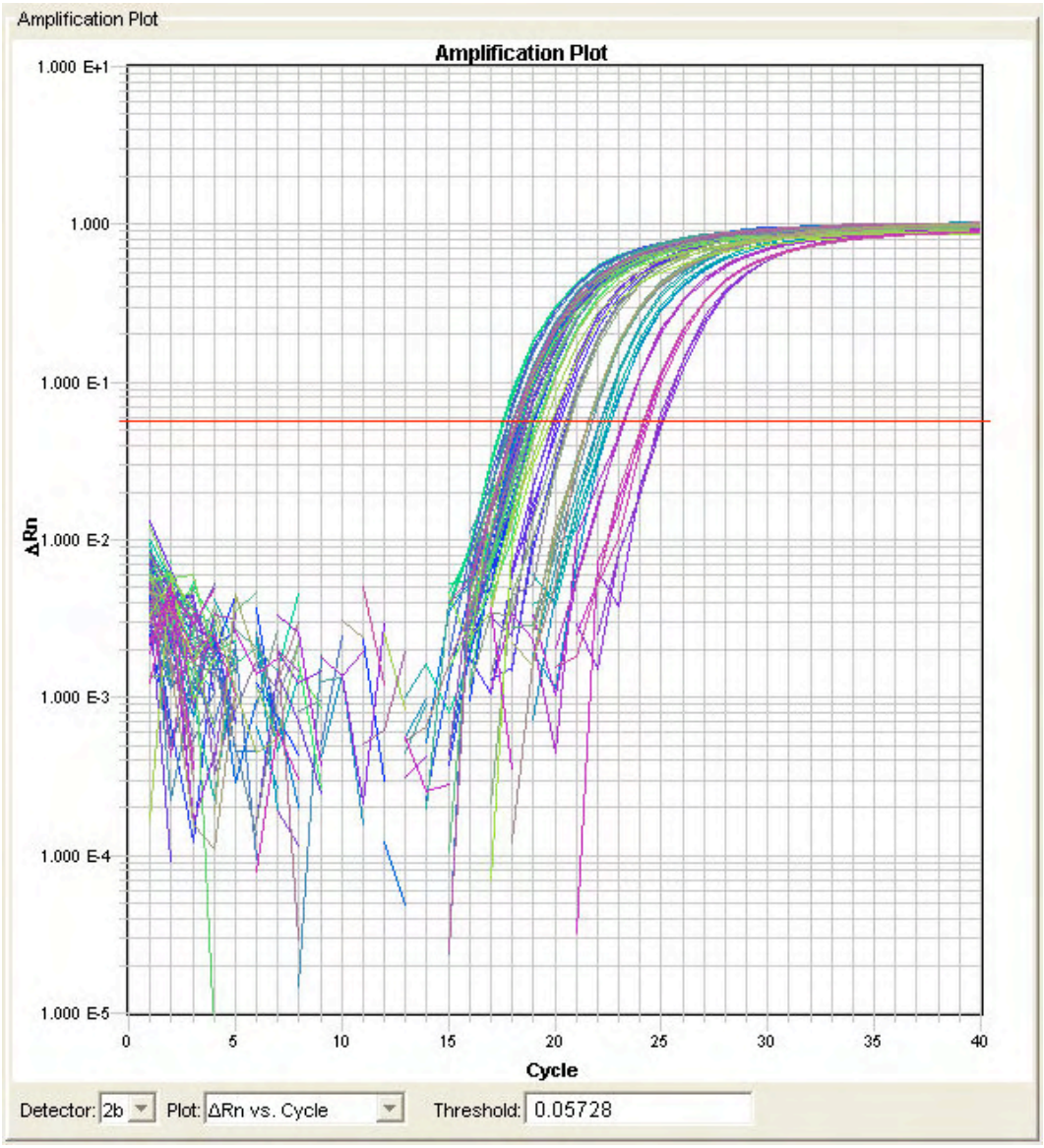

Figure 4 Representative real-time polymerase chain reaction amplification plot of MHCIIb mRNA that had a cycle threshold (horizontal red line) of 0.0573.

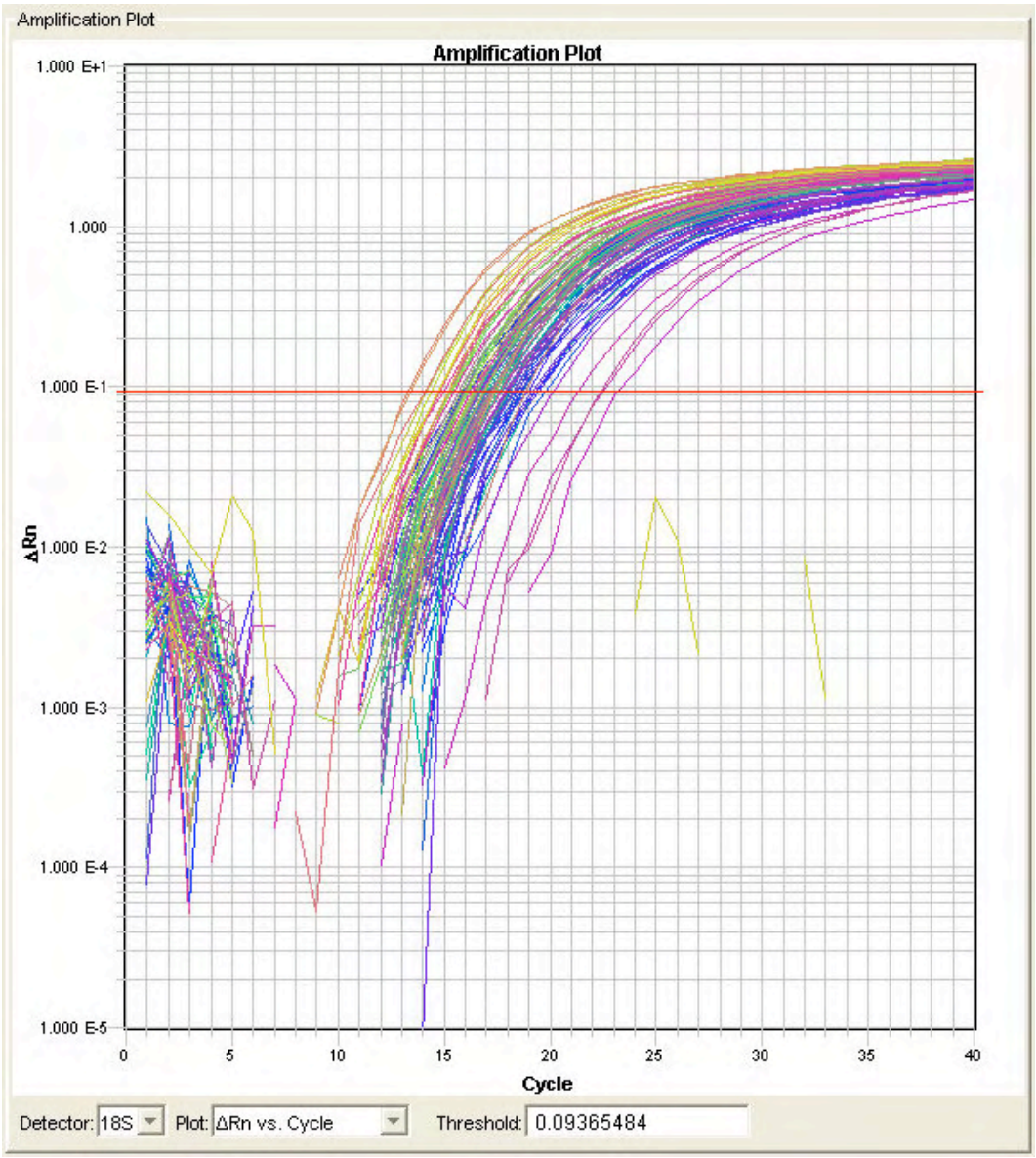

Figure 5 Representative real-time polymerase chain reaction amplification plot of 18S rRNA that had a cycle threshold (horizontal red line) of 0.0937.

APPENDIX C

Table 1. Real-time polymerase chain reaction threshold cycle (C_T) values in rat tibialis anterior muscles.

Group	Days of Stim-ulation	Condition	Threshold Cycle Values				
			MHCI	MHCIIa	MHCIId(x)	MHCIIb	18S
Control	0	Sham	31.0±0.7	23.5±0.8	25.6±1.0	23.3±0.9	19.9±0.8
Manipulated		L-NAME	25.9±0.2	20.1±0.2	20.0±0.2	18.6±0.2	20.3±1.0
	1	Control	29.0±0.6	20.6±0.3	24.5±0.3	21.4±0.2	16.8±0.4
		IRR	31.7±0.9	22.5±1.1	25.4±1.0	24.2±1.1	20.6±0.6
		L-NAME	26.6±0.6	20.7±0.4	20.6±0.4	19.2±0.6	19.0±0.6
	2	Control	28.8±0.5	21.0±0.3	23.7±0.3	21.3±0.2	15.3±0.6
		IRR	28.5±0.2	18.3±0.3	21.3±0.2	19.6±0.2	15.0±0.4
		L-NAME	26.7±0.8	20.0±0.3	20.5±0.3	19.5±0.5	18.4±0.8
	5	Control	32.1±0.1	21.8±0.3	23.6±0.3	25.0±0.7	21.4±0.4
		IRR	28.5±1.0	17.9±0.3	20.6±0.4	20.3±0.7	13.3±0.2
		L-NAME	25.4±0.7	18.8±0.6	21.5±0.7	20.8±0.5	15.7±0.7
	10	Control	31.3±0.3	21.1±0.3	24.4±0.6	26.6±0.6	22.1±0.8
		IRR	28.8±0.5	17.9±0.4	22.5±0.6	22.6±0.7	18.5±0.7
		L-NAME	25.9±1.6	19.8±0.8	23.6±0.9	22.2±0.8	16.4±1.1

Data are means ± SEM. $2^{-\Delta\Delta Ct}$ was calculated using the following formula: 2[-exponent (manipulated gene of interest$_{Ct}$ – endogenous 18S$_{Ct}$) – (control gene of interest$_{Ct}$ – endogenous 18S$_{Ct}$)].